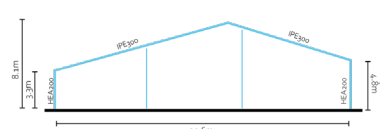
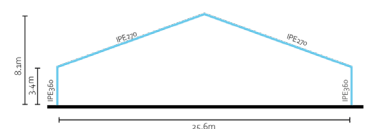
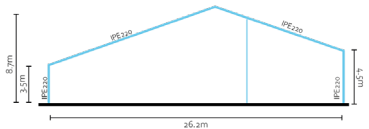
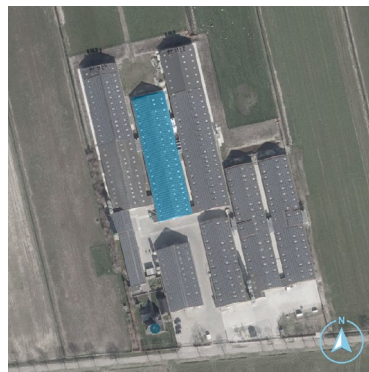
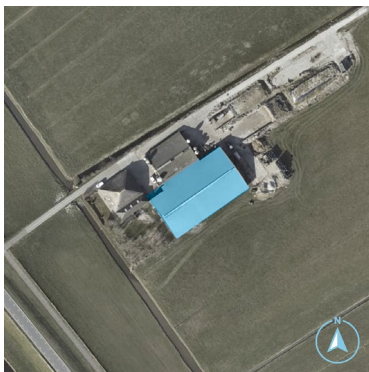
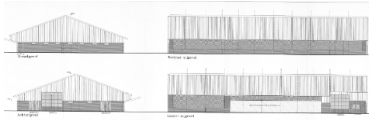


STRUCTURAL STEEL REUSE ANALYSIS



**BT Graduation Studio
Master Thesis
June 2023**

**Jelle ten Hove
4854136**

**Main mentor: Ir. A.C. Bergsma
Second mentor: prof. dr. M Overend
Board of Examination Delegate: Ir. H.W. de Wolff**

Preface

The report that is in front of you right now is the result of a graduation project at the faculty of Architecture and the Built Environment of the Delft University of Technology, within the Building Technology Master track.

At the time this report was written, the Netherlands is aiming to shift towards a circular economy in 2050, with preliminary targets of material usage reduction set for 2035. Additionally, the country faced fierce farmers' protests over the last five years as a result of the government's decisions that have been taken with regard to limiting nitrogen oxide emissions in order to save deteriorating natural landscapes. This thesis explores an unexpected overlap between these two issues as an opportunity to research the potential of mapping out reusable structural steel components that will come available in the agrarian sector due to the government's decision to buy out so-called megafarmers. It is understood that this can be considered a sensitive, political topic - however, the thesis itself is kept politically neutral and only approaches the scenario as an opportunity for research.

I hereby would like to express my gratitude to my mentors, Arie Bergsma and Mauro Overend, for guiding me in the process of this research project and for advising me along the way.

Abstract

The Dutch government was mandated by the national court in May 2019 to address high nitrogen-oxide levels, threatening construction permits to be canceled if target values are not met. As the agrarian sector contributed significantly to nitrogen-oxide emissions, reductions in this sector were necessary. Ongoing protests by farmers indicate the unresolved crisis. A government report suggests that around 500-600 high-emission agricultural businesses must cease operations for a substantial impact. Consequently, large cattle farms, known as "mega barns," will become vacant. Traditionally demolished or recycled, their materials may have the potential for repurposing, especially given the projected availability of similar buildings in the next 10-20 years.

Both the European Union and the Dutch Government have set themselves targets to convert their economies from linear to circular before the year 2050. A circular economy means a system in which products and materials are kept within the loop as long as possible, reducing the need for new raw materials and production – reducing energy needs and CO₂-emissions in the process. Recycling is currently coming up as a mainline strategy, however, it is considered to be less circular than other strategies, especially compared to reuse. The steel sector is seen as an exemplary industry that recycles a lot but would pose major environmental benefits when shifting the chain towards reuse. Yet, making this shift happen is withheld by certain barriers, especially on the designer's side. The fact that information on availability, quality and quantity of reusable components is scarce in the critical early phases of the design process, is one of these main barriers.

This thesis attempts to introduce a tool that employs reverse-engineering techniques to analyze and predict the availability of structural steel components in industrial buildings, providing designers with knowledge about potentially available materials as early in the process as possible. By utilizing publicly available data, the tool enables an accurate estimation of the length, type, quantity and quality of the elements. This is done by the use of parametric design software such as Rhino3D, Grasshopper and Karamba3D. The research explores ways of making use of existing structures' geometry and design requirements in order to predict the structural properties of the load-bearing components. The tool has been tested and evaluated on a series of cases, all of which are industrial farm halls situated in the Netherlands. This case testing has been used to improve and finetune the output results of the tool. In the end, the developed tool is able to predict steel profiles within a +/- 1 profile class range. Additional analyses are incorporated to assess cost savings, environmental benefits, and element quality.

TABLE OF CONTENTS

Preface.....	2
Abstract.....	3
1. INTRODUCTION.....	6
1.1 Context	6
1.2 The Netherlands	6
1.3 Nitrogen-oxide crisis.....	7
1.4 Problem statement	7
1.5 Objectives.....	8
1.6 Scope	9
1.7 Approach & methodology.....	10
2. BACKGROUND	12
2.1 Typology – Megabarn	12
2.2 Typology – Portal hall.....	13
2.3 Construction Steel.....	15
2.4 Circular Strategies.....	18
2.5 Steel Reuse	21
3. CASE STUDY	26
3.1 Case selection	26
3.2 Case Analysis.....	29
4. QUICKSCAN.....	30
4.1 Criteria Quicksan Tool	30
4.2 Workflow	31
4.3 Required Data.....	32
4.4 Model Set-up	34
4.5 Model Validation	40
5. TESTING.....	41
5.1 Sensitivity Analysis	41
5.2 Case Testing	45
5.3 Model iterations	59
6. DECONSTRUCTION AND REUSE.....	69
6.1 Deconstruction processes.....	69
6.2 Element quality assessment	72
6.3 Effectiveness of reuse	74
7. FINAL PRODUCT.....	77
7.1 Overview final tool.....	77
7.2 Tool application	78

7.3 Discussion: Limitations	79
7.4 Discussion: Opportunities	81
8. CONCLUSION	83
8.1 Research questions.....	83
8.2 Future Research	85
9. REFLECTION.....	86
10. REFERENCE LIST	88
Appendix A – Structural formulas	93
Appendix B – Wind table.....	94
Appendix C – Extended Case Table	95
Appendix D1-7 – Analysis Sheets	96
Appendix E – Structural verification	97
Appendix F – 3DBAG Input G2-G4	99
Appendix G – Grasshopper tool	100
Appendix H – User Interface Illustrations.....	101

1. INTRODUCTION

1.1 Context

In an action plan called 'closing the loop' (EU, 2015) the European Commission sets out concrete steps on the path towards a circular economy. A circular construction economy requires an approach that keeps resources in use within the economy for as long as possible (Lacy & Rutqvist, 2015). Several areas of special interest are mentioned in the European Commission's report, one of them being the construction and demolition sector as this sector consumes 40% of new raw materials that are introduced into the economy (Leising, 2018). Above that, the built environment puts major pressure on the natural environment and therefore, its role in transitioning to a circular economy is fundamental (Pomponi & Moncaster, 2017). Leising (2018) describes the circular economy within the built environment in more detail, stating that it is about optimizing a building's lifetime, taking into account the end-of-life phase of building in the design process and introducing new models of ownerships, considering buildings as real time material banks that store materials temporarily. Even though a transition to a circular economy is considered favourable, the construction sector is a slow-moving sector and a lot of stakeholders can seem reluctant to impose circular strategies as it might not be economically viable (Hoiby & Sand, 2019).

After the Car by Dennis and Urry (2009), however, describes a future scenario in which increasing energy hit a tipping point that will eventually lead to steep decline of transport opportunities between communities. An effect of this reduced transport is that these communities will have to transform into more locally orientated, self-sustaining hubs – on a social, economic and material level. Although being a hypothetical scenario, the start of the 2020's decade shows similarities with the vision presented in *After the Car*. Due to the recent pandemic, the war in Ukraine and other conflicts going on, energy prices have hit an all-time high (European Council, 2023). This directly translates into the world of transportation; the price for a gallon of diesel more than quadrupled, the cost of shipping a container from China increased even seven-fold between 2020 and 2022 (UNCTAD, 2022). Not only did transport costs rise, but the as the price of energy used to produce materials increased as well, construction materials became scarce and very expensive – often leading to construction projects going over budget, or even being cancelled (Dirkse, 2022). Although it is too early to say whether we reached the described 'tipping point', the high transport and material costs create an incentive for the construction industry to rethink how they source the materials needed for construction. With transport costs being high, sourcing materials locally can become economically beneficial and strategies such as reuse can be a way to avoid high material costs.

1.2 The Netherlands

Zooming in on the Netherlands, the same issues can be seen. The construction sector is a large part of the economy, but also one of the main emitters of CO₂ emissions and energy usage (CLO, 2021). As the Netherlands is part of the EU, the supranational targets of a carbon neutral and circular economy in 2050 need to be

met here as well. The Dutch government (Rijksoverheid, 2016) describes the plan to meet these targets in their report 'Nederland Circulair in 2050'. The vision summarized:

- Improving existing production processes to use less resources
- Using renewable, sustainable and available materials
- Develop new production methods and apply circular design

The goal is to ensure the Dutch economy is waste-free in 2050. As a stepping stone for reaching the goal in 2050, a preliminary milestone has been set for 2030, where the aim is to reduce the materials used in the economy with 50%. Although major steps have been taken over the last decade, with the Netherlands recycling the 3rd most per capita of all EU-27 countries and having reduced its domestic raw material consumption with 20% between 2010 and 2018 (CBS, 2020), the path towards a fully circular economy still poses a challenge to all sectors of the economy (PBL, 2021).

1.3 Nitrogen-oxide crisis

In May 2019, the Dutch national court ruled that nitrogen-oxide levels in the Netherlands were far too high, forcing the Dutch government to take action to reduce the levels drastically (NOS, 2019). Not complying with the court ruling would mean a stop on permits granted for construction of housing, roads and other infrastructural projects. As measures were taken over the full range of the economy, it was clear that the greatest reduction in nitrogen-oxide would have to come from the agrarian sector, as they have a 45% share in the national nitrogen-oxide emissions (RIVM, 2021). This led to fierce farmers protests in 2019, 2022 and 2023 and at the time of writing, the crisis is not resolved yet. It is getting clearer that the agrarian sector needs to shrink drastically with some political parties even suggesting a 50% reduction. In a report by the Dutch government, it is suggested that about 500-600 peak-emitters will have to stop business in order to make enough of an impact (Remkes, 2022). As a large number of agrarian producers will have to close their business, meaning the buildings used for these practices will become empty and available. These peak emitters are mostly large cattle farmers, running so-called 'mega barns'. Common practice currently suggests these halls will be demolished and not reused, only its materials recycled at best (Economisch Instituut voor de Bouw [EIB], Kok & Koning, 2019). Functional transformation of these buildings is a no go – their location, previous purpose and spatial properties do not lend themselves for much else than being a hall. Assuming that almost certainly hundreds of these types of buildings will become available in the next 10-20 years, it can be worth looking into the possibilities of using the materials present in these structures for other constructional purposes.

1.4 Problem statement

At first, the nitrogen-oxide crisis does not seem directly related to the topic of material reuse. However, as these industrial buildings will end up empty and ready for demolition, ways to reuse the structural components packed inside them should be analysed as they provide a source of material. To give an idea how much steel is involved here; megabarns are considered to be about 1 hectare in size. This does

not necessarily have to be one building, it can also be a collections of buildings next to each other, or a barn with multiple floors (for pigs or poultry). Following the report by Johan Remkes, 500-600 peak emitters are going to be closed. This averages out to about 550 hectares of steel hall that has potential to be reused. According to Hollander and Eldik (2007), a steel hall contains on average 22kg of steel per m², although it must be noted that this number can range between 15 and 30kg per m² depending on the type of hall. These 550 hectares of agrarian industrial hall could contain up to $22 * 550 * 10.000 = 121$ million kg of steel. Holland and Eldik note that about 77% of the steel's weight is part of the loadbearing structure, resulting in $0.77 * 121 = 93.6$ million kg of steel structural elements that could potentially be reused. To put this into perspective: that is enough steel for approximately 1.8 million metres, or 1.800 kilometre of IPE300 profile, stretching all the way from Delft to Lisbon, Portugal. If reuse could be implemented on 100% of the steel, 2 billion MJ (5.5 million kwh) of embodied energy could theoretically be saved.

From the background research (chapter 2), the following problems are identified:

- The construction sector is a very linear sector
- Reusing structural (steel) components is a niche
- The stock of industrial buildings expected to meet their end-of-life phase on a short term will end up being demolished, wasting embodied energy, if no proper plan to reuse elements is provided
- Information on reclaimable elements is limited and often available too late in the design process.

1.5 Objectives

This specific case of industrial structures being taken down can be put in a broader context; when aiming for a circular economy, one should not only focus on ensuring newly introduced materials stay in the loop, but also find ways to use what has already been used and produced. The process of seeking construction materials and components from buildings already existing is often referred to in literature as 'urban mining' (Iacovidou & Purnell, 2016). This might sound like a relatively new and modern concept, but seemingly is a lost art as Bertino et al. (2021) points out the ancient Romans already applied it. As national and supranational institutions want the construction sector to shift in a circular direction it is time to reinvent urban mining for the 21st century. The upcoming availability of these agrarian halls provides a unique opportunity to research the possibilities of mapping out, harvesting, refabricating and reintroducing structural components into a circular construction economy. To tackle the stated problems, objectives are set which this research paper intends to deal with:

1. Provide information on reclaimable components early in the process
2. Develop a tool to analyse the industrial building stock on structural reuse potential
3. Introduce a framework that will help to make the reuse of structural elements from large industrial buildings common practice.
4. Evaluate both the tool and the proposed framework from multiple perspectives

In order to meet these objectives, the research central to this paper is conducted, providing a broader perspective on why these problems occur and how to tackle these problems to reach the set objectives. The following research is attempted to be answered:

'How can structural steel elements of industrial buildings be analysed and mapped out in order to be introduced in a circular urban context?'

The following sub-questions were developed to support the answer to the research question:

- *What are current barriers for steel reuse to become common practice?*
- *What is the economic and environmental benefits of steel reuse?*
- *How can industrial buildings be analysed to provide the necessary data for potential reuse?*
- *What data is required to predict the available steel in a hall?*
- *What sources of data are available?*

1.6 Scope

Several factors impact the scope of this research paper. The four most important factors are listed down below:

1. Time span: >2035

As the nitrogen-oxide problems have created an urgent crisis, the scenario of this research is focused on the short term. This is based on the assumption that the government cannot wait too long with buying out agrarian industries, as the consequences of the court ruling have such a large impact on the country. This means current methods of reusing and recycling construction components are considered, as well as contemporary steel production processes.

2. Building type: Agrarian hall structures

Although the need to reuse materials is relevant to all sort of building types, this thesis will focus on portal hall structures, especially in the agrarian sector. This is partially because of the nitrogen oxide-crisis context, but also to properly limit the range of building properties the tool needs to be able to cover. This will help to make the tool more specific and accurate as it can be tailored to the agrarian hall and take into account the variations that occur within this building typology.

3. Country: The Netherlands

Portal hall structures are used in the agrarian sector on a global scale. However, the design requirements and regulations concerning these halls will differ per country, and sometimes even per region. Therefore the scope of this research is limited to the Netherlands, taking into the design standards and requirements that apply there. Secondly, the urgency to close farms because of nitrogen is currently a Dutch issue – other (European) countries do not have such urgent nitrogen-oxide related problems. Lastly, the Netherlands has a lot of relevant data available. Various data

sets are publicly available and contain data that can be useful setting up this tool. This data might not be available in other countries.

4. Components: Structural

Every building consists of a number of components that have a different function. These components can be categorised based on their function, resulting in:

- Façade components
- Structural components
- Installations

All of these subcategories can be analysed for reuse and should be taken into account when deconstructing and reusing building components. Some new buildings are given material passports listing all the components it is made of (Madaster, 2022). However for existing buildings these passports seldomly exist. As threequarters (Holland & Eldik, 2007) of the steel present in agrarian halls is part of the loadbearing structure, for this research focussing on the load bearing structure seems to be the most effective approach.

1.7 Approach & methodology

For this research paper, various information sources are intended to be used. The goal is to create a mix of both theoretical knowledge - especially on the material, component and structure level – practical experience from stakeholders and

1.7.1 Literature review

The literature research focused on 5 main topics. For each of these 5 main topics, various subtopics have been selected to specify what is aimed to support answering research questions with the literature research. The literature research should provide a basis to develop and evaluate the analysis tool. The various topics considered in this literature review are included in Table 1.

1. Circular Construction Economy	2. Material (Steel)	3. Steel reuse	4. Industrial Halls	5. Standards & Formulas
Why circular?	Performance	Case studies	Types	Eurocode
Current situation	Environment	Systemic studies	Design Requirements	Hall design guides
Circular strategies	Production	Current statistics	Structural properties	Steel grades
Recycle vs. Reuse	Properties	Reuse considerations	Count/location	Eco-analysis
Circularity & steel sector	Economy	Barriers		Cost-analysis

Table 1 - topics for literature review

1.7.2 Case Analysis

Central to this thesis is a case study. The case study involves a selection of agrarian halls, which are analysed to get an understanding of what kind of steel components can be expected to come from these halls once they are taken down. The findings from the case study will help to develop the criteria for the tool. Above that, the cases can function as a test case for the tool, evaluating its applicability, its effectiveness and its accuracy. It is important that the cases are diverse, covering a range of different hall setups (e.g. asymmetrical, different location, animal type). This is crucial to ensure the tool does not get too specific for one hall type.

1.7.3 Research by Design

A tool will be developed to reverse-engineer and analyse existing structures. During the development, the tool will be extended bit by bit, with the goal of evaluating and improving the results and ensuring the tool is applicable to as many situations as possible. Although this does not immediately sound like a design process, it resembles the iterative nature of one. The main goal of apply this method is to:

- Evaluate and improve the accuracy of the tool
- Extend the applicability of the tool
- Improve the tool's efficiency

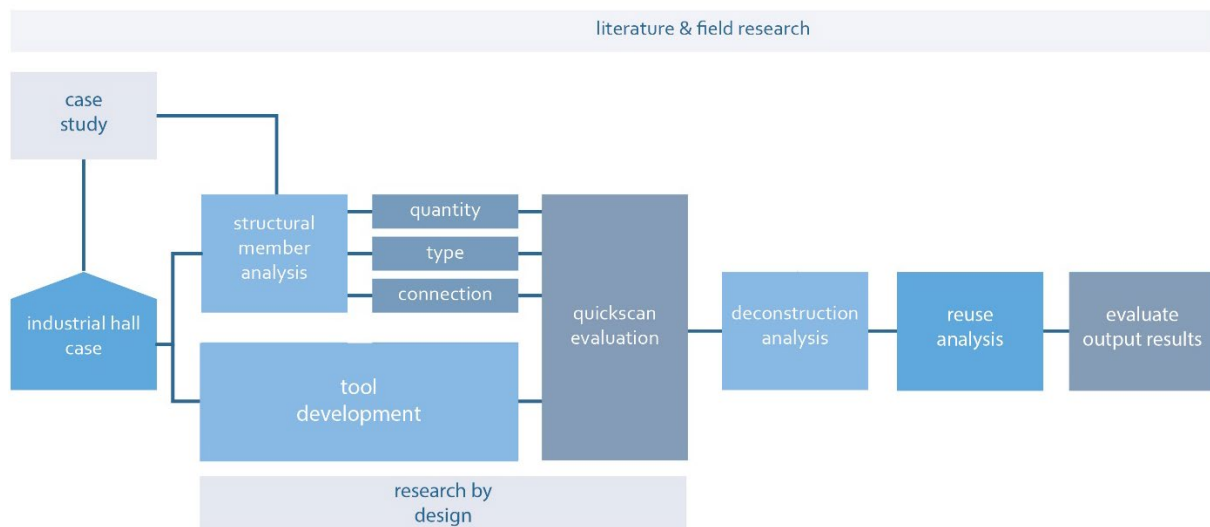


Figure 1 – research setup

2. BACKGROUND

This chapter aims to provide the background information that is needed in order to develop the analysis tool. The building type, material properties, circular strategies and reuse potential are discussed in this section.

2.1 Typology – Megabarn

The halls this research is focussed around are categorized as mega-barns. Although the analysis and quick-scan that will be developed could cover smaller industrial halls as well, the ongoing nitrogen-oxide crisis creates an urgency to focus on these larger halls first as they are most likely to be taken down in the near future, thus requiring a plan of action to stimulate the reuse their structural components.

2.1.1 Definition

An agrarian company is considered to have a mega-barn when it has room for at least the following populations of livestock given in Table 2. In order to keep such populations, a hall of 10.000-12.000m² is required to provide enough space to comply with the animal welfare standards set by the government (Nieuwenhuis, 2019). The reason for these properties is that 10-12 hectare is the area of a standardized agrarian plot – making optimal economic use of the available space. An important note here is that a 'mega barn' might consist of a collection of halls that are built side to side. Nevertheless, there are examples of singular halls covering the 10-12 hectare.

Count	Animal type
120.000	laying hens
220.000	broilers
7.500	meat pigs
1.200	breeding pigs
1.250	veal calves
250	dairy cows
1.500	goats

Table 2 - animal count, based on: Wakker Dier (2022)

2.1.2 Megabarns in figures

According to Wakker Dier (2022), the Netherlands has over a 1.000 of these mega-barns in operation across the country, with about a quarter of them located in the southern province of Noord-Brabant (see Figure 2). Contrary to what would be expected regarding the ongoing developments concerning nitrogen-oxide emissions, the number mega-barns in the Netherlands has steadily grown in the last decade. About 54% of all the mega-barns are used for dairy cows and veal calves, 29% is used for pig farming, and about 8-9% is used for poultry and goats respectively.

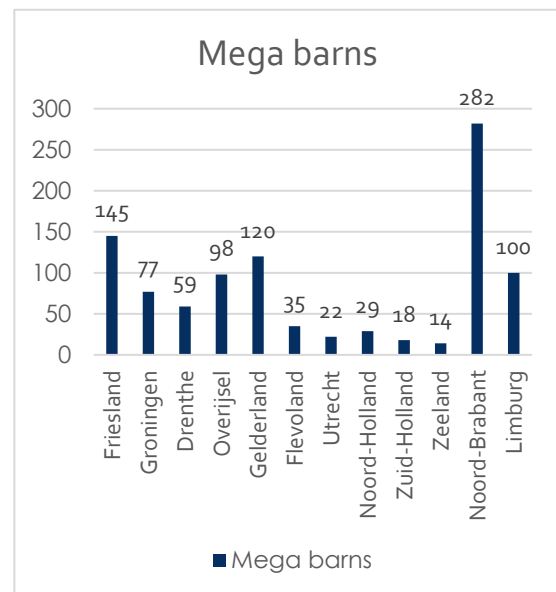


Figure 2 - megabarns per province based on: Wakker Dier, 2021

The hall typology can differ per animal type. For laying hens and broilers, and sometimes even for pig farming, it possible to introduce multiple floors, creating even more farm space on every square meter of available land. The effects of different typologies on the structural behavior will be discussed in more detail.

2.2 Typology – Portal hall

2.2.1 Structural Setup

Around 90% of all the (industrial) halls in the Netherlands are designed as a portal structure (Hollander & Eldik, 2007). This means the span in width is made by a structural portal and the portals are repeated on a (often fixed) distance from each other in the length direction, creating an unobstructed open space underneath the portals. Facades and roofing span from portal to portal. Figure 3 shows a simplified diagram of different portal structure. Depending on the functional and aesthetic requirements, the roof can either be flat or pitch. An overview of possible hall shapes can be found in Stalen Hallen (Barendsz et al., 2019). In the agrarian sector, pitched roofs are most common, in part because they refer to traditional stables.

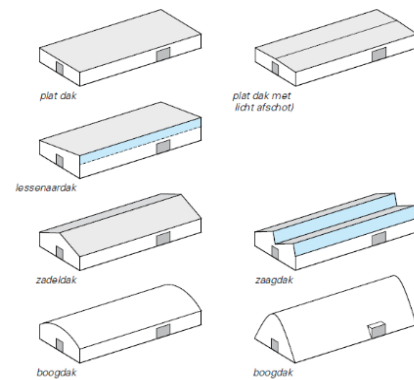


Figure 3 - roof typologies (source: Barendsz et al., 2019)

2.2.2 Structural Elements

Due to the cross sectional properties of steel beams, columns of portal structures are generally HEA profiles, whereas the steel girders are IPE profiles (Oosterhoff, 2013). The sizes of the cross section depend on various factors: maximum span, spacing between portals, mechanic typology and weight of the exterior cladding (Hollander & Eldik, 2007). According to an analysis by Casadata (2017), the most commonly used steel beams used in typical barns are:

- | | | |
|----------|-----------|----------|
| - IPE160 | - IPE 200 | - HEA120 |
| - IPE180 | - IPE 220 | - HEA140 |

However, larger profiles up to IPE600 are used, generally in cases of larger spans, high wind loads or special cases. In some cases standard profiles do not suffice, for which the use of steel trusses can be a solution. This is not considered an option for pitched roofs. According to Hollander & Eldik (2007), on average 77% of the steel used halls is part of the main load bearing structure, either as a column or as a girder. However, these structural elements only make up about 7-8% of the investment cost for a steel hall.

2.2.3 Mechanics typology

There are several ways to mechanically construct a steel portal, but a different static set-up has a large influence on the forces acting on the portal. In principal, there are 4 ways to set up a portal for a steel hall, of which diagrams are shown in Figure 4.

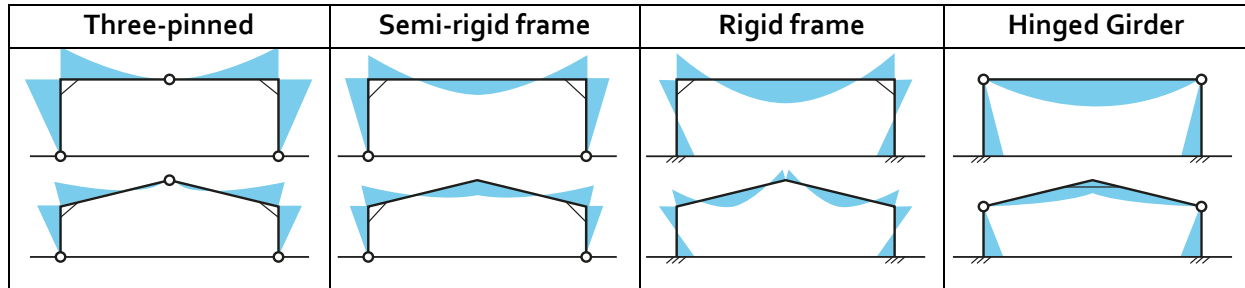


Figure 4: static setup portals, based on: Hollander & Eldik, 2007

The diagrams show that the mechanical setup of the portal defines both the location as the intensity of the maximum moment that occurs. This dictates the profiles that are used, the connections between elements that are applied and the spacing between the portals.

2.2.4 Design requirements for portal structures

Load bearing structures of portals have to meet certain structural requirements set by national standards. These requirements have been taken into account during the design phase and have strong influence on the structural elements that were chosen for the final design. Understanding what these requirements are can therefore be useful to be able to predict what elements can be retrieved from deconstructing the structures. The requirements are defined in two different categories: Ultimate Limit State (ULS) and Serviceability Limit State (SLS). The ULS is about the limit of loading at which a given material fails and breaks, whereas the SLS is about the limit of bending or deformation that is considered to be serviceable (Bekaert, 2020; Arends, 2020).

The ULS is defined by the maximum stress that occurs in a beam or column. Stresses are caused by normal forces, shear forces and moments that occur because of the loads acting on structural members. For steel structural members, the maximum stress that is allowed to occur at the ULS depends on the steel class that was selected. For most construction projects, either S235, S275 or S355 is chosen, where the 3-digit number indicates the ULS-stress in N/mm². For structural members, the length and the section modulus define the maximum stresses occurring. For columns, the risk of buckling also needs to be taken into account. Buckling occurs at once when axial forces exceed the limit, so safety margins here are relatively large.

The SLS is defined by the maximal deformation that is allowed. This is defined according to standards and depends on the length of a member. The main properties of a structural member that are relevant in designing for the SLS are its length and the second moment of area of the cross section. A large second moment of area indicates a higher resistance against bending. Formulas used to calculate the ULS and SLS are added to the appendix (A). Figure 5. displays the various load cases that can act upon a portal structure. These load cases are

caused by the deadload of the structure, wind and snow. Deadload is always present, but snow and wind load vary throughout the year and can even coincide. A structure needs to be designed to be able to handle these combined load scenarios as well. For steel halls, various load case combinations need to be considered (Hollander & Eldik, 2007), these combinations can be found in appendix A. Agrarian halls are considered to be a buildings of the lowest safety class (CC1) because in case of structural failure, only animals are endangered and the eurocode regulations regard the loss of animal life as an economical loss, which is not similar to the loss of human life.

BG1 is structure related, BG2 is a standard set for all of the Netherlands, however BG3, 4 and 5 are influenced by the location of the structure as well as the height. Values for wind calculations can be found in *kracht+vorm* (Oosterhoff, 2013) and are added to the appendix (B). For each of the load cases, the required safety margins have been included – providing the load cases for which the portal structure will have to be designed.



Figure 5: load scenarios, based on: Hollander & Eldik, 2007

2.3 Construction Steel

As construction steel is the main material used for loadbearing structures of agrarian halls, a broader material perspective is discussed in this section. Steel is looked at on a global level, on a component level and on a material level and from an environmental, economic and circular perspective.

2.3.1 Global production

Iron ore is the main ingredient needed to produce steel. Globally, about 2500 Mt of iron ore is mined from quarries each year. Figure 6 shows a map of the annual output of iron ore on a global scale. Australia is a main supplier of iron ore, producing 900 Mt annually (34,6%), followed by the BRIC-countries, who together have a similar share of production (US Government, 2022). Iron ore is then treated in production plants and converted into crude steel, that can be used for multiple purposes.



Figure 6: iron ore production worldwide, source:

According to the World Steel Organization (2021), around 1900 megaton of crude steel is produced annually. Major steel producing countries are China, Japan, India, the USA and Russia. It must be noted that China, number one crude steel producer, is responsible for almost 55% of the annual crude steel production – producing 10 times more than India, being number 2. Europe as a whole has only 10% of the

production share. About 52% of the world crude steel production is used for infrastructural purposes. This includes buildings, transport and energy systems. As the world population is expected to grow with another 2 billion people over the next two decades, this share is expected to increase. In the Netherlands, about 900.000 tonnes of structural steel is used every year, and an added 550.000 tonnes is used as reinforcing steel bars (Blois, Korevaar & Blok, 2019).

2.3.2 Production process

In Figure 7 the process of steel production is depicted. There are two main types of steel production; oxygen steel making (70,8% of global production; World Steel Org. 2022) and electric arc steelmaking (28,9% of global production; World Steel Org. 2022), see also Figure 8. In both cases, a mix of iron ore, coal slack and scrap metal is melted in a furnace. The contents of the mixture and the purity of the ingredients have a strong influence on the properties and the quality of the material being produced. The mixture is melted at a temperature of approximately 1.600 degrees Celsius (Britannica, 2022). The hot, liquified mixture is then poured out over rollers, forming blooms, billets and slabs. These elements are then further shaped by hot- and cold-rolling, forming plates, rods, bars, tubes and profiles that follow industry standards.

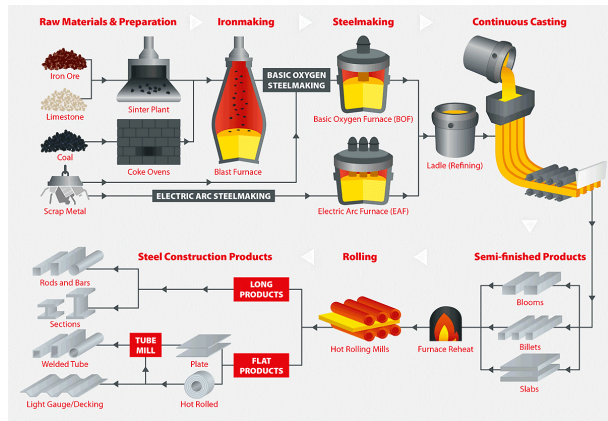


Figure 7: steel production process, source:

There are four main types of industry steel available (HQTS, 2022):

- Carbon steel: Mostly iron, maximum of 2% carbon, few other minerals
- Stainless steel: Iron, 10%> chromium, rust resistance
- Alloy steel: Specific combination of materials to perform certain duty
- Tool steel: 75% scrap steel, often heat strengthened

Carbon steel is the most commonly applied steel in the construction sector. It contains up to 0,3% of carbon. The production of this steel is a very energy-intensive process, due to the high temperatures that are required to melt the steel. This translates into a high level of embodied energy for steel. Table 3 shows that steel has one of the highest embodied energy levels per kilogram of all building materials, even with the average recycle rate (80%) included. The longer lifespan of steel adds some nuance to the embodied energy impact to some extent, reducing the average amount of embodied energy per year of service closer to the levels of concrete (Neenu, 2022). The benefit of reuse over recycling becomes clear as well; for every time that steel is recycled, about 16-20 MJ of energy per kg has to be added again, whereas for reuse, 0 MJ is added.

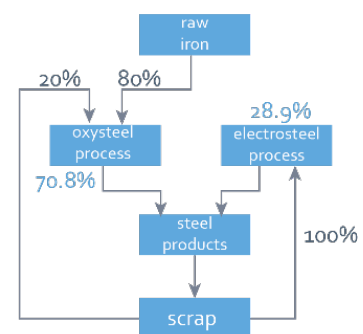


Figure 8: steel production processes, based on: Bouwen met Staal, 2019

Material	Energy MJ/kg	Carbon co ₂ /kg	Material density kg/m ³
Aggregate	0.083	0.0048	2240
Concrete (1:1.5:3)	1.11	0.159	2400
Bricks (common)	3	0.24	1700
Concrete block (medium density)	0.67	0.073	1450
Aerated block	3.5	0.3	750
Limestone block	0.85		2180
Marble	2	0.116	2500
Cement mortar (1:3)	1.33	0.208	
Steel (general, av. Recycled content)	20.1	1.37	7800
Stainless steel	56.7	6.15	7850
Timber (general, excludes sequestration)	8.5	0.46	480–720

Table 3: embodied energy of construction materials, source: Bath University & Neenu, 2022

The steel industry itself is looking for ways to reduce the impact on the environment. A promising technique is to use hydrogen as fuel source in order to melt the steel, instead of coal which is now the most commonly used fuel for steel production (Liu et al., 2021). However, this method is still in development and being researched after and requires a hydrogen energy infrastructure to really take flight. Tests have been executed with a hydrogen powered steel plant in Norway. Although technically feasible, experiments and calculations show a 40% increase in cost compared to the regular oxysteel process (Bhaskar et al., 2022). This goes to show that hydrogen steel, though promising, is still relatively far away from commercial viability. Therefore the standard production methods of steel are considered for the rest of this research paper.

2.3.4 Properties

A small overview of the different properties of (construction) steel is given in Table 4.

Material Property	Value
Density ρ	$\approx 7850 \text{ kg/m}^3$
Unit weight γ	$\approx 78.5 \text{ kN/m}^3$
Modulus of elasticity E (Young's modulus)	210000 MPa
Shear modulus G	$G = E / [2 \cdot (1 + \nu)] \approx 81000 \text{ MPa}$
Poisson's ratio in elastic range ν	0.30
Coefficient of linear thermal expansion α	$12 \times 10^{-6} \text{ }^\circ\text{K}^{-1}$

Table 4: steel properties, source:

Some of the properties, such as the yield strength differ per class of steel. As this research is focussed on the construction sector, only steel classes commonly find in that industry will be discussed. Different steel classes are listed in Table 5. Most European countries, the Netherlands included, follow the European EN standard to define the steel grade. The most commonly applied steel in the construction sector is S235JR (Vanilla Steel, 2022).

Steel Class:	S235	S275	S355	S450
Yield strength	235	275	355	440
Ultimate strength	360	430	490	550

Table 5: steel strength classes, source:

2.4 Circular Strategies

Shifting towards a circular construction economy requires implementing strategies that will help to close the loop. The Ellen McArthur foundation published the *Butterfly Diagram* in 2019, showing how these different strategies add to an economy that will optimally make use of the materials that are introduced. The following strategies are distinguished:

1. Recycle
2. Refurbish/Remanufacture
3. Reuse/Redistribute
4. Maintain

Each of the strategies is applicable to products and materials that circulate in the global and local economy. As this thesis focuses on material reuse, the maintain strategy is not discussed as it does not involve applying any material in another project.

2.4.1 Recycle

In the case of recycling in the construction industry materials are retrieved during or after the demolition of a building. The state and quality of the retrieved elements is secondary here because the components are broken down to raw materials, which are then shaped into new elements, sometimes with a completely new purpose. In this way, the materials are kept in the loop and do not end up at landfills or incineration plants (Allwood, 2014, EMF, 2019). Recycling can be closed-loop, but more commonly occurs as an open-loop process (Huysman et. al., 2015). In a closed-loop process, the materials being recycled retain their qualitative value (or even gain value by the process of upcycling) whereas in an open-loop process, the recycled material is used in a new situation with lower requirements as the material's quality degraded. Although closed-loop recycling is considered to be completely circular, there are considerable downsides to the strategy of recycling. Extra energy needs to be introduced in order to transport and reshape these materials (Thormark, 2001, WRAP, 2008). This heavily depends on the material, the requirements for the new product after recycling and the distance of transport (Iacovidou & Purnell, 2016). In some cases the environmental benefits of recycling can become nihil, making almost no impact but being more expensive than regular demolition (Mahpour, 2018). In the case of open-loop recycling, a term that is often used is downcycling. Helbig et. al. (2022) defines downcycling as *'the phenomenon of quality reduction of materials reprocessed from waste relative to their original quality'*. This open-loop recycling is common practice in the construction sector (Cowther, 2018), however, does result in a loss of (economic) value of the material and still requires new functional construction elements and materials to be introduced that do have these intrinsic qualities. Allwood (2014) therefore calls the practice of downcycling *'fundamentally wasteful'* stating that materials should better be kept in their high-quality state – downcycling should only be seen as an option of last resort.

2.4.2 Reuse/Redistribute

In a building component reuse strategy, elements are removed from a structure and used in the same way for another project (Bertino et al. 2021). Components generally do not require any processing to take place to be applied in a new project (Xing et. al., 2020). A reuse strategy aims to extend a construction element's lifespan further than that of the building it was a part of and therefore helps to keep the materials in the loop. The main benefit of reusing components is the embodied energy that has been put into the component is being exploited as much as possible (Tingley & Davidson, 2011). Instead of introducing new embodied energy into forming a new product, the energy can be saved by using components that have already been produced for earlier projects. The extra energy that is used in the process of reusing is for the transport of components to and from the storage location. For new designs, various strategies can be applied to deliver buildings which components are relatively easy reusable; design for deconstruction (DfD), design for reuse (DfR) and design for manufacturing and disassembly (DfMA) are examples of such strategies (Iacovidou & Purnell, 2016). Once components are introduced into the cycle, one needs to keep track of them to know when materials become available (Xing et. al., 2020). To apply a reuse strategy on a broader scale, material databanks need to be introduced to keep track of materials that are in use (Kim et. al., 2020). Producers of building materials can provide the elements, but it offers the opportunity for them to also offer lifespan extending services. It would be possible for companies within the industry to remain the owner of the product in a system that is called 'operational lease' (Ploeger et. Al, 2019). A practical example of this strategy is a system called ClickBrick (Wienerberger, 2016). This façade system is designed in a way that the bricks used for the façade can simply be removed and reused in the same way in another project without any mortar to deal with. In the case of ClickBrick, after a period of use, the company purchases back the bricks for a fraction of their original price. This is based on an evaluation of the remaining quality of the bricks and the duration of the use (Wienerberger, 2020).

Reusing building structures can basically be achieved in three different ways according to Gorgolewski (2008):

1. Leave the loadbearing structure in place and transform its function, retrofitting it
2. Deconstruct the loadbearing structure, set it up exactly the same way on a new location
3. Deconstruct the load bearing structure, salvage the individual components and reuse these components in a variety of new projects

As mentioned earlier, the case of industrial halls that is central to this thesis, does not allow for the first method of reuse to be implemented, as a functional transformation is almost impossible due to the configuration and location of the structure. The second method is practically feasible and might in some cases be desirable. Companies like Portal Power are specialized in re-selling portal structures, both on location or by transporting the portal structure to a new location (within the UK). The

third method allows for reuse in another context and will therefore be the method of reuse this thesis will continue to focus on.

2.4.3 Refurbish/Remanufacture

In the strategy of remanufacturing, components are removed from the structure and transported to the manufacturer where the product is brought back to its original state, sometimes even being improved (Ijomah, 2010). The process of remanufacturing can save both energy and financial resources (Seitz & Peattie 2004; King et al. 2006)). According to King et al. (2006) the process of remanufacturing only requires 20-25% of the energy that manufacturing new components would require. In order for remanufacturing to be properly implied, components need to be designed with the remanufacturing process in mind (Yang et al., 2015) often referred to as design for remanufacture (DfRem). According to Ijomah (2010) products that are designed according to DfRem principle can be easily disassembled without damage to the product that affects its functional performance. In practice this leads to components that exist of core elements, which can be stripped, cleaned, sometimes slightly repaired to then be put together to be applied again. 2. Although remanufacturing allows for more control over the quality of the end product, it is the most complicated of the three circular strategies discussed here. The need for refurbishment can vary per element that is brought back to the manufacturer, thus making it more labour-intensive and in some cases therefore cost in-efficient (Hatcher et. al., 2011). Other factors according to Hatcher (2011) that can negatively influence the effectiveness of remanufacturing components are:

- Materials in core elements that can break can make remanufacturing impossible
- Component joints and connections that make disassembly practically impossible
- Cost-raising features regarding remanufacturing (materials, knowledge, labour)

2.4.4 Strategies compared

All of the mentioned strategies are nowadays more or less implemented in new products, services and materials that are introduced to the economy (CBS, 2020). It is considered to be much more difficult to implement these strategies to products that are already designed, produced and used, as these were not necessarily designed to be circular. In the construction sector, the terms of urban mining or urban harvesting (Cossu & Williams, 2015) are used to describe processes and methods that go and search for circular opportunities in the built environment. Although applying any of the aforementioned strategies is considered to be a circular approach, reuse is in essence more circular than recycling and refurbishment (EMF, 2019; Geyer et al., 2002; WRAP, 2008). This is the reason why the European Waste Framework Directive (2015) prioritizes reuse of waste over recycling whenever technically feasible and financially possible. In some situation, products and materials do not lend themselves well for reuse – when components are non-retrievable, break during deconstruction or have no demand in being reused, it is still better to recycle than to have it end up at a landfill. The hierarchy between circular strategies is often visualised using the so-called R-ladder or R-pyramid. This ladder shows which circular strategy is preferred

above the others. Each step up the ladder requires less material and embodied energy input - resulting in a smaller eco-impact during the manufacturing process. Figure 9 shows the R-pyramid, Figure 10 the R-ladder.



Figure 9: R-pyramid, source: Cattermole Consulting



Figure 10: R-Ladder, source: Cattermole Consulting

Both the ladder and the pyramid show two extra circular strategies: reduce and refuse or prevention. These strategies refer to the (questionable) need for new products. Better than to use reused or recycled products, is not using any material at all. For the construction sector, this strategy translates to the transformation and repurposing of structures that have met the end of their user-life-cycle but have not met their functional end-of-life stage. As mentioned before, these strategies do not apply to industrial halls due to their properties. Within the steel sector, about 95 percent of the reclaimed materials is being recycled, and only 5 percent is being reused. This goes to show that within the steel construction sector, there is a lot of potential to improve the circularity of the industry by shifting from recycling to reuse, climbing two steps on the R-ladder. Shifting from recycling to reuse in the steel industry would mainly result in savings regarding the added embodied energy of the steel that is being drawn out over a longer service life rather than having to keep adding extra energy at every recycling cycle.

2.5 Steel Reuse

The following section contains a literature review on reuse in the specific case of construction steel. Current practice, methods and theories will be discussed, as well as barriers currently preventing reuse from becoming a mainstream method.

2.5.1 Current Status of Steel Reuse

The steel sector tends to proudly put forward that it is a circular sector that keeps almost all the material in the loop. Sources point to about 99% of the raw material being kept in the loop (Construction Steel Info, n.d.). This indeed can be considered than other construction material sectors, such as concrete (20% recycle; 75% downcycle) and timber (13% recycle; 13% reuse). Clear data is hard to find and can differ strongly per country, but somewhere between 6 and 10% of reclaimed steel is reused, and the other 90-94% recycled (Hopkinson et al. 2019; Geyer et al. 2002). Only 1% of steel ends up on landfills (see Figure 11). The

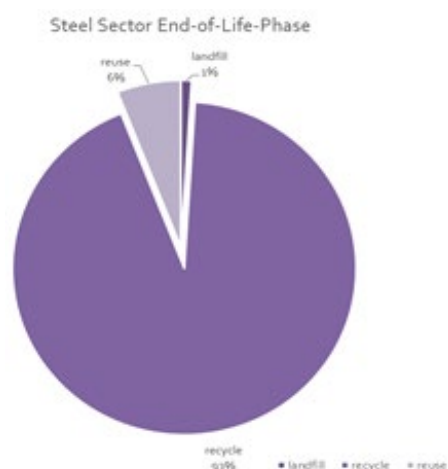


Figure 11: Steel sector end-of-life phase, source:

problem with recycling steel, as mentioned before, is that in order to melt steel and shape it into a beam again, a lot of energy has to be introduced. According to reclaimed building products manual by WRAP (2008) various types of steel building components can be worth reclaiming. Structural steel, tubes, plates and bars, metal cladding, fencing and portal frames are all elements that can be reclaimed and will most likely have a cost saving effect and are all labeled to have 'some availability'. It has to be noted that this goes for UK construction projects, the cost effectiveness and availability can differ per country (Gorgolewski & Morretin, 2009).

2.5.2 Considerations for Steel Reuse

The reuse of structural components is possible, but not yet common practice in the building industry (Gorgolewski, 2008; Huuhka & Hakanen, 2015). It is therefore important to analyse the barriers that keep component reuse from being a more widely applied strategy and to get clear what challenges might come up during the process of reusing components. Geyer et al. (2002) applied a systemic analysis, using a simplified model of the steel construction cycle to identify why reuse is currently uncommon practice. In an ideal scenario, where technical feasibility and market demand play no role, both cost and energy are maximally saved when 100% of components is reused and 0% recycled. However, in reality both technical feasibility and market demand influence the share of components that can actually be reused. This leads to the following scenarios as displayed in Table 6.

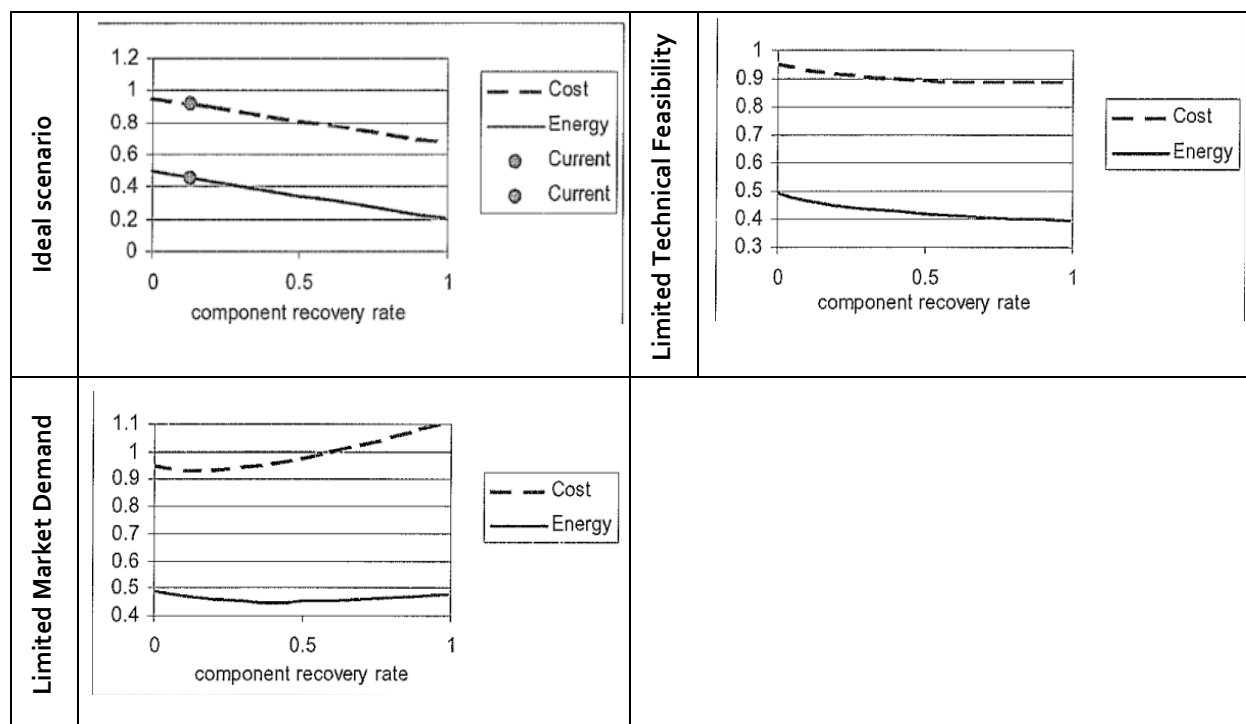


Table 6: steel reuse scenarios, source: Geyer et al., 2002

Given that both LTF and LMD scenarios occur in real-life, financial incentives become the main bottleneck, keeping the reuse share low (20% max) as LTF and LMD cause different points of optimum. Most barriers for steel reuse becoming common practice that can be found in literature revolve around the issue of technical feasibility [T] and

the issue of market demand [M]. In a study by Tingley et al. (2017) into the barriers regarding steel reuse, the following six barriers were found to be most present among stakeholders in the industry:

- Lack of client demand [M]
- Lack of supply chain coordination and integration [M]
- Storage of recovered materials
- Construction sector inertia [M]
- Lack of information about existing structure and materials [T]
- Jointing technique [T]

These six barriers act on different levels in the industry – on a design level, on an economic level and on a system level – and show the complexity of reuse in practice, both technically and market-wise. According to Huuhka & Hakanen (2015) add to this stating that the barriers for steel reuse on a component level revolve around cost [M], quality [T], quantity [M&T], perception [M] and trust [T]. So apart from the technical side and the market side, barriers can also be identified on system-level and component-level. Gorgolewski and Morretin (2009) go into more detail regarding the practical process of structural component reuse within a design project, putting forward three aspects to consider:

1. Responsibility of providing and sourcing materials.
2. Procedures for grading reclaimed components need to be established and regulatory frameworks need to be researched.
3. The economic (dis)advantage of using reclaimed components is a complex balance between saving material cost but added costs because of labour.

In another research paper, Gorgolewski (2008) adds that including salvaged components in a design project requires a different design approach because of the unexpected nature of reclaimed materials; the supply of available material might not match with the dimensions or quantities a specific design requires. Therefore a flexible

design strategy is required. Being able to gain accurate information about the

availability of reclaimed components early in the design process can help to adjust the design to include reusable materials. Figure 12 summarizes of all the different barriers that can be encountered while aiming to reuse steel components in construction projects. The barriers occur on a systemic level and on a component level and regard either market demand or technical feasibility. Softening these barriers will potentially help to make steel reuse more common practice and enable designer to implement such a strategy in their designs.

	system level	component level
market demand	lack of trust added costs lacking incentive	supply v. demand legal barriers planned availability
technical feasibility	storage & transport regulation & codes integration in design	material loss deconstruction process unknown properties

Figure 12: summary of potential barriers in steel reuse, source: own work

2.5.3 Properties of Reclaimed Elements

Each of the elements that can be reclaimed for the purpose of reuse has properties that define what new cases the elements can be used for. Based on literature (Gorgolewski, 2008; Kim et. Al, 2020; Tingley, 2011) the following properties can be considered relevant for reusing structural steel components and are listed in Table 7.

General	Geometry	Physical	Material
<ul style="list-style-type: none">- Location of elements- Current usage	<ul style="list-style-type: none">-Type: (H/I/C/Tube/Combined)-Section Modulus- Dimensions: (Width/height/length)- Curvature	<ul style="list-style-type: none">- Unit weight- Yield strength- Extension value- Age	<ul style="list-style-type: none">- Chemical composition- Quality- Steel class

Table 7: properties relevant for reuse

The hierarchy of importance of each of the properties differs per case of reuse but in early design processes, the geometric properties, yield strength and unit weight are relevant. Knowing these specific properties early on can benefit designers in implementing reused steel components in their projects (Gorgolewski & Morretin, 2009).

2.5.4 How to Incentivize Steel Reuse

Steps to streamline the process, making information available earlier in the process and good, up-to-date information availability are key factors in making steel reuse more common practice. According to New Steel Construction(2017), or NSC, the following directions need to be taken into account when it comes to structural steel reuse:

1. Provide clear documentation of all steel members used in a structure
2. Keep records of the steel supplied.
3. Steel members should have a permanent marking or tagging

These directions indicate a larger theme that can be found in the literature regarding steel reuse and reuse in general: setting up an economy in which one can keep track of the materials that are in use (Xing et al., 2020; Kim & Kim, 2020). For all three directions provided by NSC, a footnote needs to be added that these directions are much more easily applied to newly introduced elements, rather than to existing structures and components. Fujita et al. (2023) add to this that to promote steel reuse research needs to establish a procedure to quantify the remaining structural performance, properties and quantities of reclaimed steel and ensuring it is reapplied with connections that can easily be dismantled.

Most of the barriers in steel reuse are there because steel reuse has not been applied numerously yet, and no systems are in place to guide the process. Assumed is therefore that what is necessary to get steel reuse to become more common practice, is a method to kickstart steel reuse. Several issues that now prevent reuse

have to be overcome once - introducing the material into the circular loop. As can be seen in the figure on the right, once these barriers are passed further reuse is becoming easier to implement, thus more likely to become common practice and guidance for new steel reuse projects. Stakeholders in the process should be incentivised to invest in breaking the barriers and setting up the system once, to then profit from the benefits that further reuse offer (see Figure 13).

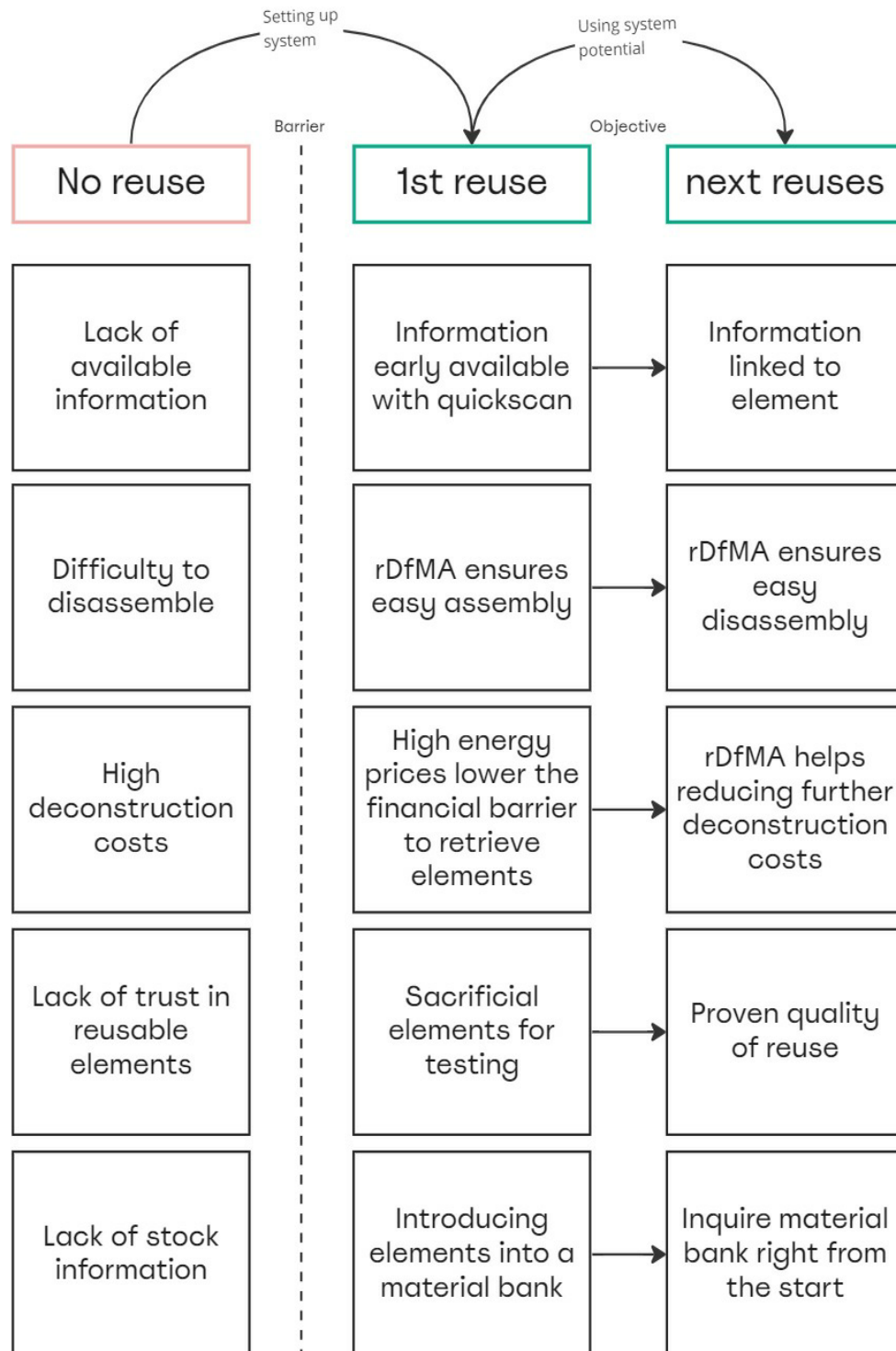


Figure 9: Overcoming barriers in steel reuse, source: own work

3. CASE STUDY

This chapter provides the analysis of the available case material. Various agrarian halls are analysed to better understand what kind of structural components to expect from these halls. The analysed halls will also function as a test cases to evaluate the tool during its development

3.1 Case selection

3.1.1 Available Case Material

Multiple methods of acquiring case material have been employed, however, without the desired result of getting the drawings of an actual mega-barn that is 10.000m². The potential case studies that were found are listed in Table 8. Case G is a collection of 4 different halls on one location, all of which have drawings available. The properties of these halls are listed in in a seperate Table 8a. An extended table including address information is added the appendix (C), the locations of the halls are shown in Figure 14. A separate list of case material sources is added to the reference list (Chapter 10).

case	Type	width [m]	length [m]	height [m]	spacing [m]	symmetrical	drawings/static analysis
A	Pigs	17	122	6,5	4,8	Yes	Both
B	Poultry	30	54	9	4,8	Yes	Drawings
C	Dairy	26	50	8,9	4,6	No	Drawings
D	Dairy	26	50	7,8	5	Yes	Static analysis
E	Dairy	34,5	93	9,8	5	No	Static analysis
F	Veal calves	32,9	70	10	5,4	Yes	Drawings
G	Pigs	-	-	-	-	Yes	Drawings

Table 8: case studies, source: own work

case	Width [m]	length [m]	height [m]	spacing [m]
G1	30,3	160	7,3	5,5
G2	17,1	111	5,7	5
G3	14,8	46,5	5	5
G4	14,8	92,5	5	5

Table 8a: case studies

3.1.2 Case Assessment

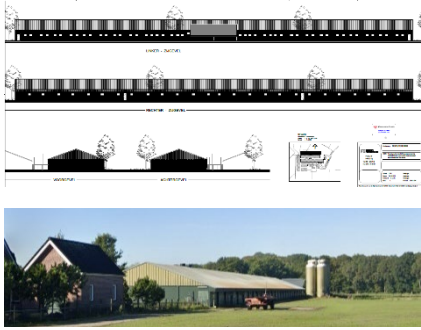

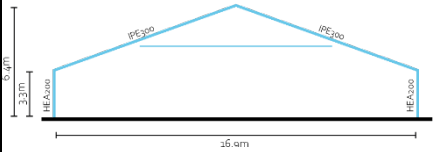
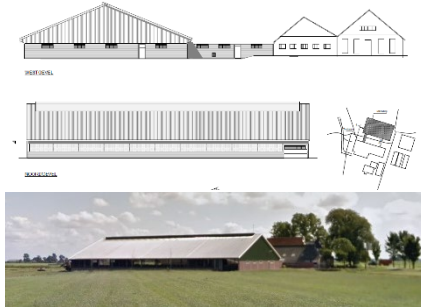

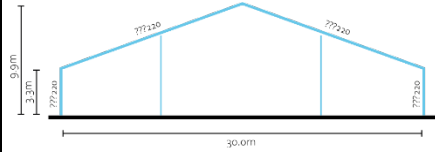
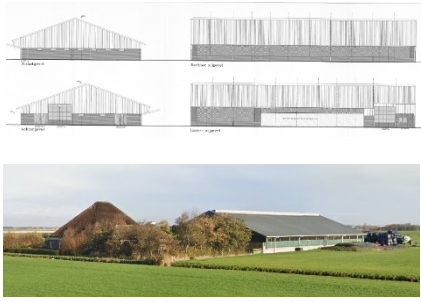
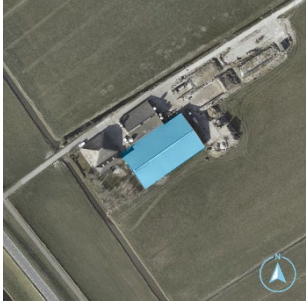
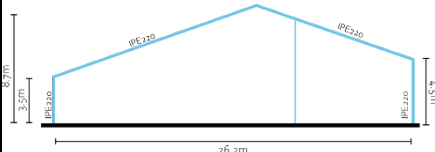

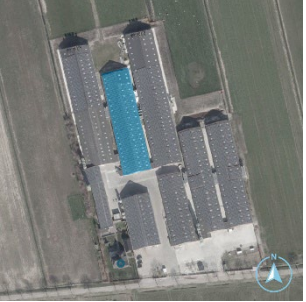
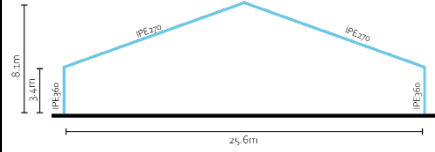

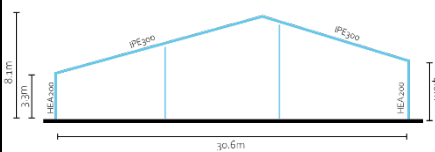
In this paragraph, the various case studies that have been found are assessed based on their suitability to function as a case analysis for the purpose of this research. To introduce each case study, Table 9 gives an over view of the halls analysed for this research. The following factors are taken into account assessing the suitability:

1. Ground floor area
2. Quality of available drawings
3. Availability of information on structural members
4. Resemblance to mega barn
5. Availability 3DBAG data
6. Moment is was found

The first five are related to the structure itself. The last one is not necessarily about the suitability of the hall itself, but the later a case study was found, the lesser it's impact on the research will be due to the time frame in which this research paper has been conducted. The assessment of the cases can be found in Table 10.



Figure 14: location case studies, source: own work

	Drawings/Images	Satellite	Principal Section
A			
B			
C			
D			
E			

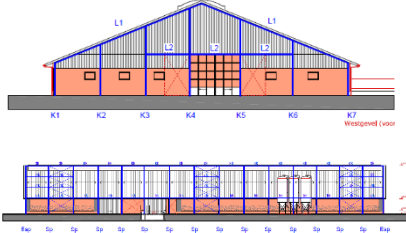
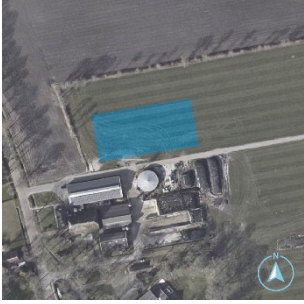
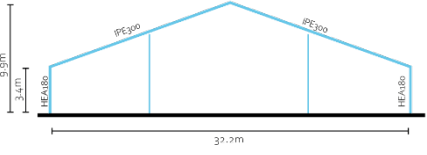
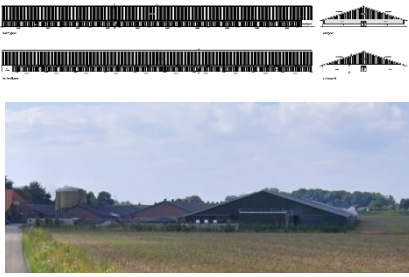
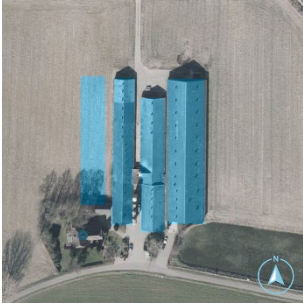
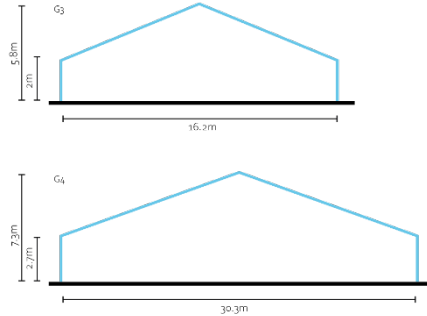
F			
G			
	Image source: Google Streetview	Source: pdokviewer.nl	Source: Own work

Table 9: case studies; images, satellite & principal section, source: various

case	area [m2]	quality drawings	information on structural members	resemblance mega barn	availability 3d data	rating 1-5	found when?
A	2.074	High	Extensive	High	No	4	February
B	1.620	High	Medium	Medium	No	2	January
C	1.300	High	Limited	Medium	Yes	2	March
D	2.340	-	Extensive	Very high	Yes*	4-5	April
E	3.209	-	Extensive	High	Yes	3-5	April
F	2.566	High	Extensive	High	No	4	April
G	8.803	High	Limited	Very high	Yes*	4	May

Table 10: case assessment, source: own work

The assessment (Table 10) aims to give each hall a rating based on the first five assessment criteria. The higher the rating, the better the case fits the scope of the research and the more accurate the results will likely be. The low scores for case B and C indicate that their results might not be fully representative regarding the research's scope. They do not really resemble a mega barn due to their smaller size. However, as they were found early in the process they have been used as early test cases for the development of the tool. For case A, D and E static reports were found, not only providing information on the structural members but also giving insight on the structural calculations that were executed to define the profile sizes. This will help to compare and possibly improve the calculations made by the quickscan tool. Case G poses an interesting scenario where drawings of all four halls on a megafarm are provided. This will help to get an estimate of the amount of steel that can be expected to be reused by closing one megafarm.

3.2 Case Analysis

Each of the selected cases has been analysed in detail and will function as reference structures for setting up the quickscan tool. An overview of the findings from this analysis is included in Table 11. As the quickscan tool will be developed to generate a list of reclaimable steel profiles, a similar list (Table 11a) has been comprised of the data found while analysing these halls.

case	column type	column length [m]	beam type	beam length [m]	n portals
A	HEA200	3.3	IPE300	9.4	23
B	HEA220	3.3	IPE220	15.6	10
C	HEA220	3.5/4.5	IPE220	14.9/12.0	11
D	IPE360	3.4	IPE270	13.5	18
E	HEA200	3.3/4.8	IPE300	17.4/15.0	17
F	HEA180	3.4	IPE300	13.8	14
G1	IPE270	2.5m	IPE300	15.9	28

Table 11: structural elements per case study

For each case an analysis sheet is included in the appendix (D). These drawings are part of the documentation that was found. This sheet shows the analysis of the principal section, floorplan, AHN-section, assumed static setup and connections. A separate table referencing the sources of this documentation is added to the reference list. Based on the analyses, some assumptions can be made that will help to shape the framework for which the tool has to be designed. These assumptions are listed down below:

- Agrarian halls have span of 15-35 metres
- All analysed halls have bolted connections
- Spacing between portals is around 5000mm
- Halls can have secondary elements that might influence the load bearing behaviour, such as extra columns or tension rodss
- Static setup remains guesswork without extra information
- In general, HEA-profiles are used for columns, IPE profiles are used for spanning beams

These assumptions, together with the data gathered from the analyses, will form the basis for the development in the tool, which will be discussed in the next chapter.

case	column type	length [m]	quantity
A	HEA200	3.3	46
	IPE300	9.4	46
B	HEA220	3.3	20
	IPE220	15.6	20
C	HEA220	3.5	11
	HEA220	4.5	11
	IPE220	17.4	11
	IPE220	15.0	11
D	IPE360	3.4	36
	IPE270	13.5	36
E	HEA200	3.3	17
	HEA200	4.8	17
	IPE300	17.4	17
	IPE300	15.0	17
F	HEA180	3.4	28
	IPE300	13.8	28
G1	IPE270	2.5	56
	IPE300	15.9	56

Table 11a: reclaimable elements output list, source: own work

4. QUICKSCAN

The goal is to construct a digital structural analysis model that resembles the structural behaviour of industrial halls and to use this model to reverse engineer the range of profiles that is most likely to have been used for construction. In order to do this, the available data and required input need to be determined. A workflow is set up to determine how the input should be converted to useful output data. Because of the repetitive structural nature of the halls central to this thesis, there is no immediate need for a 3D-analysis and it is assumed that a 2D-analysis will suffice.

4.1 Criteria Quickscan Tool

The main principle behind the tool is to reverse-engineer the required section modulus of the profiles that make up the portal and use these to select a potential profile type, as shown in Figure 15. Combining the profile type with the geometrical properties of the hall will result in a list of structural members, including their length, their quantity and their assumed profile type, which can then be provided to designers seeking to use reclaimed elements. To properly develop the tool, criteria need to be set for the tool to reach.

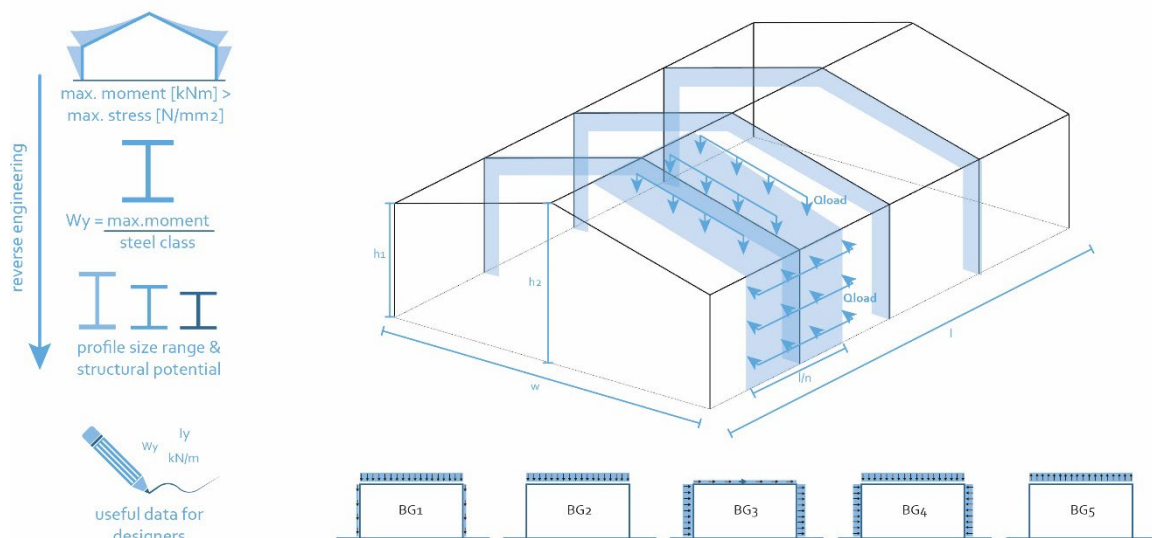


Figure 10: initial idea for quickscan, source: own work

For this research, the objective is set to develop a tool that indicates the profile length, quantity and type of the columns and the spanning beams separately, deviating by a maximum of 1 profile, although no deviation would be preferable. The tool should provide results for HEA and IPE profiles, as those are the profile types found in these structures. All input values should either be definable by literature or by calculation, with data from sources that are publicly available. The tool functions as an indicator, attempting a solid approach rather than a perfect analysis. In case of deviation, underestimating a profile is preferred over overestimating one as potential underperformance of a profile estimated too strong can lead to structural failure in a design. The tool should aim to factor in as much variables as possible, such as steel degradation and material loss due to deconstruction, providing designers with a broad package of information to help inform them to make the

right decision. A list of values is shown in Table 12, indicating what factors should be included in the tool.

Element length	Element type	Element quantity	CO2-savings	Cost savings
Element degradation	Location	Element age	Potential reuse impact	Effects of deconstruction

Table 12: Factors to include in tool, source: own work

4.2 Workflow

In order to set up a proper analysis model, that actually results in output that is useful to the larger scope of this thesis, a flowchart and a model definition will be set up. The flowchart serves as the basis of the model and will show the necessary input, the desired output and the path between the two.

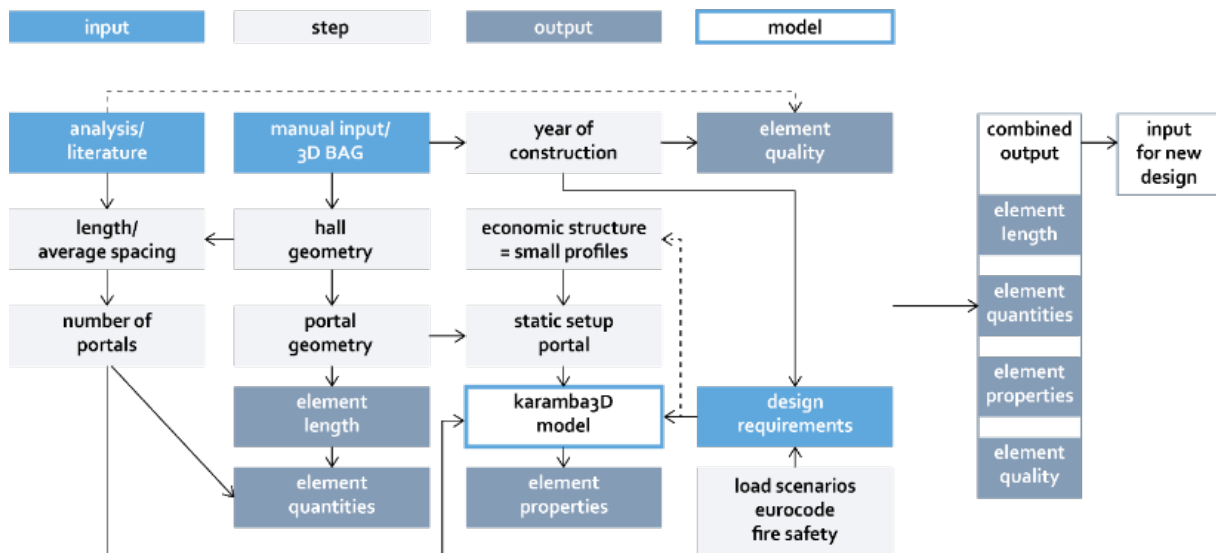


Figure 16: quickscan workflow, source: own work

The workflow is illustrated in Figure 16. The most important input factor is the geometry of the hall itself. This will determine most of the output elements, such as element length and quantity and the setup of the portal. This is also the feature that is least standardized and differs for each hall. The research from literature and the analysis of existing structures function as input to standardize the model. As the goal of the quickscan tool is to get a broad overview of the available structural members, the input for the tool can and should not be too detailed. This means some factors will have to be determined based on assumptions. To make these assumptions as accurate as possible, information from these sources will help to reduce the required input data and will help to make the tool more easily applicable. The last source of input are the design requirements. These define the performance that the structural elements will have to meet and in reverse define the type of elements that can be found in industrial halls. The main function of these requirements is to prevent a structure from collapsing, meaning elements used in the hall – no matter their cross sections, quality and connections – will have the structural performance to deal with these loads, given the structure is still standing.

4.3 Required Data

4.3.1 Internal elements

The required data for setting up a structural analysis model can be divided in two categories; internal and external elements. Internal elements are related to the structure itself, such as dimensions, portal spacing, supports and connections. External factors concern the loads that are applied on said structure – wind, snow and other variable loads. The deadload of the structure itself plays a role as well, however is intrinsic to the internal elements of the model and therefore not considered external.

4.3.2 Internal elements

In order to setup a portal model, the dimensions of a horizontal section of a hall structure are required. For a symmetrical hall, only three dimensions are required to set up a portal. An asymmetrical hall requires a few extra dimensions. For both scenarios, dimensions are given in Table 13.

symmetrical			asymmetrical		
property	symbol	unit	property	symbol	unit
Width	w	[m]	Width	w	[m]
Minimum height	h1	[m]	Position max. height	x	[m]
Maximum height	h2	[m]	Minimum height A	h1.1	[m]
			Minimum height B	h1.2	[m]
			Maximum height	h2	[m]

Table 13: required dimensions to setup symmetrical and asymmetrical portal, source: own work

The data required to set up the section of the portals is available online, from multiple sources. The dimension of a hall can be derived from mapping tools such as Google Earth. Actueel Hoogtebestand Nederland (AHN) offers a height map that covers all of the Netherlands, based on LiDAR data, with a resolution of 8 points per square meter. This data can be used to take a section of a structure and retrieve the outline. This is the data needed to set up the shape of the portal. Examples of this are shown in the analysis of the previous chapter. The AHN data is being updated and renewed and is currently running on what is labelled AHN3. There is an updated and improved AHN4 on its way (Actueel Hoogtebestand Nederland, n.d.; 3D Geoinformation TU Delft, 2021). An even more sophisticated source of data is 3DBAG. This dataset (3D Geoinformation TU Delft, 2021) combines the aforementioned AHN3 height data with BAG-data from the Dutch Register Office, creating a dataset of all Dutch buildings and structures in various level of detail (LoD). The output data of 3DBAG is validated by val3dity with 98%, meaning that 98% of geometries rendered by 3DBAG are valid and actually represent the building volume of the building correctly. In 9.69 million buildings are included in 3D BAG, which is about 92% of all buildings in the Netherlands registered. It is therefore considered a reliable and valid source of input data to generate the hall geometries for the quickscan tool. The 3DBAG data will be discussed in more detail later.

The spacing between the portals defines how many portals the structure contains and how much load is distributed to one portal. There is no direct way to retrieve this information from an online source, apart from some halls showing a visible structure, repetitive pattern in cladding or roof openings. An interior photo could be a helpful resource as well. If the spacing between portals cannot be defined, a well-educated estimate could suffice as the model is not an exact representation but an analytical approximation of the structural situation. On average, the portals for are spaced out 5-6 meters from each other, as result of economic optimization. The spacing distance could further be finetuned given that $n \cdot \text{spacing [m]}$ should correspond the total length of the hall. The number of portals would then equal $\text{length/spacing} + 1$. The structural setup of the portal needs to be defined, selecting support types and connection types. According to Hollander and Eldik (2007), two type of steel connections are relevant: stiff connections and flexible connection. These types are also referred to as fixed connections and hinged/pin connections respectively. Each connection within the portal has to be defined as either one of these options, which influences the structural setup, relating to paragraph 2.2.3.

4.3.3 External elements

The external elements that have to be defined al revolve to a large degree around the load cases (Figure 17). The three main external elements that need to be considered are: wind load, snow load and cladding.

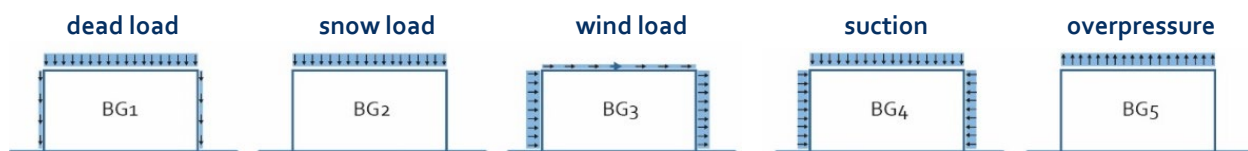


Figure 17: Load scenarios, based on: Hollander & Eldik, 2007

First of all the maximum wind load. This value is defined by three factors: location, surroundings and building height. As the map in Appendix B shows, the Netherlands is divided in three wind regions (I, II, III), with each region having its own specific maximum wind pressures. The surroundings are categorized as coast, open area or built environment. Region III has no values for coast, as these regions are landlocked. The maximum height of the building (h_2) will define the maximum wind pressure exerted on the building in kN/m^2 . A table with these values can be found in the appendix (B). As the shape of the building influences whether wind will act as pressure or as suction, coefficients are applied to correct for this. For pitched roofs, the coefficients are given according to the values provided by Oosterhoff, 2013.

In case of overpressure or suction (BG4 & BG5), the selected value for wind pressure applies as well. However, the direction of the pressure differs from regular wind pressure, and different coefficients apply. TNO (1992) provides formulas to calculate these loads, which are listed in Table 14.

Suction	Overpressure
$C_{pi} = (1,0 - 0,1 \log \frac{V}{A})$	$C_{pi} = -(0,44 - 0,02 \log \frac{V}{A})$
met $0,3 < C_{pi} < 0,8$	met $-0,4 < C_{pi} < -0,3$

Table 14: formulas for BG4/BG5, source: TNO, 1992

Secondly, the snow load needs to be considered. The maximum snow load that needs to be taken into account is uniform for the whole Netherlands and is set at 0,7kN/m² (Arends, 2020). As snow will slide of a sloped roof, the value is multiplied with a coefficient of 0,8; resulting in a maximum snow load of 0,56kN/m². The cladding weight heavily depends on the chosen materials, however from an economical point of view it should be as light as possible – especially when it's only function is to shelter from wind and rain. Table 15 shows the weight of several cladding options (The Steel Construction Institute, 2008). To simplify the model input, the re-cladding weight is categorized as low (0,10), medium (0,20) or high (0,30), values in kN/m² respectively. Medium in this case is considered to be the normal, a higher or lower value can be picked if there is knowledge of the presence of a specifically light or heavy (e.g. solar panels) cladding systems.

	Weight kN/m ²
Steel roof sheeting (single skin)	0.07-0.20
Aluminium roof sheeting (single skin)	0.04
Insulation (boards, per 25 mm thickness)	0.07
Insulation (glass fibre, per 100 mm thickness)	0.01
Liner trays (0.4 mm – 0.7 mm thickness)	0.04-0.07
Composite panels (40 mm – 100 mm thickness)	0.10-0.15
Purlins (distributed over the roof area)	0.03
Steel decking	0.20
Three layers of felt with chippings	0.29
Slates	0.40-0.50
Tiling (clay or plain concrete)	0.60-0.80
Tiling (concrete interlocking)	0.50-0.80
Timber battens (including timber rafters)	0.10

Table 15: cladding load, source: SCI, 2008

4.4 Model Set-up

In order to setup the model in a proper way including all the necessary elements, a workflow has been setup to approach constructing a functioning script. This workflow is depicted in . It shows when and where certain input is applied to the model. To generate a 2D section geometry, both a manual input and a 3DBAG input will be developed. In case a hall structure's data is not yet available in the 3DBAG-data set, the manual input can be used instead. The generated geometry is then converted into a

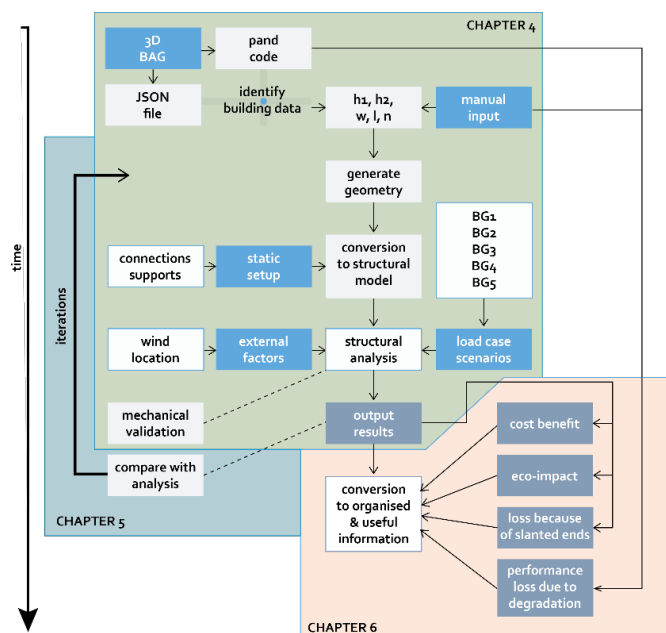


Figure 18: Extended workflow model, source: own work

Karamba3D, a Grasshopper plugin specialised in executing parametric structural calculations. Load scenarios based on literature and data about external factors such as wind and location are constructed and applied to the model. Karamba3D will then analyse the model, putting out a maximum occurring moment in each separate element. This value is then converted to a required profile size, linked with the length of the element and quantity of the element based on the geometry generated in the first step. The execution of each of the steps is described in more detail on the following pages (See Figure 18).

Step 1.1: Hall Geometry - Manual input

For the manual input, five points are generated that form the basis model for the portal. Support A is set at a fixed point (0,0), ensuring the rendered portal will always be anchored at this specific point. Support B ($w,0$) is set at w distance [m] from support A. Point A ($0,h_1$) is defined as a ($h_1,0$) translation from point (0,0). Point B (w,h_1) is a similar translation, starting from ($w,0$). Point C (xw, h_2) is the top of the roof. For symmetrical halls, $x = 0.5$. The generated points are then connected to form line elements that represent the structural members. Line 1 and 2 represent columns, line 3 and 4 represent beam elements. A summary of this model definition is given in Table 16.

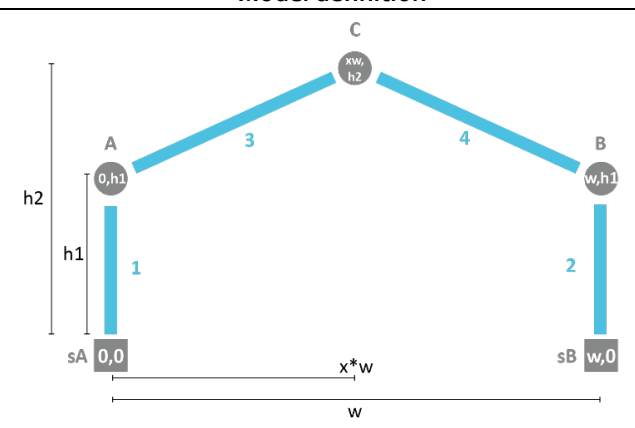
Point	Coordinate	<div> <p>Model definition</p>  </div>
sA	(0,0)	
sB	(w,0)	
A	(0,h1)	
B	(w,h1)	
C	(xw,h2)	
Line	Points	
1	sA, A	
2	sB, B	
3	A, C	
4	C, B	

Table 16: manual input model definition, source: own work

Step 1.2: Hall Geometry - 3DBAG input

The 3D-BAG data is retrievable as a CityJSON file. Each building in the data set contains a data element that includes a list with properties. A full list of available properties is added to the appendix (E), but the most relevant are listed in Table 16. Data item 0 - object name - refers to a BAG-code. Every building has a unique BAG-code that can be used to identify the building within the dataset. The BAG-code of every building in the Netherlands is publicly available, making it a useful piece of information to trace down a building in the dataset. For each building, the dataset provides a maximum height (item 12), a minimum height (item 13). These values provide the required h_1 and h_2 after being corrected by a subtraction of the ground level height (item 14), see also Table 17. Not included as separate values in the dataset, but retrievable using Grasshopper are coordinates of the corner points of the buildings projected area. Using these points, the width and the length of the structure can be determined. All the required data can thus be retrieved from the

3D-BAG dataset and organised following the same steps of setting up the portal as in the manual input. The only extra step that needs to be added is an inward offset of the outline of the structure. The data provided by 3DBAG will give the geometry of the outer shell of the structure, which in most cases will be the façade. The centre line of the structural elements that Karamba3D uses to generate the beam elements does not coincide with the outline of the building, but lays half a profile height + the thickness of the facade underneath that line. Including this offset has almost no effect on the static calculations, but does influence the length of the available elements. Including this offset ensures the provided element lengths are as close to reality as possible.

Data item	information	unit
0. Object Name	BAG-code	
4. Object dak_type	Roof type: flat/slanted	-
5. Object data_area	Building area	m ²
12. Object h_dak_max	h ₂ + *	m
13. Object h_dak_min	h ₁ + *	m
14. Object h_maaiveld	*	m

Table 17: retrievable 3DBAG data, source: 3DBAG

Step 2: Karamba3D Definitions

Points sA and sB are defined as **support**. A value selector functions as input variable, selecting the degrees of freedom (dof) that define the support type (rigid, no dof; pinned, dof rotation in y-dir). Point A, B and C are defined as **joint**. Similar to **support**, the input variable is selecting the dof that define the connection type (rigid, no dof; pinned, dof rotation in y-dir). Lines 1-4 are defined as **beam** with a default profile size set. This profile only functions as a starting point for the calculations and does not have to match the actual profiles used, as will later be shown in the verification. The beams are connected by the definition **beam-joint agent** for A, B and C, and the connected beams are supported by sA and sB (see also Table 18). Loads in Karamba3D are defined as **beam load**, expressed in kN/m. This means all loads need to be converted from kN/m² to kN/m by multiplying the load with the portal spacing distance.

Point	Type
sA	Support
sB	Support
A	Connection
B	Connection
C	Connection
Line	Beam
1	ld1
2	ld2
3	ld3
4	ld4

Table 18: Karamba3D definition, source: own work

BG1 is a combination of structure weight (BG1.1.) and cladding load (BG1.2.). To define BG1.1, Karamba3D component **load - gravity** is used. This multiplies the weight of the structure (length of elements * specific weight per meter of cross section) [kg] with the gravitational acceleration (9,81m/s²) to give the weight of the structure in kN. This load is applied in the z-direction. BG1.2 is calculated by selecting a cladding type (light = 0,10/medium = 0,20/heavy = 0,30), multiplying the load with the portal spacing distance and the length of each element to give a load in kN/m. This load is applied to each separate line element as a **beam load**. The load is applied in the negative z-direction, equal to BG1.1.

BG2 involves loads caused by snow. This unit multiplies the standard snow load value with a constant for sloped roofs (0,8; VMRG, n.d.). This results in a value in kN/m². Multiplying this value with the portal spacing distance gives a snow load value in kN/m. This load is applied as a **Beam Load** on elements id3 and id4 in the negative z-direction.

BG3 involves wind load. The input values of BG3 are based on the aforementioned wind pressure table. A region and surrounding type can be selected in the input menu, the height can be retrieved from the geometry setup and thus the correct wind pressure is picked out of the table and applied to each individual beam. This load is applied in the positive x-direction, simulating wind from the left side. Wind from the right side can be simulated by applying the loads in the negative x-direction. For the sake of the scope of this research paper, only wind from the left side is considered for now, keeping the script simpler. The wind pressure has been multiplied by the corresponding coefficients (Oosterhoff, 2013) and is applied based on the local orientation of the element. Some halls have open walls that will not be affected by the wind pressure. Therefore wind loads on id1 and id2 need to be able to be switched of simultaneously or separately based on a halls design. Karamba3D does not allow a load to be simply switched off, instead a **Value list** element is added to deactivate this load on id1 and/or id2 by overriding the applied wind input value with an input value of zero – which equals no wind load.

BG4 introduces the effects of suction. The applied loads are based on the wind pressure, and work in a similar to BG3, only the direction of the applied forces is set inwards. This means a different load direction needs to be applied to each specific element (Table 19). A coefficient is applied to the wind pressure that depends on how open or closed off a structure is. Based on research by TNO (1992) a simplification has been made to simulate four scenarios: All walls open, left wall open, right wall open, no walls open (see Table 20). When a wall is selected to be open, executed as described in BG3 using a **Value list** component, the suction force is not applied to the column element supporting the wall by overriding the input value with 0.

Beam	Load direction
id1	+ x
id2	- x
id3	- z
id4	- z

Table 19: load directions, own work

Scenario	coefficient
All walls open	0,8
L-wall open	0,55
R-wall open	0,55
No walls open	0,3

Table 20: suction coefficients, based on: TNO, 1992

BG5 includes the loading effect of overpressure. Overpressure applies only to elements id3 and id4, and is based on the wind pressure. It is applied in the positive z-direction, as overpressure creates an upward force. A coefficient of 0,35 is applied (TNO, 2022). and is not affected by selecting opened walls as described in BG3 and BG4.

In order to test the portal for safety, various load case scenarios need to be analysed. For each of the loadcases, different safety factors apply. This has been incorporated into the grasshopper model by not by separately combining each load case, but making four load cases including all load scenarios, applying a safety factor 0 in order to 'switch off' a load. This is done to maintain the data structure Karamba3D uses to compute and apply the loads. Table 21 shows the applied safety factors.

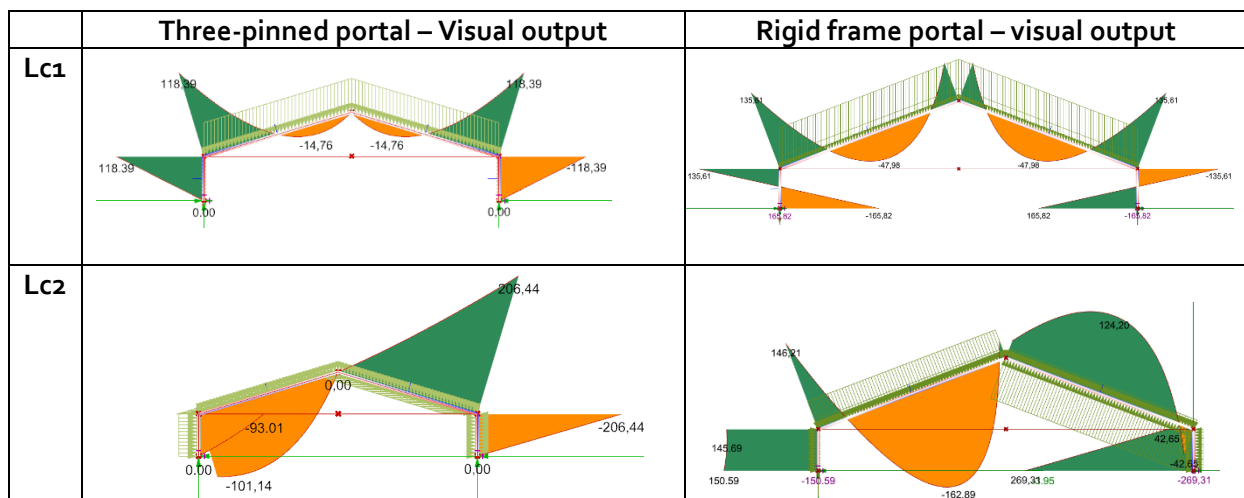
Scenario/Loadcase	Lc1	Lc2	Lc3	Lc4
BG1	1,1	1,1	1,35	1,3
BG2	1,3	0	0	0
BG3	0	1,3	0	0
BG4	0	1,3	0	0
BG5	0	0	0	0,9

Table 21: loadcase safety factors, based on:

Step 3: Structural Analysis

All the separate elements are brought together in the Karamba3D **model assembly** element. The input for this elements concerns the point coordinates of the nodes (supports & connections), the line elements that are converted to beams, the load cases and the support and connection conditions. The assembly element translates these components to a model that is then mathematically analysed by component **analyze model**. The output of this element can be graphically displayed, showing where the maximum stresses and maximum moments occur using the **beam view** component. As the model is set up in a parametric way, changes to the geometry of the hall can be directly calculated into new results. Karamba3D offers a visual output, examples of which are shown in Table 22.

The moments occurring in the beam can be calculated for different points of the portal. Because of the various directions of occurring loads and different mechanical set ups, the location of the maximum moment can change. This is why an extra element is added to the script of the model, calculating the moment occurring in each beam at 100 different points, listing them and selecting the maximum occurring value. The values are first converted to absolute values, to ensure the script considers -150 kNm to be a bigger occurring moment than + 120 kNm.



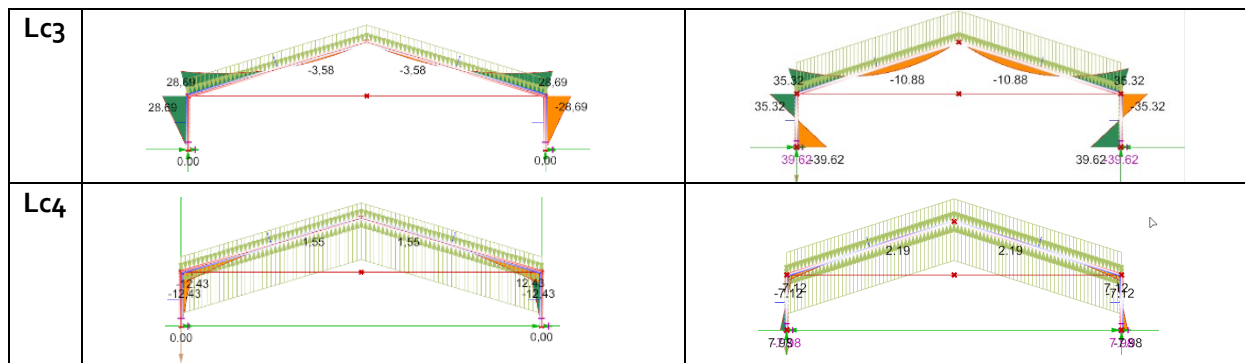


Table 22: Karamba3D visual output, source: own work

Step 4: Conversion of results

The maximum moment occurring in a beam is then used to reverse calculate the required section modulus in mm^3 , by dividing the maximum moment value by the maximum allowed stress (equal to the steel class) for steel. In the case of industrial hall structures this value is 235 N/mm², but the quickscan tool could easily be adapted and expanded to cover other steel classes as well. However for the scope of this research, this is considered unnecessary.

The output value of this step results in a section modulus [mm^3] that can then be used to select potential steel profiles that provide the structural strength to deal with the maximum moment. Tables of both HEA and IPE profiles (Staal tabellen, n.d.) provide the section modulus of each profile. These tables are added in appendix H. An extra unit of script is added that selects the section modulus value from the list of profile properties that is closest to the output of the calculation, making sure it rounds towards the ceiling, as rounding towards the floor would result in a profile selection that is too weak to deal with the occurring stresses. It then links this rounded value with the corresponding profile number and combines it with the profile type, either HEA or IPE, to create a profile suggestion as output. This part of the script is depicted in Figure 19.

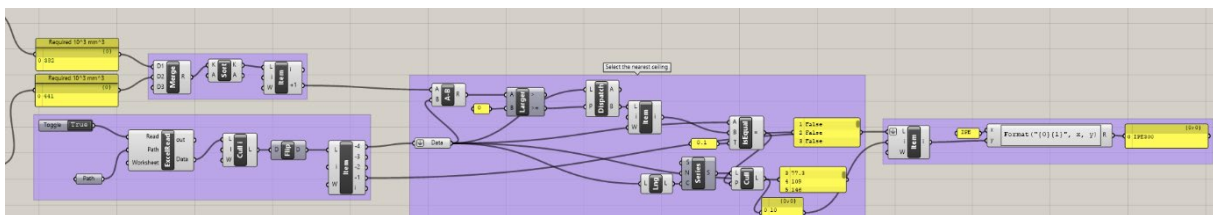


Figure 11: Profile selection script, source: own work

Step 5: Organisation of Output Data

The output data is then organised and structured by the model. Not only the total length of retrievable elements is relevant, more than that the length of each individual beam matters. 100m of profile cannot span 12m in a new project if all the elements are 10m each. The decision has been made to organise the output per id-element, given that in cases of non-symmetrical halls, the lengths of

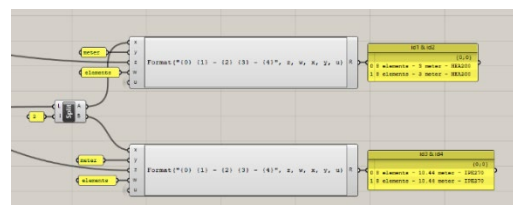


Figure 20: Output data organization script, source: own work

these elements can be different. The output result will therefore have the following structure (see Figure 20):

[n elements, element length, element profile, id1]
 [n elements, element length, element profile, id2]
 [n elements, element length, element profile, id3]
 [n elements, element length, element profile, id4]

The part of the script organizing the output data is shown in The number of elements is defined by the total number of portals minus the portals (n-2) at both ends of the hall, as these tend to have a completely different structural set up – more or less a wall rather than a portal. In chapter 7 it is explained in more detail how this information, together with the information an extra set of analyses, is formatted to an excelsheet.

4.5 Model Validation

In order to validate the model and prove the results the quickscan tool gives are proper calculations, the output results are compared with a series of hand calculations. This does not prove yet how close the results come to reality, just whether it the mechanics behind it is sound. For this process, the manual input version is selected to set up a portal that is more manageable to calculate by hand (See Table 23). The calculations have been added in appendix E.

4.5.1 Model properties

Portal properties	Value	Model definition
w	20m	
h1	3m	
h2	6m	
Spacing	5m	
Cladding	Light	
Wind area	II - built	
Mechanical setup	Three-pinned	

Table 23: manual input for performing calculations, source: own work

5. TESTING

In this chapter the model will be tested to evaluate its accuracy and effectiveness. First of all, a sensitivity analysis is applied in order to understand to what extent the input values affect the result. To measure how effective the tool is in predicting what type of steel beams can be retrieved from a hall structure, the analysed halls of chapter 3 are used as input to compare the output data of the model with the real world, giving insight to what extent the model represents reality. Some of these halls led to the model being updated, reworked or experimented with. These iterations are included in paragraph 5.3.

5.1 Sensitivity Analysis

The goal a sensitivity analysis is to see how certain factors influence the output result. Most input factors, such as geometry and wind region are relatively certain, however, input factors such as cladding weight, portal spacing and the mechanical setup of the portal can influence the output results when they are wrongly assumed. As a basis for the sensitivity analysis, the setup used in paragraph 4.5 is used again, see Table 24.

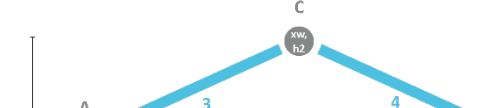
Portal properties	Value	Model Definition
w	20m	
h1	3m	
h2	6m	
Spacing	5m	
Cladding	Light	
Wind area	II - Built	
Mechanical setup	Three-pinned	
Pre-selected profile	IPE220	

Table 24: model input sensitivity analysis, source: own work

This setup functions as the calibration point of the sensitivity analysis. In this analysis the effect of the preselected profile type, cladding, portal spacing and static setup will be tested.. The effects are measured for loadcase 1 (lc1) and loadcase 2 (lc2) as these are the two most significant loadcases. For each analysis, only the input factor being analysed is changed; the other input factors remain as stated in Table 24. To compare the changes in output more precisely, not the profile output, but the section modulus output is considered. Table 25 shows the required section modulus for each elements based on the given set up. Values for the section modulus from now on will be given in 10^3 mm^3 .

element	10^3 mm^3 lc1	10^3 mm^3 lc2
ld1	504	41
ld2	504	306
ld3	504	333
ld4	504	357

Table 25: section modulus output sensitivity analysis, source: own work

element	10^4 mm^3 lc1	10^3 mm^3 lc2
ld1	504	41
ld2	504	306
ld3	504	333
ld4	504	357

Table 25: section modulus output sensitivity analysis, source: own work

5.1.1 Analysis 1 – Preselected Profile Type

For Karamba3D to be able to make a calculation, the beams must be assigned a cross section. As mentioned in chapter 4, an IPE220 profile has been selected as an average profile size to stand in, assuming the effect of the profile weight compared to other loads such as wind and snow can be ignored. To check whether that assumption is correct, various other profiles were put in place to analyse to what extent this profile pre-selection affects the output results. Two smaller profiles (IPE180 and IPE200) and two bigger profiles (IPE240 and IPE270) have been tested. The section modulus output of each element is given in Table 26.

Element	Lc1				Lc2			
	Id1	Id2	Id3	Id4	Id1	Id2	Id3	Id4
IPE180	493	493	493	493	52	295	334	354
IPE200	499	499	499	499	47	301	333	355
IPE220	504	504	504	504	41	301	333	357
IPE240	511	511	511	511	35	313	333	359
IPE270	519	519	519	519	27	321	333	362
Avg. Deviation per step	1,4% 6,5 mm ³	1,4% 6,5 mm ³	1,4% 6,5 mm ³	1,4% 6,5 mm ³	12% 6 mm ³	1,4% 6,5 mm ³	0,1% 0,2 mm ³	0,6% 2 mm ³

Table 26: results sensitivity analysis 1, source: own work

The required section moduli output increases by an average of 1.4%. The values for Lc2 show varying deviations per element, with Id1 being the most affected percentage-wise. Yet, the absolute difference per profile step is similar to that of all elements in loadcase 1. The difference between Id1 and Id2 is due to wind load direction, but the tool selects one profile type for both based on the highest required section modulus, making the percentual deviation of Id1 irrelevant. The deviation per profile step for Id2 is similar to that found for elements in loadcase 1. Id3 and Id4 are practically unaffected, with Id4 having a deviation of less than 1% per profile step and Id3 having no deviation. The small deviations lead to the conclusion that the pre-selected profile has no significant effect on the output result, especially as the average percentual deviation is smaller than the calculation model's margin of error.

5.1.2 Analysis 2 – Cladding Weight

Cladding for economical and industrial structures is relatively light compared to facades of housing and utility buildings, due to the incentive to save cost and their purely functional usage. The range of cladding weight is small, but as it is multiplied by the portal spacing and the length of all elements its effect can be significant. The default cladding is considered to be medium (0,20kN/m²). The section modulus output of each element is given in Table 27.

Cladding type	Lc1				Lc2			
	Id1	Id2	Id3	Id4	Id1	Id2	Id3	Id4
Light	504	504	504	504	41	301	333	357
Medium	565	565	565	565	21	367	333	383
Heavy	626	626	626	626	82	428	334	428
Avg. Deviation per step	10,8% 61 mm ³	10,8% 61 mm ³	10,8% 61 mm ³	10,8% 61 mm ³	50-100% 41 mm ³	1,4% 64 mm ³	0,1% 0,5 mm ³	9,1% 35 mm ³

Table 27: results sensitivity analysis 2, source: own work

The cladding type has a greater impact than the pre-selected profile type. A difference of $61 \cdot 10^3 \text{ mm}^3$ can result in a profile selection that is one or two classes off, particularly in lower profile classes. The large percentual deviation in required section modulus for id1 with lc2 is similar to analysis 1, with only id2's result being relevant for profile selection. As the deviation of 10.8% is much larger than the calculation's margin of error, the cladding type should only be changed if the user knows it is either light or heavy cladding

5.1.3 Analysis 3 – Static Setup

The static setup of the portal is the biggest unknown factor within the model. Although a three-pinned portal is considered to be the status quo, in some cases a rigid frame or semi rigid frame has been considered a more fitting solution for a hall. Most likely a setup has been chosen during the design process that requires the smallest profile sizes – being the most economically attractive option. The required section modulus output of each element is given in Table 28. Visual outputs of lc1 and lc2 applied on the four setups are included in Table 29, to give a better understanding of the different structural behaviour of each setup.

Portal Setup	Lc1				Lc2			
	Id1	Id2	Id3	Id4	Id1	Id2	Id3	Id4
Three-pinned	504	504	504	504	41	301	333	357
Hinged girder	973	973	270	270	87	433	315	167
Semi-rigid	449	449	449	449	53	294	341	351
Rigid frame	376	376	328	328	179	361	224	174
Range size	597	597	234	234	138	137	117	190

Table 28: results sensitivity analysis 3, source: own work

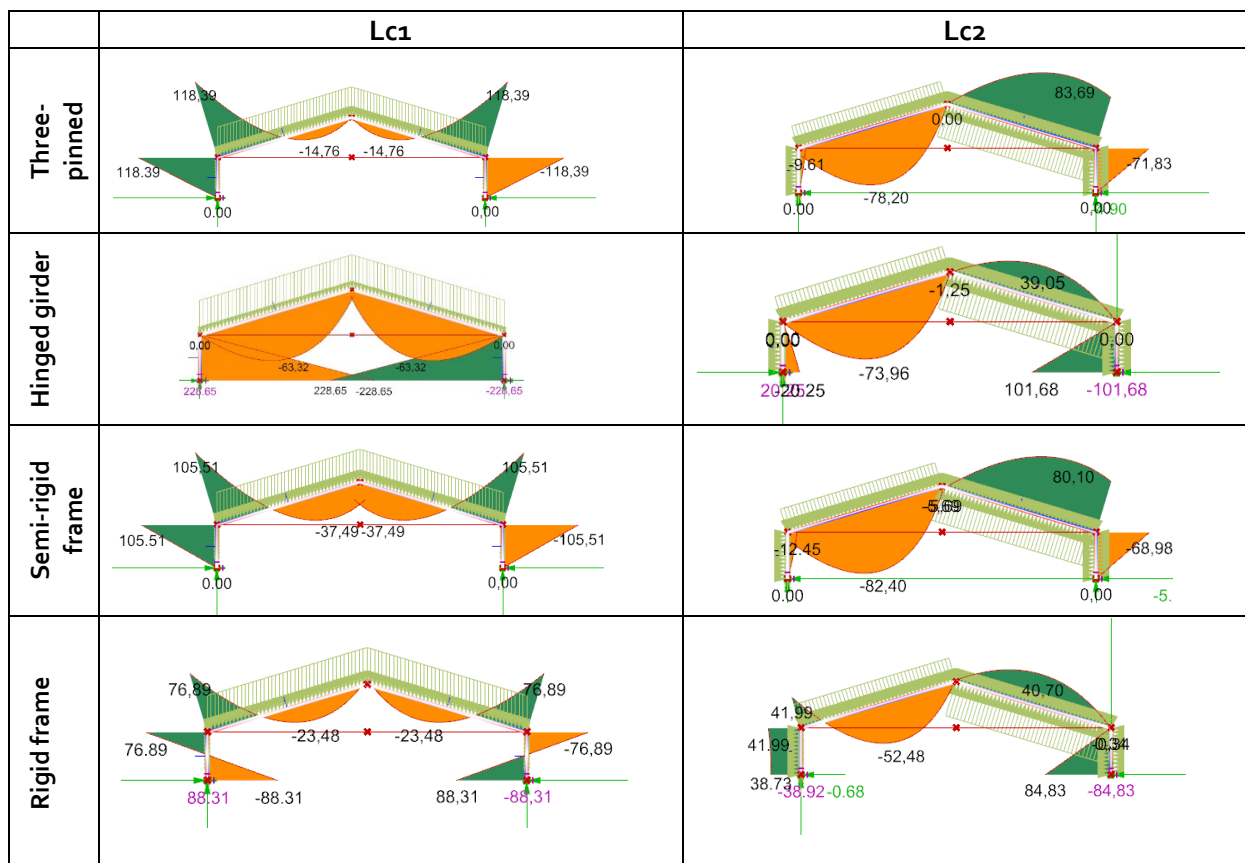


Table 29: visual output sensitivity analysis 3, source: own work

The output results for the three-pinned portal and the semi-rigid frame come really close to each other, with comparable margins like those caused by different types of cladding. The hinged girder setup provides the largest deviation, compared to the other setups as well as within itself; for loadcase 1, the required section modulus for id1 and id2 is quadruple that of id3 and id4. The rigid frame provides the lowest required section modulus on average for all elements, indicating a structurally optimized setup for this specific portal. It must be noted that the effects of a different portal setup can differ strongly based on the overall geometry of the hall. This is why an extra component of model script was developed to optimize the portal setup in a structural way, providing the lowest average section moduli for all elements. In case the portal setup of a structure is unknown, because of the economical and functional use of the structure, this optimized portal scenario is the most likely to be applied (see paragraph 5.3).

5.1.4 Analysis 4 – Portal Spacing

The case studies discussed in chapter three show that the range of spacing between portals varies between 4,5 and 5,5 meters. The portal spacing is a manual input to be selected by the user of the tool, with 5m being the default spacing. For the sensitivity analysis, three variants have been tested: 4,5m, 5m and 5,5m. The required section modulus output of each element is given in Table 30.

Portal Spacing	Lc1				Lc2			
	Id1	Id2	Id3	Id4	Id1	Id2	Id3	Id4
4.5 m	458	458	458	458	33	279	300	322
5 m	504	504	504	504	41	301	333	357
5.5 m	551	551	551	551	49	333	367	391
Avg. Deviation per 0.5m step	9,1% 46 mm ³	9,1% 46 mm ³	9,1% 46 mm ³	9,1% 46 mm ³	17% 7 mm ³	8,9% 27mm ³	9,9% 33 mm ³	9,2% 33 mm ³

Table 30: results sensitivity analysis 4, source: own work

A difference of 0.5m in portal spacing has a smaller impact then changing the cladding type has. A difference of $\pm 40 \cdot 10^3$ mm³ can result in a profile selection that is one about one class off, particularly in lower profile classes. The percentual deviation in required section modulus is relatively constant, making the effect of increasing portal spacing predictable. Similar to analysis 1, for load case 2 only id2's result being relevant for profile selection, so the higher percentual deviation of id1 can be ignored.

5.1.5 Conclusion Sensitivity Analysis

These results show that cladding and portal spacing have rather limited effects on the profile output, as the difference in profile classes is just one step which can be considered to be within the margin of error. However, the static setup strongly influences the outcome. The hinged girder setup deviates the strongest, suggesting profiles for columns that deviate 4 classes from the actual profile and suggesting profiles for spanning beams that are 2 classes lower than the actual profile. These differences are significant and although the three-pinned setup and the rigid frame are much more common, this deviation cannot be ignored.

5.2 Case Testing

All of the cases described in chapter 3 have been used as input to evaluate and improve the output results of the quickscan tool. The results of each case testing are listed in this paragraph.

5.2.1 Case A – Meatpig Hall, Breda

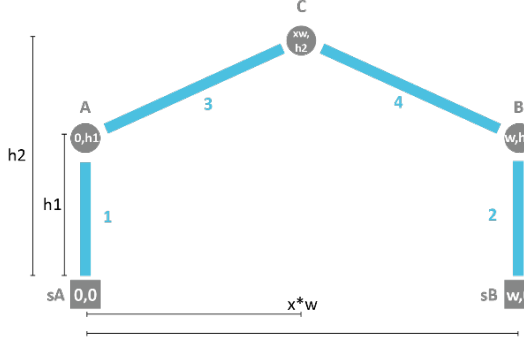
Portal properties	Value	Portal Definition
w	20m	
h1	3.3m	
h2	6.5m	
Spacing	4.8m	
Cladding	Medium	
Wind area	III open	
Mechanical setup	Three-pinned	

Table 31: input values case A, source: own work

This case hall is not included in the 3DBAG dataset (but it probably will be with AHN4). Therefore the manual inputs as shown in Table 31. have been used. These input values are based on the available drawings of the hall. The input values were then converted to a portal by the Karamba3D model, resulting in the following visual output listed in Table 32.

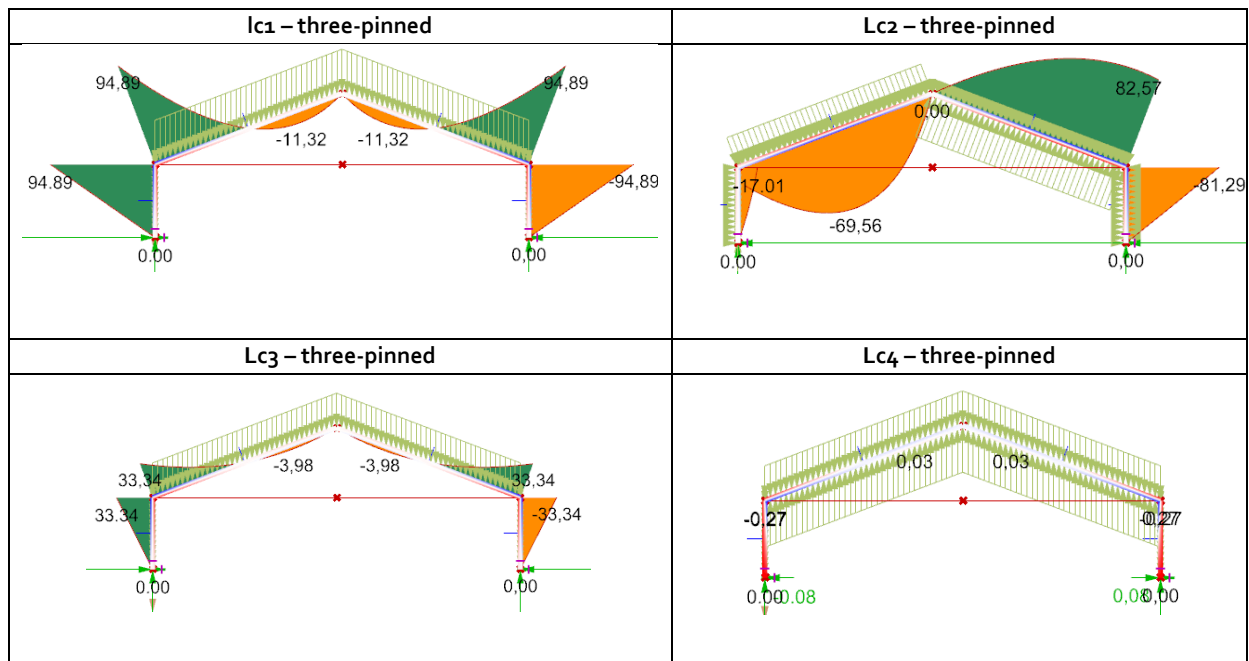


Table 32: visual output structural analysis case A, source: own work

As Table 33 shows, lc3 and lc4 cause occurring moments that are much smaller than those caused by lc1 and lc2. The output results for lc3 and lc4 will therefore not be relevant as the suggested profiles of these load cases deviate significantly from reality and should therefore be ignored. For other halls, or in general for other input values, this might not be the case. The quickscan output is shown here in Table 33.

Element	Length [m]	Quantity	Profile type lc1	Profile type lc2	Profile Selection	Reality
ld1	3.3	23	HEA220	HEA200	HEA220	HEA200
ld2	3.3	23	HEA220	HEA200	HEA220	HEA200
ld3	9	23	IPE300	IPE270	IPE300	IPE300
ld4	9	23	IPE300	IPE270	IPE300	IPE300

Table 33: output quickscan case A, source: own work

Comparing the quickscan output with the real scenario, it seems the model predicts the length and the quantity of the model correctly. Moreover, the suggested profile types are correctly predicted in case of elements id3 and id4, in this case as IPE300. The largest suggest profile size is leading, a profile might suffice for one load case but not for another. The output for element id1 and id2 only slightly deviates, suggesting HEA220 profiles, whereas in reality HEA200 profiles are used. A potential reason for this deviation is that in the case of this specific hall, some extra structural elements are added such as a horizontal IPE200 beam that functions as a tension rod. This element is not included in the model but has some structural consequences, reducing the stress occurring in the columns. As none of the other case halls have such a horizontal element and the results are considerably close, no attempt will be made to include such elements in the tool for now.

5.2.2 Case B – Poultry Hall, Jeth

Portal properties	Value	Portal Definition
w	30m	
h1	3.3m	
h2	8.6m	
Spacing	4.8m	
Cladding	Medium	
Wind area	II open	
Mechanical setup	Three-pinned	

Table 34: input values case B, source: own work

This case hall is not included in the 3DBAG dataset (but probably will be with AHN4). Therefore the manual inputs as shown in Table 35 have been used. These input values were then converted to a portal model, giving the following visual shown in Table 35 on the next page.

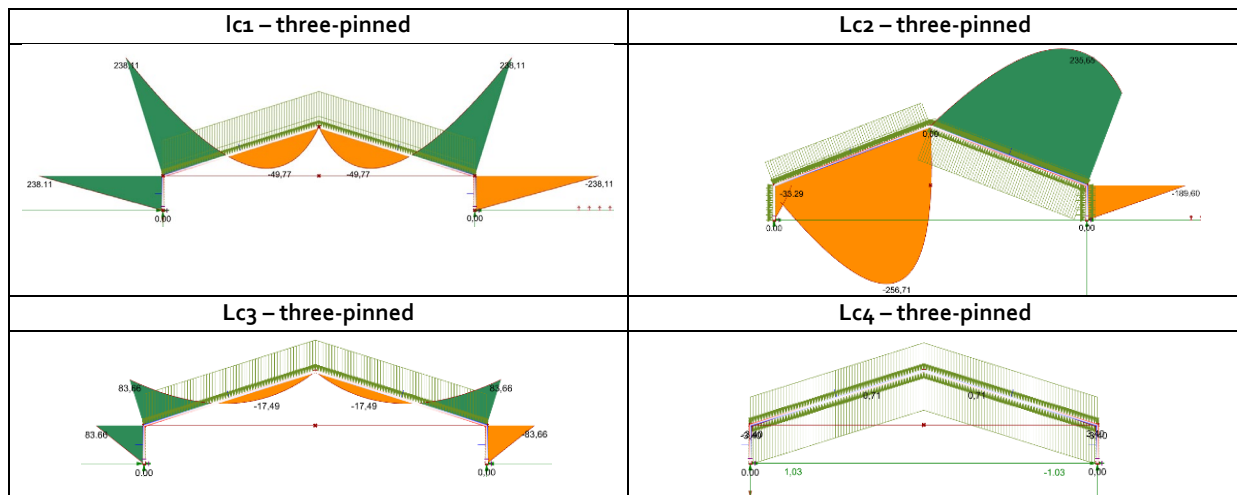


Table 35: visual output structural analysis case B, source: own work

The output of the quickscan tool are listed in Table 36. Compared to the the real scenario, the model strongly overestimates the profiles, suggesting profiles for id3 and id4 that are 6 classes larger than what actually can be found in the structure. This is far beyond the margin of error.

Element	Length [m]	Quantity	Profile type lc1	Profile type lc2	Final Profile Selection	Reality
ld1	3.3	10	HEA280	HEA260	HEA280	HEA220
ld2	3.3	10	HEA280	HEA260	HEA280	HEA220
ld3	15.6	10	IPE400	IPE400	IPE400	IPE220
ld4	15.6	10	IPE400	IPE400	IPE400	IPE220

Table 36: quickscan output case B - three-pinned, source: own work

There are some factors that could be the cause of these strongly deviating results:

1. Error in input values
2. Static setup of the portal
3. The role of secondary supporting elements

The input values were checked and do not show any errors (Figure 21).

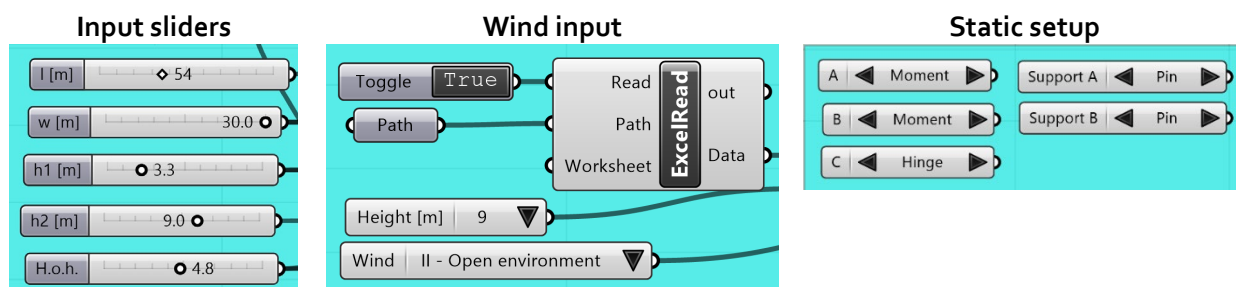


Figure 21: input sliders and value lists case B, source: own work

The assumed static setup used for this analysis is a three-pinned portal. Other static models have been tested to see if that would bring the profile suggestions by the quickscan tool closer to the profiles actually present in the hall.

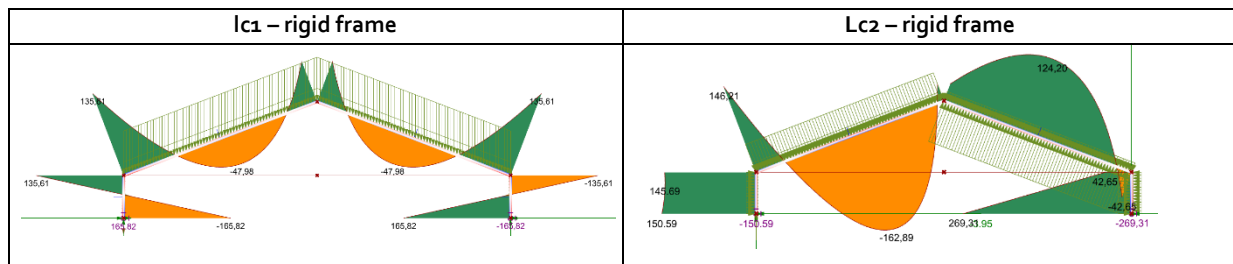


Table 37: visual output structural analysis case B - rigid frame, source: own work

Element	Length [m]	Quantity	Profile type lc1	Profile type lc2	Final Profile Selection	Reality
ld1	3.3	10	HEA280	HEA300	HEA300	HEA220
ld2	3.3	10	HEA280	HEA300	HEA300	HEA220
ld3	15.6	10	IPE330	IPE360	IPE360	IPE220
ld4	15.6	10	IPE330	IPE360	IPE360	IPE220

Table 38: quickscan output case B - rigid frame, source: own work

The results shown in Table 37 and Table 38 are based on a rigid-frame setup. These results are only marginally better than the original output and still deviate 3-4 classes from the actual profiles used in this hall.

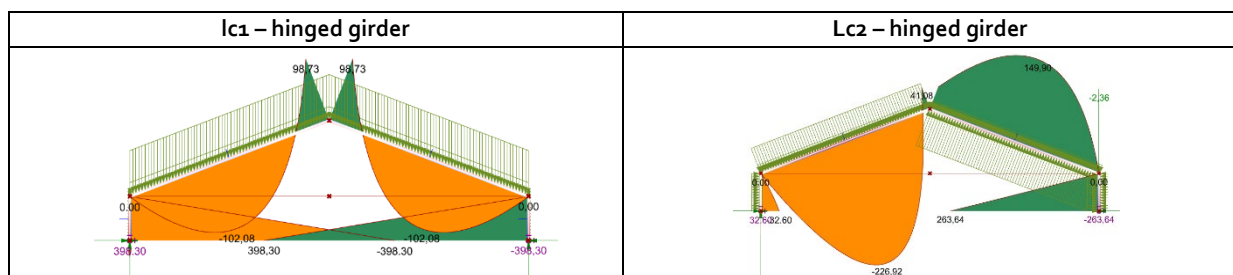


Table 39: visual output structural analysis case B- hinged girder, source: own work

Element	Length [m]	Quantity	Profile type lc1	Profile type lc2	Final Profile Selection	Reality
ld1	3.3	10	HEA360	HEA300	HEA360	HEA220
ld2	3.3	10	HEA360	HEA300	HEA360	HEA220
ld3	15.6	10	IPE300	IPE400	IPE400	IPE220
ld4	15.6	10	IPE300	IPE400	IPE400	IPE220

Table 40: quickscan output case B - hinged girder, source: own work

The results in Table 39 and Table 40 are based on a hinged-girder setup. They present no improvement on the original output as they still deviate up to 6 classes from the actual profiles used in this hall. As the output is still off by a significant margin, an attempt was made to rework the Karamba3D model in a way that secondary structural elements can be added as well. The steps behind this iteration are discussed in more detail in paragraph 5.3. This iteration of the script led to the decision to reconsider the default static setup to be a rigid frame portal. In this case both spanning beams are supported by a smaller column. This scenario gives the lowest occurring moments and is therefore the most likely applied scenario, as this results in the smallest profiles. Visual outputs are shown in Table 41 on the next page.

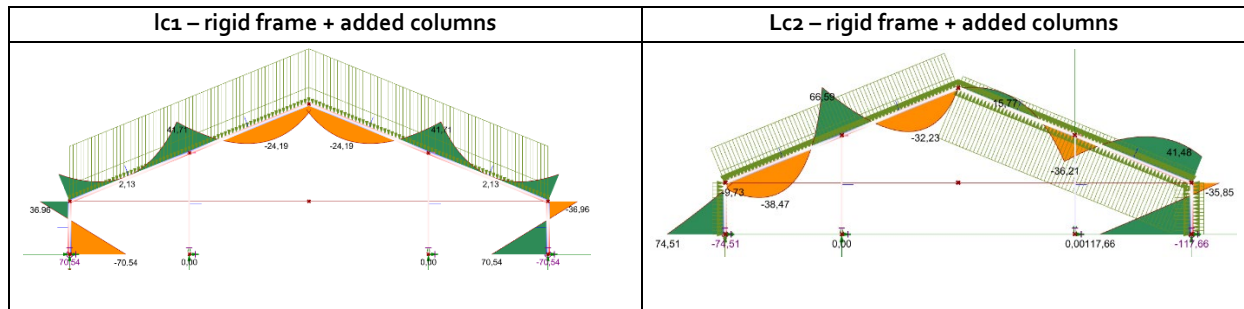


Table 41: visual output structural analysis case B - rigid frame + added columns, source: own work

Element	Length [m]	Quantity	Profile type lc1	Profile type lc2	Final Profile Selection	Reality
ld1	3.3	10	HEA200	HEA220	HEA220	HEA220
ld2	3.3	10	HEA200	HEA220	HEA220	HEA220
ld3	15.6	10	IPE220	IPE240	IPE240	IPE220
ld4	15.6	10	IPE220	IPE240	IPE240	IPE220

Table 42: quickscan output case B - rigid frame + added columns, source: own work

The results (Table 42) come much closer to the real situation suggesting profiles that only deviate one class from the actual situation. The addition of extra secondary structural columns is a likely feature of halls with larger spans such as this case study. However, their presence cannot be retrieved from any of the available data sources mentioned in paragraph 4.2. This means the extra columns can be introduced in the analysis based on assumption, or extra information (e.g. a photo taken from inside the hall) is required in order to know whether or not to add these columns to the analysis.

5.2.3 Case C – Dairy Hall Callantsoog

This hall provides a series of challenges to deal with: asymmetry, an extra supportive column and located in a windy area. This hall is included in the 3DBAG dataset. As the 3DBAG input has not yet been redeveloped to work for the script including one supporting column, the accuracy of the 3DBAG-input is checked with the simple version of the tool (no extra supporting column. These geometrical values are then used as manual input in the script that does include a supporting column. The input values for case C are listed in Table 43.

Portal properties	Value	3DBAG visual	Attribute list
Data tile	310		Tile number <input type="text" value="310"/>
Pand code	0476100000003241		identificatie <input type="text" value="NL.IMBAG.Pand.0476100000003241"/>
Spacing	4.8m		h_maalveld <input type="text" value="-0.023"/>
Cladding	Light		h_dak_70p <input type="text" value="7.0924325"/>
Wind area	I open		dak_type <input type="text" value="slanted"/>
Mechanical setup	Three-pinned		pw_bron <input type="text" value="ahn3"/>
			pw_datum <input type="text" value="2015-12-01"/>
			val3dity_codes <input type="text" value="[]"/>

Table 43: input values case C, source: 3DBAG, own work

The original version of the 3DBAG-input script assumes a symmetrical hall. Above that, because of the way this lot has been registered, the hall itself and the smaller attached building are seen as one geometry. The minimum height resulting from the dataset is not the lower roof ridge of the main hall, but the lower roof ridge of the attached building. Furthermore, defining ridges and lines as the longest/second-longest/third-longest etc. does not lead to desirable results in case of combined geometries such as this hall. In this case, the roof ridge of the smaller building was selected as the sloped roof line for the main hall, messing up the generated geometry. These problems were dealt with by reworking the 3DBAG-input script, which is described in detail in paragraph 5.3. Table 44 shows the geometry output given by the model based on the reworked version of the 3D-BAG input.

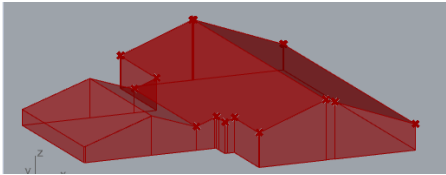
	3DBAG output	Real value	Deviation	Geometry in Rhino by Grasshopper
h1.1	3,6m	3,5m	+2,8%	
h1.2	4,7m	4,5m	+3,1%	
h2	9,0m	8,9m	+1,1%	
w	25,6m	25,7m	-1,1%	
l	49,9m	49m	+1,8%	
x	0,56	0,55	+2,0%	
ld1 length	3,6m	3,5m	+2,8%	
ld2 length	4,7m	4,5m	+3,1%	
ld3 length	14,9m	14,9m	0%	
ld4 length	11,8m	12,0m	-1,6%	

Table 44: geometry output case C based on 3DBAG, source: own work

The 3DBAG input comes very close to the real scenario, showing a maximum deviation of +3,1% for the output element length of id2. As the deviation is generally overestimating dimensions, the inward offset described in paragraph 4.4 could be slightly increased to counter the overestimation. However, this adjustment will not be applied before more geometries are evaluated. As aforementioned, the provided geometry values are used in the manual input to include the extra supporting column. The input is listed in Table 45. Only one extra supporting column is added, which is positioned on the right side of the hall. The position on the x-axis is labelled wb and represents the distance between support sA and the support for the extra column. The visual outputs for loadcase 1 and 2 are shown on the next page in Table 46.

	3DBAG output
h1.1	3,6m
h1.2	4,7m
h2	9,0m
w	25,6m
l	49,9m
x	0,55
wb	0,55

Table 45: manual input for case C

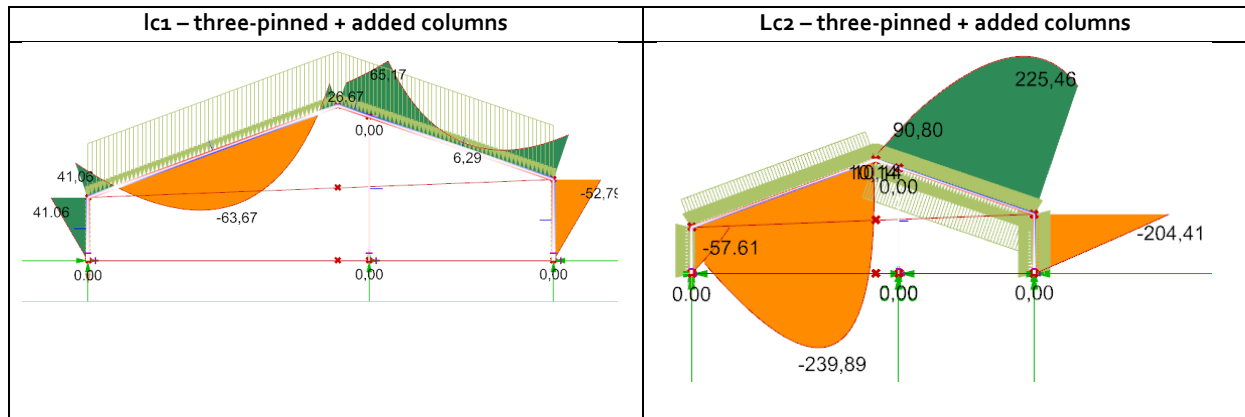


Table 46: visual output structural analysis case C, three-pinned + extra column, source: own work

The visual output shows a considerable difference between moments occurring due lc1 and lc2. A check was done to make sure the model selects the right windpressure (area: I, environment: open, height: 9m = 0,98) which it does select. The results of quickscan output are listed down below in Table 47.

Element	Length [m]	Quantity	Profile type lc1	Profile type lc2	Final Profile Selection	Reality
ld1	3.6	9	HEA200	HEA280	HEA280	HEA220
ld2	4.7	9	HEA200	HEA280	HEA280	HEA220
ld3	11.8	9	IPE220	IPE400	IPE400	IPE220
ld4	14.9	9	IPE220	IPE400	IPE400	IPE220

Table 47: quickscan output case C - three-pinned + extra column, source: own work

Table 48 shows strongly deviating results, mainly caused by the high profile suggestions suggest because of the large effect the wind load has on the portal structure. The profile suggestion based on lc1 does come close to the real scenario, indicating the structural setup and the portal geometry can be assumed to be correct. Other structural setups also lead to vast overestimation of both columns and beams. This would leave only the coefficients that are applied separately to each element as a possible error (see Figure 22) . These values might either be too high or too general and not applying to this specific situation. If strong deviations occur in other cases because of the wind load being too high, further research into these coefficients is needed to improve these values.

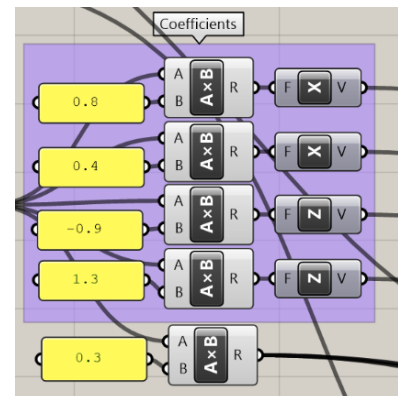


Figure 22 pressure coefficients in model, source: own work

5.2.4 Case D – Poultry hall ELSHOUT

This case hall has no drawings available, only a static report on the portal structure. This prompts an opportunity to compare the calculations made by the Karamba3D model with the calculations made by the structural engineer's computer program. The hall is part of a megabarn located in Elshout. The hall can be found in the 3DBAG data set. As the image in Table 48 shows, multiple hall structures are located on this address, however the highlighted barn is the only one that has technical data available. The 3DBAG input is shown in Table 48.

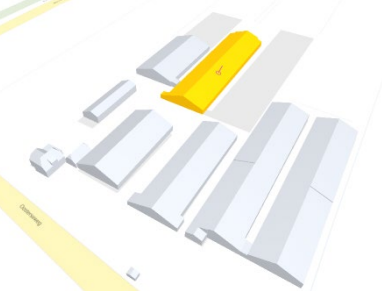
Properties	Value	3DBAG visual	Attribute list																		
Data tile	1393		<table><thead><tr><th>Attribute</th><th>Value</th></tr></thead><tbody><tr><td>Tile number</td><td>1393</td></tr><tr><td>identificatie</td><td>NL_IMBAG_Pand.0797100000030356</td></tr><tr><td>h_maaiveld</td><td>1.06</td></tr><tr><td>h_dak_70p</td><td>7.4837937</td></tr><tr><td>dak_type</td><td>slanted</td></tr><tr><td>pw_bron</td><td>ahn3</td></tr><tr><td>pw_datum</td><td>2016-12-01</td></tr><tr><td>val3dity_codes</td><td>[]</td></tr></tbody></table>	Attribute	Value	Tile number	1393	identificatie	NL_IMBAG_Pand.0797100000030356	h_maaiveld	1.06	h_dak_70p	7.4837937	dak_type	slanted	pw_bron	ahn3	pw_datum	2016-12-01	val3dity_codes	[]
Attribute	Value																				
Tile number	1393																				
identificatie	NL_IMBAG_Pand.0797100000030356																				
h_maaiveld	1.06																				
h_dak_70p	7.4837937																				
dak_type	slanted																				
pw_bron	ahn3																				
pw_datum	2016-12-01																				
val3dity_codes	[]																				
Pand code	0797100000030356																				
Spacing	5.0m																				
Cladding	Heavy																				
Wind area	III-open																				
Mechanical setup	Three-pinned																				

Table 48: input values case D, source: 3DBAG, own work

As there are no further secondary supporting elements involved in this hall, the 3DBAG geometry can directly be converted into the portal used for the structural analysis. The 3DBAG input is listed in Table 49 and compared with the real scenario. For this hall the 3DBAG data turns out to be very accurate, with an average deviation of just -0,6%. The portal will now be generated and structurally analysed by Karamba3D. The visual output is depicted in Table 50.

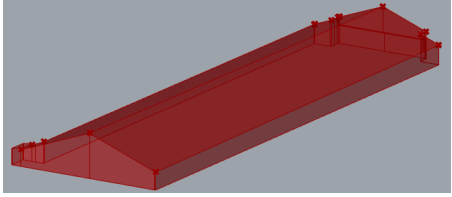
	3DBAG output	Real value	Deviation	Geometry in Rhino by Grasshopper
h1.1	2,94m	2,95m	-0,3%	
h1.2	2,94m	2,95m	-0,3%	
h2	7,5m	7,6m	-1,3%	
w	25,7m	25,6m	+0,4%	
l	90,4m	90m	+0,3%	
x	0,5	0,5	0	
ld1 length	2,94m	2,95m	-0,3%	
ld2 length	2,94m	2,95m	-0,3%	
ld3 length	13,5m	13,6m	-0,7%	
ld4 length	13,5m	13,6m	-0,7%	

Table 49: geometry output case D based on 3DBAG, source: own work

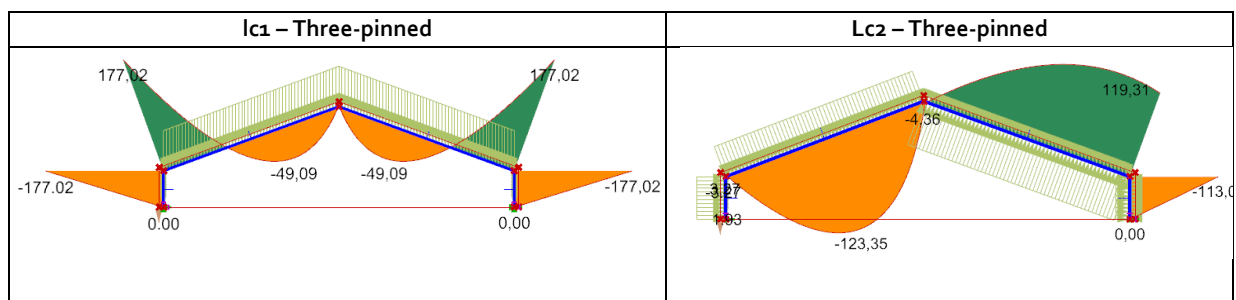


Table 50: visual output case D, source: own work

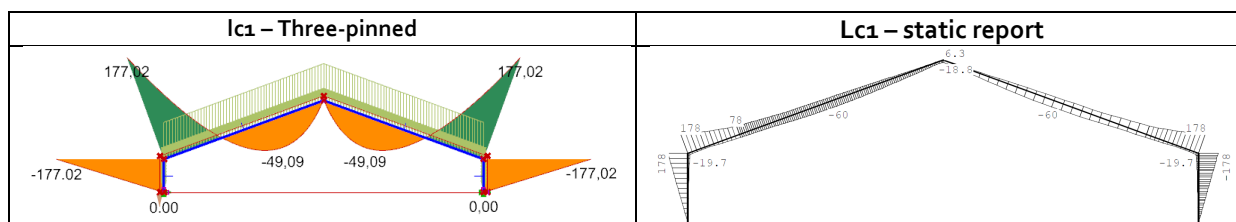


Table 51: visual output case D compared to static report, source: own work

Load case 1 is also visualised in the static report of the hall. For comparison, both the Karamba3D output and the static report visualisation are shown next to each other in Table 52. The maximum occurring moment is almost exactly the same (177 vs. 178 kNm). However, within the spanning beams, the maximum moment suggest by Karamba3D is significantly lower (49 vs 60 kNm). This might be local loads places on a portion of the roof, such as solar panels. In the end, it has no effect on the selection of the profile in the script, as that is based on the maximum occurring moment. The output results of the quickscan tool are given in Table 52.

Element	Length [m]	Quantity	Profile type lc1	Profile type lc2	Final Profile Selection	Reality
ld1	2.95	18	IPE360	IPE300	IPE360	IPE360
ld2	2.95	18	IPE360	IPE300	IPE360	IPE360
ld3	13.5	18	IPE360	IPE300	IPE360	IPE270
ld4	15.5	10	IPE360	IPE300	IPE360	IPE270

Table 52: quickscan output case D - three-pinned, source: own work

Although the model predicts the columns right, there appears to be a strong deviation for the profiles suggested for id3 and id4. After further inspection, it turns out that in the real scenario, beam id3 and id4 are hybrid beams, consisting of two different profiles. The first 2,5 meters of each beam is a HEA280 profile (1013*10³mm). The remaining 10,5 meters of each beam is an IPE270 profile (428*10³mm). The HEA profiles are used to deal with the high moments occurring at the corners of the profile, whereas the lighter, slimmer IPE270 spans the parts of the hall where lower moments occur. This is most likely done to save cost. Although its name suggests otherwise, a HEA280 profile is 270mm high, just like an IPE270. The much more expensive HEA profile is only applied where it is needed. A quick calculation (Table 53) shows a combination of HEA280 + IPE 270 to be about 300 euros cheaper than using just an IPE360 (similar structural performance). Given that there are 36 spanning beams present, this would possibly save more 10.000 euro. None of the other case halls have such a hybrid profile combination but the fact that these combined beams can possibly occur in structures like these does have a significant impact on the validity and reliability of the quickscan tool. There is no reason for the tool to assume a combined profile is used and even if that knowledge is available, it cannot predict what profiles are used and what percentage of the beam consists of which type of profile. The implications of this will be discussed in chapter 8.

Cross section	Price/m [euro]	Length per beam	Total cost	Combined cost
IPE270	66	11	726	1080
HEA280	142	2,5	355	
IPE360	105	13,5	1417	1417

Table 53: cost calculation, source: <https://www.limtrade.nl/>

5.2.5 Case E – Dairy hall, Baak

This case involves an asymmetric hall with two extra columns supporting the portal frame. In that respect it shares some similarities with case C. The hall can be found in the 3DBAG dataset. The input values for the model are listed in Table 54. Similar to case C, the 3DBAG-generated geometry is compared to the real scenario and then used as input in a manual model to include the two supporting columns. A comparison between the 3DBAG geometry and the reality is given in Table 55.

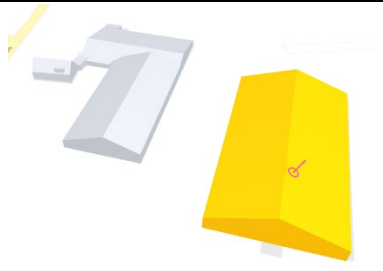
Portal properties	Value	3DBAG visual	Attribute list																		
Data tile	2827																				
Pand code	1876100000033530																				
Spacing	5.0m																				
Cladding	Medium																				
Wind area	III-open																				
Mechanical setup	Three-pinned																				
			<table><thead><tr><th>Attribute</th><th>Value</th></tr></thead><tbody><tr><td>Tile number</td><td>± 2827</td></tr><tr><td>identificatie</td><td>NL_IMBAG_Pand_1876100000033530</td></tr><tr><td>h_maalveld</td><td>8.734</td></tr><tr><td>h_dak_70p</td><td>18.538559</td></tr><tr><td>dak_type</td><td>slanted</td></tr><tr><td>pw_bron</td><td>ahn3</td></tr><tr><td>pw_datum</td><td>2017-12-01</td></tr><tr><td>val3dity_codes</td><td>[]</td></tr></tbody></table>	Attribute	Value	Tile number	± 2827	identificatie	NL_IMBAG_Pand_1876100000033530	h_maalveld	8.734	h_dak_70p	18.538559	dak_type	slanted	pw_bron	ahn3	pw_datum	2017-12-01	val3dity_codes	[]
Attribute	Value																				
Tile number	± 2827																				
identificatie	NL_IMBAG_Pand_1876100000033530																				
h_maalveld	8.734																				
h_dak_70p	18.538559																				
dak_type	slanted																				
pw_bron	ahn3																				
pw_datum	2017-12-01																				
val3dity_codes	[]																				

Table 54: input values case E, source: 3DBAG, own work

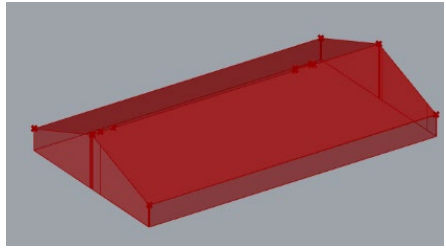
	3DBAG output	Real value	Deviation	Geometry in Rhino by Grasshopper
h1.1	3,4m	3,3m	+3%	
h1.2	4,9m	4,8m	+2,8%	
h2	10,0 m	9,6m	+4%	
w	31,1m	30,6m	+1,6%	
l	68,8m	70m	-1,7%	
x	0,540	0,533	+1,2%	
ld1 length	3,4m	3,3m	+3%	
ld2 length	4,9m	4,8m	+2,8%	
ld3 length	17,6m	17,4m	+1,1%	
ld4 length	15,2m	15,0m	+1,3%	

Table 55: geometry output case E based on 3DBAG, source: own work

The 3DBAG is relatively accurate, but does tend to overestimate dimensions. The deviations are within an acceptable margin, comparable to the margins the Karamba3D calculations have. The portal will now be generated and structurally analysed by Karamba3D. The visual output is depicted in Table 56. The results of the quickscan are listed in Table 57.

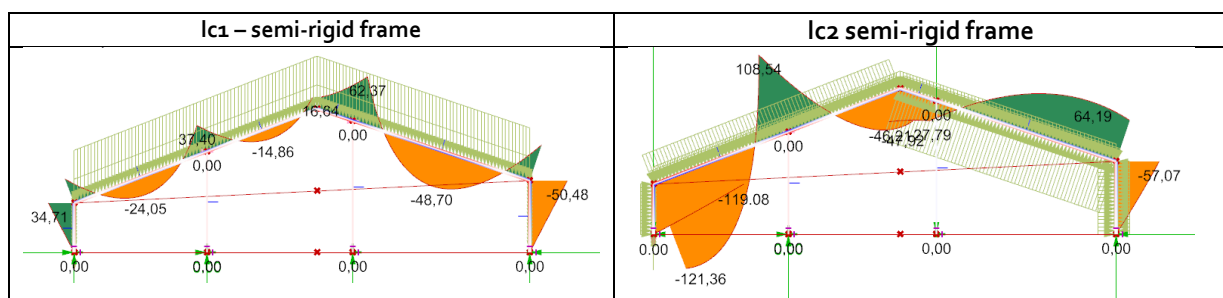


Table 56: visual output structural analysis case E, source: own work

Element	Length [m]	Quantity	Profile type lc1	Profile type lc2	Final Profile Selection	Reality
ld1	3.3	10	HEA140	HEA220	HEA220	HEA200
ld2	3.3	10	HEA160	HEA220	HEA220	HEA200
ld3	15.6	10	IPE200	IPE300	IPE300	IPE300
ld4	15.6	10	IPE240	IPE300	IPE300	IPE300

Table 57: quickscan output case E – semi-rigid frame, source: own work

Comparing the quickscan output with the real scenario, it seems the model predicts the length and the quantity of the model correctly. Moreover, the suggested profile types are correctly predicted in case of elements id3 and id4, in this case as IPE300. The largest suggest profile size is leading, a profile might suffice for one load case but not for another. The output for element id1 and id2 only slightly deviates, suggesting HEA220 profiles, whereas in reality HEA200 profiles are used.

5.2.6 Case F – Dairy hall, Een

This case can be considered somewhat hypothetical, as the hall itself has not been constructed yet. However, the set of drawings found for this hall also refers the structural calculations that have been executed, this means the columns and beams listed in the drawings are not merely suggestive but backed by structural engineers. Therefore case F can still be considered a valid case that can be used to evaluate the quick scan tool.

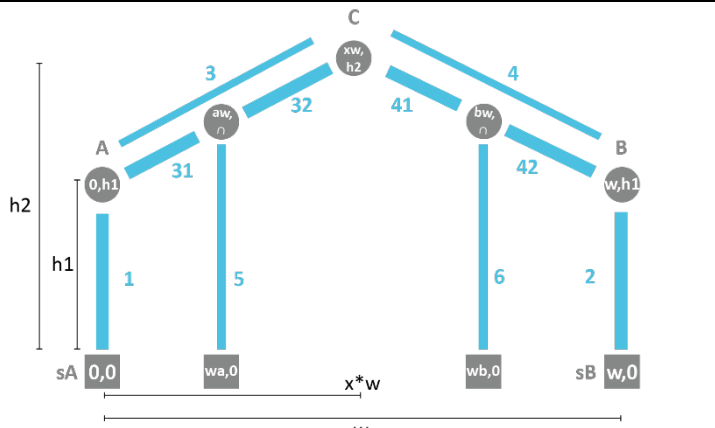
Portal properties	Value	Portal Definition
w	32.4m	
h1	3.4m	
h2	9.9m	
wa	8.2m	
wb	24m	
Spacing	5.4m	
Cladding	Medium	
Wind area	III-open	
Mechanical setup	Semi-rigid frame	

Table 58: input values case F, source: own work

This case hall is not included in the 3DBAG dataset, as it has not been built yet. Therefore the manual inputs as shown in have been used, based on the construction plans of the hall. The input values were then converted into a portal by the Karamba3D model, resulting in the following visual output listed in Table 59.

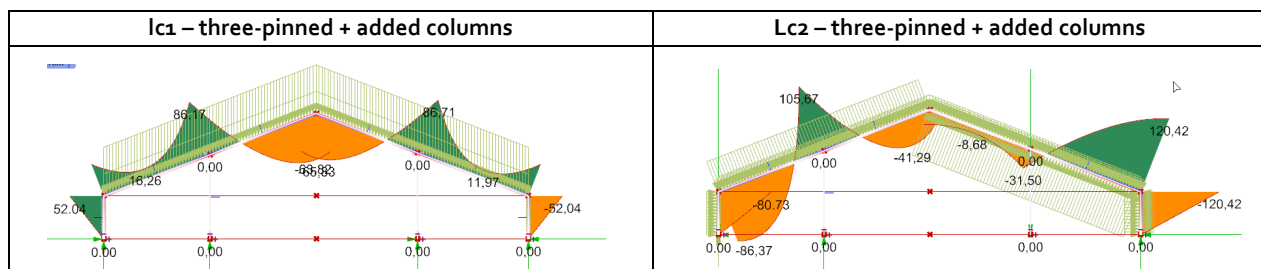


Table 59: visual output structural analysis case F - three-pinned + added columns, source: own work

Element	Length [m]	Quantity	Profile type lc1	Profile type lc2	Final Profile Selection	Reality
ld1	3.3	13	HEA180	HEA200	HEA200	HEA180
ld2	3.3	13	HEA180	HEA200	HEA200	HEA180
ld3	13.8	13	IPE270	IPE300	IPE300	IPE300
ld4	13.8	13	IPE270	IPE300	IPE300	IPE300

Table 60: results output quickscan, source: own work

Comparing the quickscan output with the real scenario (Table 60), it seems the model predicts the length and the quantity of the model correctly. The quantity of the elements is also correctly predicted. Moreover, the suggested profile types are correctly predicted in case of elements id3 and id4, in this case as IPE300. The largest suggest profile size is leading, a profile might suffice for one load case but not for another. The output for element id1 and id2 only slightly deviates, suggesting HEA200 profiles, whereas in reality HEA180 profiles are used.

5.2.7 Case G1 - Meat Pig Hall, Hengelo

This is one of the four halls located on one farm. It is the biggest hall of not only these four, but all the cases included in this research. Sections of all 4 halls on this location have been found, however, this is the only hall of which more detailed information is available. The other 3 halls (G2-G4) can still be used to test the accuracy of the 3DBAG input, as they are all included in the 3DBAG-data. These analyses have been included in the appendix (F). Input for the analysis of hall G1 is included in Table 61. The output based on the 3DBAG is listed in Table 62 and is compared to the real scenario.


Portal Properties	Value	3DBAG visual	Attribute list																		
Data tile	787		<table><tr><th>Attribute</th><th>Value</th></tr><tr><td>Tile number</td><td>± 787</td></tr><tr><td>identificatie</td><td>NL_IMBAG_Pand.1876100000010142</td></tr><tr><td>h_maaiveld</td><td>10.724</td></tr><tr><td>h_dak_70p</td><td>17.168281</td></tr><tr><td>dak_type</td><td>slanted</td></tr><tr><td>pw_bron</td><td>ahn3</td></tr><tr><td>pw_datum</td><td>2017-12-01</td></tr><tr><td>val3dity_codes</td><td>[]</td></tr></table>	Attribute	Value	Tile number	± 787	identificatie	NL_IMBAG_Pand.1876100000010142	h_maaiveld	10.724	h_dak_70p	17.168281	dak_type	slanted	pw_bron	ahn3	pw_datum	2017-12-01	val3dity_codes	[]
Attribute	Value																				
Tile number	± 787																				
identificatie	NL_IMBAG_Pand.1876100000010142																				
h_maaiveld	10.724																				
h_dak_70p	17.168281																				
dak_type	slanted																				
pw_bron	ahn3																				
pw_datum	2017-12-01																				
val3dity_codes	[]																				
Pand code	1876100000010142																				
Spacing	5.5m																				
Cladding	Medium																				
Wind area	III-Open																				
Mechanical setup	Rigid frame																				

Table 61: input values case G1, source: 3DBAG, own work

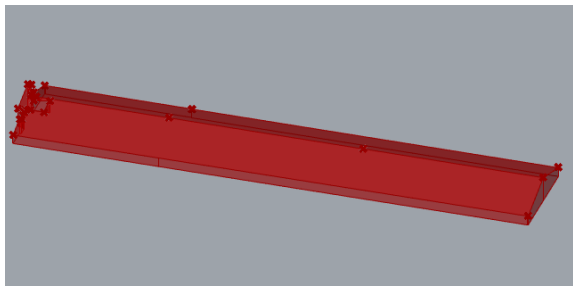
	3DBAG output [m]	Real value	Deviation	Geometry in Rhino by Grasshopper
h1.1	2.7	2.6	+3,8%	
h1.2	2.7	2.6	+3,8%	
h2	7.8	7.7	+1,3%	
w	30	30.3	-0,9%	
l	162	160	+1,2%	
x		0.5	0	
Id1 length	2.6	2.5	+4%	
Id2 length	2.6	2.5	+4%	
Id3 length	15.2	15.8	-3,9%	
Id4 length	15.2	16.8	-3,9%	

Table 62: geometry output case G1 based on 3DBAG, source: own work

The 3DBAG is relatively accurate, but does tend to overestimate the dimensions. The deviations are within an acceptable margin, comparable to the margin of error the Karamba3D calculations have. The portal will now be generated and structurally analysed by Karamba3D. The visual output is depicted in Table 63. The results of the quickscan are listed in Table 64.

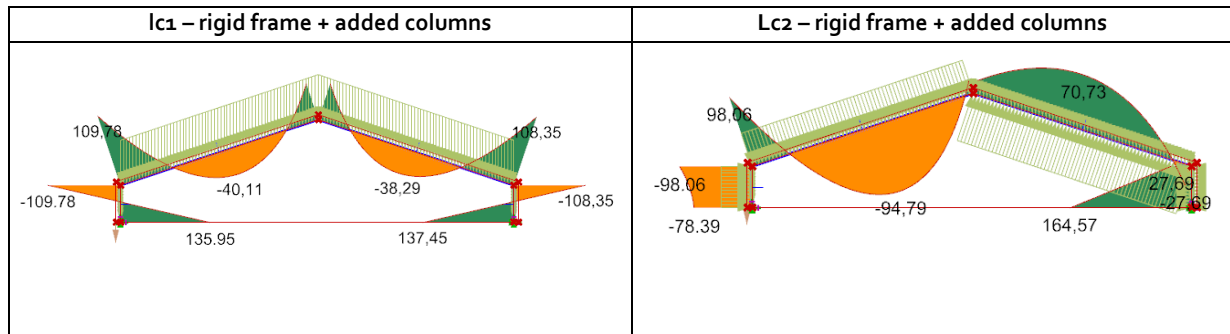


Table 63: visual output structural analysis case G1 - rigid frame, source: own work

Element	Length [m]	Quantity	Profile type lc1	Profile type lc2	Final Profile Selection	Reality
ld1	2.6	28	IPE300	IPE330	IPE330	IPE270
ld2	2.6	28	IPE300	IPE330	IPE330	IPE270
ld3	15.2	28	IPE300	IPE240	IPE300	IPE300
ld4	15.2	28	IPE300	IPE240	IPE300	IPE300

Table 64: output results quickscan case G1, source: own work

Comparing the quickscan output with the real scenario, it seems the model predicts the length and the quantity of the model correctly. It underestimates the length of id3 and id4, but in the case of retrieving elements it is better to underestimate than to overestimate. The quantity of the elements is also correctly predicted. The output for element id1 and id2 deviates 2 classes, suggesting IPE330 profiles, whereas in reality IPE270 profiles are used. No direct cause of this deviation could be found. Other static setups lead to even bigger deviations, and even with a smaller portal spacing (5m) and light cladding it remains deviated 2 classes.

5.2.8 Conclusions based on case study

Based on these analysis, conclusions on the accuracy of the predictions made by the tool can be drawn. The predictions are assessed on three of the four main factors the tool intends to map out: element length, element quantity and element type. Element quality will be assessed in the next chapter.

• Element lengths

Whenever the manual input was used, the accuracy of the element length is practically 100%, as the dimensions that can be found in the drawings of the halls have been used. More interesting is to assess the accuracy of the 3DBAG output, as this script is going to be used when drawings or reports on a hall are not available. Percentual deviations of all analysed elements are shown in Table 65. As the values shows, the average deviation set well below 3%. Columns are overestimated, whereas spanning beams are under estimated. Correction factor of the average column deviation could be implanted in the script to counter for this, even when it means that in some cases, columns are underestimated because underestimation of length is preferred for designers aiming to reuse these components.. If designers assume a larger length the beams can always be cut to shorter lengths. Having to extend a beam that was assumed to be longer creates more problems. Nevertheless, the target set in paragraph 4.1 of a maximum deviation of 5% is reached.

	C	D	E	G1	G2	G3	G4	Average
Id1	+2,8%	-0,3%	+3%	+4%	+1,2%	+5%	0%	+2,24%
Id2	+3,1%	-0,3%	+2,8%	+4%	+1,2%	+5%	0%	+2,26%
Id3	0%	-0,7%	+1,1%	-3,9%	+2,2%	+1,3%	+3,3%	+0,62%
Id4	-1,6%	-0,7%	+1,3%	-3,9%	+2,2%	+1,3%	+3,3%	+0,42%

Table 65: 3DBAG accuracy analysis, source: own work

- **Element quantities**

Element quantities have been predicted 100% accurately, which is no surprise as the portal spacing is the factor that most strongly influences this output, and was given for all the halls analysed. Another factor that could influence this output would be the length of the hall, which in the case of manual input is accurately known. The length analysis of the 3DBAG could have had an effect on the quantity, however the deviations here are much smaller than the average portal spacing and therefore do not affect the results to a significant degree (see Table 66).

	C	D	E	G1	G2	G3	G4	Average
Length	+1,8%	+0,3%	-1,7%	+1,2%				+2,38%
Absolute	+0,9m	+0,4m	-1,2m	+2m				

Table 66: 3DBAG accuracy analysis b, source: own work

- **Element type**

The output results of the quickscan tool in case A, B, E and F meet the target that was set; maximum of one profile in deviation. Case D and G1 both have elements overestimated with two classes. For case D, this is caused by the sue of hybrid profiles as spanning beams, whereas the reason of the extra deviation for hall G1 cannot directly be explained. Case C presents a complete mismatch, which is caused by the results of loadcase 2, indicating the used wind pressure coefficients on these elements might not be correct for the situation applied in the analysis. The wind direction might also be a cause of the large deviations. The deviations per element are listed in Table 67. It shows the average deviation for both columns and beams is +1,15. It must be noted that this relatively high value is mainly cause by the strong deviation od case C. Therefore, an extra table (Table 67) is added in which only loadcase 1 is considered for case C, assuming the loadcase 2 calculation is invalid. This shows an average deviation closer to overestimating about half a profile. The developed tool matches the accuracy target set in paragraph 4.1 , provided that the deviating results of hall C are caused by an error in the lc2 analysis.

	A	B	C	D	E	F	G	Average
Id1;id2	+1	0	+3	0	+1	+1	+2	+1,15
Id3;id4	0	+1	+5	+2	0	0	0	+1,15

Table 67: Profile deviation quickscan output, source: own work

	A	B	C (lc1)	D	E	F	G	Average
Id1;id2	+1	0	-1	0	+1	+1	+2	+0,57
Id3;id4	0	+1	0	+2	0	0	0	+0,43

Table 68: Profile deviation quickscan output V2, source: own work

5.3 Model iterations

During the process of testing and evaluating, some issues showed up that required to rework the Karamba3D model. Some of these iterations are an evolution of the general model, other iterations ended up as a separate version that could be applied to a specific scenario. The process of developing iterations was also used to explore the broader applications for this tool.

5.3.1 Input for asymmetric halls

In order to analyse asymmetric halls, the list of manual input values needs to be extended, as id1 and id2 will have different heights. The portal is still generated using 5 points, of which point A, B and C define the (asymmetric) shape of the hall (. The definition of point A and B slightly changes, distinguishing a h1.1 and h1.2. For point C, the input value of x needs to become parametric, defining the horizontal location of the ridge as a factor of the total width. The definition of point C does not change. For the manual input this means extra input sliders for h1.1 and h1.2 were added. The h1 slider remains and a button is included to switch between symmetrical and asymmetrical halls, the former requiring just h1 as input, the latter both h1.1. and h1.2. Above that, the slider to change value x (for symmetrical halls considered to be 0.5) should be included in the input tab.

Point	Coordinate
sA	(0,0)
sB	(w,0)
A	(0,h1.1)
B	(w,h1.2)
C	(xw,h2)

Table 6g: Point definition, source: own work

The current conversion from 3DBAG data to portal assumes the hall is symmetrical. The BAG-3D viewer however depicts the correct shape of the hall. This indicates there should be a way to retrieve this asymmetric shape from the data set and use it as input in this iterated version of the model. This requires a deeper understanding of how the 3DBAG data is structured. As mentioned before, the AHN data consists of height points measured by a satellite using LiDAR technology. The current AHN data has a resolution of 8 points per square meter. Each of these points has an x,y,z-coordinate, resulting in a point cloud that looks like Figure 23

Put in a very simplified way, the coordinates of these point clouds are then compared to the BAG-data. By comparing these two sets of data, it is possible to locate which points fall within a building's footprint and are part of the building's geometry. A maximum

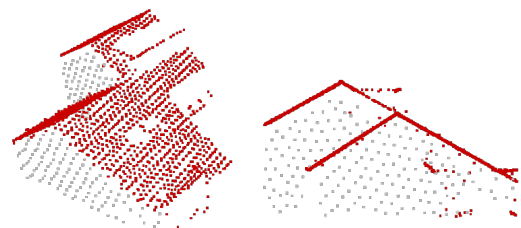


Figure 12: Point clouds, source: 3DBAG

height, minimum height and roof angle can be derived from the information; these are the lines of information in the dataset that have been used to derive the geometry of the portal before. However, within the JSON file that is used for the BAG-input of the quickscan tool, these point clouds are fully included. The point clouds are used to generate the surfaces of a building, displaying the volume of the building in Grasshopper, the 3DBAG viewer or other JSON-viewers such as Ninja. These surfaces can be used to gain more detailed information on the exact shape of the building.

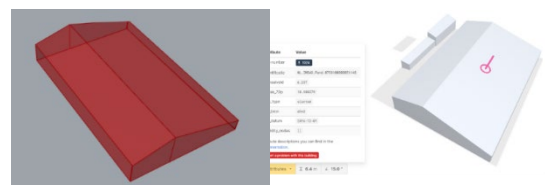


Figure 24: Example geometry, source: 3DBAG + own work

To show how this information can be retrieved an example of a clearly asymmetrical hall is used as a case (Figure 24).

The 'pand code' of the building is used as input to select and only display this specific building. The grasshopper conversion shows the generated surfaces that are based on the point clouds. Each of these separate surfaces can be selected and analysed on their geometry. To define the geometry of the section, it would seem logical to pick the section walls, as they give the shape of the portal. However, the surfaces are randomly listed, which means the list first needs to be sorted (based on a specific property) to pick the right surfaces. As these surface walls are split up in two separate surfaces and the number and order of surfaces in the list can vary per selected building, it is hard to sort the list in a general way to identify these surfaces for all different sorts of buildings. This is why the choice has been made to select the floor and roof surfaces for this analysis instead. These can be easily sorted out, as these three surfaces have the largest surface area. By sorting the list of surfaces based on area, the top surface on the list is the floor surface, followed by the two roof surfaces. Using the outer vertices of these surfaces, h1.1, h1.2, h2 and w can be defined (Figure 25). To find these vertices, the short sides of the roof surfaces need to be identified. This works in a similar way, where the randomly organised list is organised on a property, in this case length. The longest line will be in the length direction of the hall. The length value retrieved from one of these lines can be used as the length input for the model.

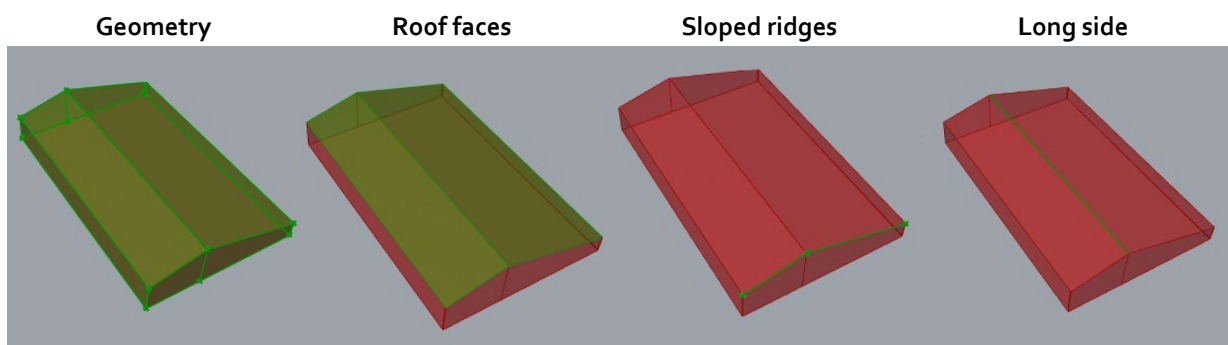


Figure 25: Surface selection, source: own work

In case of a perfectly generated geometry, the third and fourth longest line of the roof surface would be the sloped ridges. However, due to the way they are generated, this does often not apply, especially to geometries of combined buildings such as the example of case C (see Figure 26). In this specific case the line connecting the roof surface of the larger and the smaller volume is considered the third largest, and the free roof ridge that is left over turns out to be the fourth longest. This is incorrect and cause the wrong geometry to be generated. A property the lines of the sloped roofs have in common is that they are angled $0^\circ < 90^\circ$ compared to the z-axis, whereas the horizontal lines make perfect 0 or 90 degree angles with this axis. By removing lines that have an exact 0 or 90 degree angle from the list, your left over with just the sloped lines. Of these, the first and second longest actually can be

considered the sloped roof ridges. The line selection within script has been adjusted applying this selection method for the sloped sides.

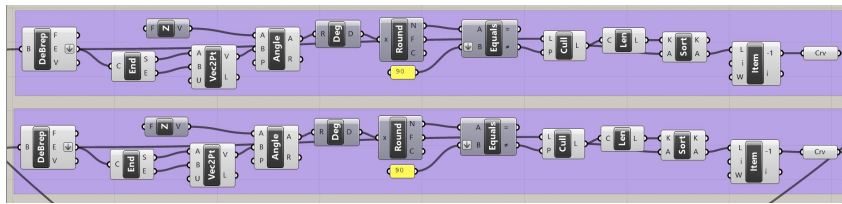
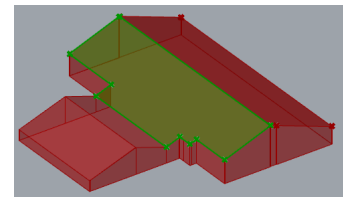


Figure 13: Line selection on complex surface, source: own work



Because of the random order of the list, it can vary per geometry which short side of the roof and floor surface is selected. For the z-coordinates of these points that does not matter, but it does for the x- and y-coordinates. Above that, the orientation of the building is based on the location of the building on map. This orientation needs to be taken into account when defining the position of the end points. This issue can be tackled by using relative distance and relative position. First, the length of h1.1 and h1.2 is defined. This can be done by subtracting the z-coordinate of point A/B with the z-coordinate of point sA/sB. For an asymmetrical hall, the horizontal distance between A-C and B-C is different. This means not just w, but w1 and w2 need to be defined. Note that $w_1 + w_2 = w$, with w1 being A-C and w2 being B-C. By subtracting the x- and y-coordinates of the endpoints of the diagonal of the roof surface, the relative x- and y-distance can be found. Applying Pythagoras theorem (Figure 27), the diagonal of the triangle created by relative distance x and y equals either w1 or w2, based on which roof surfaces is selected. The formula to define w1 and w2: $\sqrt{dx^2 + dy^2}$. Because of dx and dy are squared, it does not matter for the calculation whether dx and dy are positive or negative.

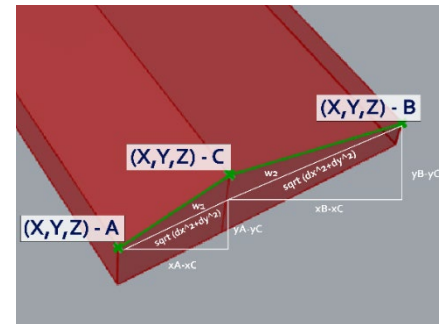


Figure 14: Defining relative distance, source: own work

Now that h1.1, h1.2, w1 and w2 are defined (Table 70), the portal can be generated. The new input points slightly differentiate to incorporate the difference between h1.1/h1.2 and w1/w2, but the principle behind it is the same. These five point are used to generate 4 lines, which contrary to the symmetrical output all have different lengths. This means the calculations performed by the tool will provide different outputs per element, and can end up suggesting 4 different profiles that make up the portal. This though is very unlikely to occur in reality due to practicality and economics, especially in cases where the difference between w1/w2 and h1.1/h1.2 are relatively small. It is likely that the columns (id1, id2) and the beams (id3, id4) are similar in size due to economic reasons and connection design (Hollander & Eldik, 2017). This means the larger profile between them can be assumed profile selected for both members. The described iteration of the BAG input conversion is added into the original quickscan

Point	Coordinate
sA	(0,0)
sB	(w1+w2,0)
A	(0,h1.1)
B	(w1+w2,h1.2)
C	(w1,h2)

Table 70: Point definition based on 3DBAG, source: own work

model, replacing the former BAG input tab. Although this conversion is more complicated, even minor asymmetries are now accounted for.

5.3.2 Secondary supporting elements

The input given for hall B resulted in the quickscan suggesting profiles almost twice the actual size. As aforementioned, the most likely reason of this error is the presence of secondary supporting columns, having a more significant structural function than expected beforehand. Case C, E and F also shows extra columns possibly supporting the roof, suggesting that these type of columns occur more often and as they can influence the end result, the tool should provide an option to include them in the analysis. Two main steps need to be taken to include these columns:

1. Define and generate the column's geometry
2. Assemble the column into the structural Karamba3D analysis

The geometry of the column can be approached as a line that spans vertically between a point on line sA-sB and a point on line A-C or B-C. The column always stands on a 90 degree angle with sA-sB, the angle with A-C and/or B-C will depend on the geometry of the hall. A point or a set of points can be generated on line sA-sB at a set distance (w_a , w_b) from sA. These points (sA' , sB') will function as supports for the columns. Distances w_a and w_b are most likely unknown. These values can be based on estimation. In case of a symmetrical hall like hall B, these points are assumed to be at $1/4^{th}$ ($= 0,5*w_1$) and $3/4^{th}$ ($= w_1 + 0,5*w_2$). A second point or set of points can be generated on the spanning beams, line A-C and/or B-C, by drawing a vertical line with a length longer than h_2 (for example h_2+1m) in the z-direction and using the intersection between these vertical lines and A-C and B-C as the end points for the columns. These points will be labelled 'ac' and 'bc' depending between which main points it is situated (see Table 71).

Point	Coordinate	Model definition
sA	(0,0)	
sB	(w1+w2,0)	
A	(0,h1.1)	
B	(w1+w2,h1.2)	
C	(w1,h2)	
sA'	(wa,0)	
sB'	(wb,0)	
ac	$\cap (A-C;w_a)$	
bc	$\cap (B-C;w_b)$	

Table 71: Model definition added elements, source: own work

columns can be HEA, box- or even circular tube-profiles. The latter two come in various thicknesses, all influencing the structural properties of the cross section. Above that, the uncertainty of the position of the added columns makes their actual length a more uncertain property compared to id1-id4. Therefore the information on these column is relatively suggestive, but can still be useful for designers looking for smaller steel profiles. However, as the exact positioning of these columns is generally unknown, the output length that is coupled with these profiles has a much larger margin of error. Added to that is the fact that for these columns, not only HEA-profiles but box-profiles and tube-profiles might be used, so these output results should be considered relatively unspecified for now.

The steps required to add these columns require the script to be reworked to a large extent. The addition of extra points, connections and beam elements make that this iteration is hard to implement in the main model, especially given that with the columns turned off, the connections at point ac and bc become problematic as they have an unidentified member. This iteration can however be included as an extra branch of the tool. If the hall has no extra supporting columns, the tool should select the original script. If a hall has one extra supporting column, it should select a script in which only one column is generated, and similarly with two columns. This is impossible to pull off with grasshopper itself, but a more developed version of the quickscan could select a script before it continues to accept further input (see Figure 29). The possible input values would differ per script, and so would the component tagging. These adjusted scripts are linked to the manual input, but the BAG-input can be included over time.

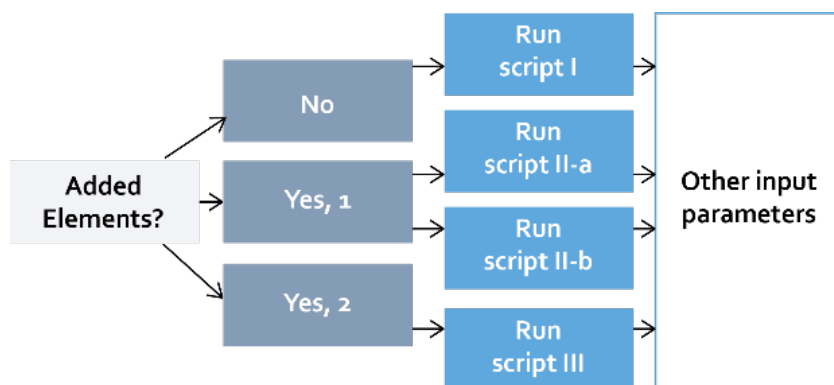


Figure 16: Script selection, source: own work

5.3.3 Structural optimization

Grasshopper allows for the use and integration of optimization software within the script. Although the quickscan tool is used to analyse existing structures rather than designing new ones, optimization software can be used to predict better results in case of unknown input factors. As the sensitivity analysis showed, the static setup of the portal has a great influence on the output of the model. However it is also the input factor with the highest uncertainty, given that the directly available geometric and visual data do not provide any clue of the static setup. The only assumption that can be made, is a static setup that is as cost-effective as possible, since most hall structures have a solely economic purpose. The simplest way of reducing cost is to reduce material, meaning smaller profiles are generally more desirable. **Source.** Instead of having to manually try out every possible static setup and then comparing the results, an optimization tool can be linked to this process, running all possible static scenario's and selecting the one suggesting the smallest profiles. The static setup is defined by the 5 connection points, which can either be a hinge connection/support or a moment connection/support. This means in total 32 (2^5) possible static setups can be considered by the quickscan tool.

A grasshopper plugin that can be implemented in order to achieve this selection, is Galapagos. This component runs multiple calculations and seeks either a maximum or a minimum value. Table 72 shows how Galapagos input relates to the quickscan tool.

Galapagos	Description	Quickscan tool
Genome	Parameter	Static connections
Fitness	Optimization goal	Lowest [mm ³]

Table 72: Galapagos relation to quickscan, source: own work

The genome input must be connected to a **number slider**, requiring defined connection types represented as values on a slider. A moment connection is assigned 0 and a hinge connection is assigned 1, allowing a 0-to-1 slider to be connected to each component defining the connections. The same method can be used for supports. However, a risk of this strategy is that out of the 32 possible static setups, an illogical setup may be wrongly identified as the most beneficial scenario. This is because the wind load analysis only considers wind from one direction, while in reality, the wind can come from multiple directions. An illogical setup example would be having sA as a pin support and sB as a fixed support due to wind loading, which would need to be flipped when the wind comes from the opposite direction. To avoid this issue, only preselected static setups actually applied in practice should be considered. This can be achieved by translating these static setups into numerical lists, identifying each support or connection type with a number (Table 73). These lists can then be linked to a **list item** component, to which a **number slider** component can be connected.

Point/setup	Three-pinned	Semi-rigid	Rigid Frame	Hinged girder	Supports
sA	5	5	0	0	5 = pin 0 = fixed
sB	5	5	0	0	
A	1	1	1	0	Connections
B	1	1	1	0	0 = hinge 1 = moment
C	0	1	1	1	

Table 73: numerical translation of static setup, source: own work

This adjustment not only makes the input ready for a Galapagos application, but also simplifies the input of the mechanical setup from five individual **value list** controlling every single support and connection to one **value list** controlling all five points, allowing the user to select a preselected static setup. This improved script element is added to all versions of the script. The various load cases affect each individual structural element differently. As a consequence, a really low section modulus for one element does not necessarily mean it is the optimal situation when other profiles suggestions are much larger. A potential way to tackle this would be to not consider the calculated section modulus of each individual structural member, but to consider the calculated sum of all. This will result in the tool selecting a static setup that is on average the most efficient. After selecting the setup, the tool will proceed in a regular way, analysing each specific structural member and calculating a suggested profile size for each element.

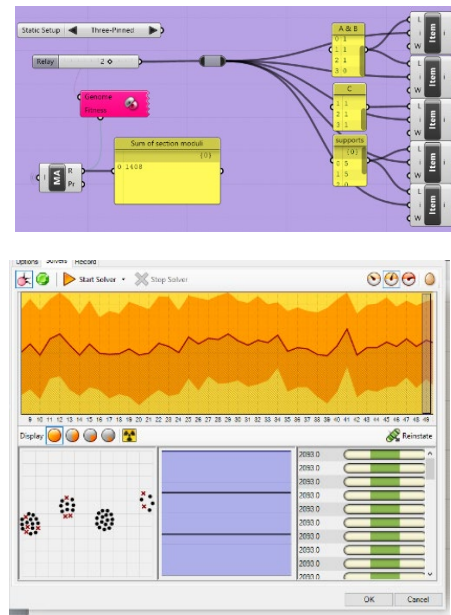


Figure 17: Static optimization in grasshopper, source: own work

To check the optimization (Figure 30) and the hypothesis that the lowest sum of section moduli is results in the smallest profile output, the basic portal setup used in paragraph 5.1 is used again. The results of these tests are listed in Table 74 and 75. After an analysis for loadcase 1 and loadcase 2, Galapagos concluded that the rigid frame setup would lead to the lowest sum of section moduli.

Lc1	Id1	Id2	Id3	Id4	Sum
Three-pinned	HEA220	HEA220	IPE300	IPE300	2016
Rigid frame	HEA200	HEA200	IPE270	IPE270	1408
Semi-rigid frame	HEA220	HEA220	IPE300	IPE300	1796
Hinged girder	HEA280	HEA280	IPE270	IPE270	2486

Table 74: optimization results lc1, source own work

Lc2	Id1	Id2	Id3	Id4	Sum
Three-pinned	HEA200	HEA200	IPE270	IPE270	1037
Rigid frame	HEA200	HEA200	IPE220	IPE220	938
Semi-rigid frame	HEA200	HEA200	IPE270	IPE270	1039
Hinged girder	HEA220	HEA220	IPE240	IPE240	1002

Table 75: optimization results lc2, source: own work

Connecting Galapagos to the selection procedure turned out less practical than assumed. The optimization keeps running for a long time before giving a definitive answer, even though it only has to compare 4 outputs. This probably has to do with the nature of the Galapagos component, that was designed to go through a bulk of options to then start inching in on an optimization. The optimization is too simple for Galapagos, which causes it to keep looking for answers. To put it metaphorically: it's like trying to hit a small nail with a giant sledgehammer. A simpler solution would be to have the sum of the section moduli displayed close to the static setup input, so users of the tool can judge themselves which static set up to pick.

5.3.4 Correction Factor

The results the tool provides are generally overestimations of the actual profiles that can be found within the halls. As described earlier, overestimations could lead to designers assuming stronger profiles than what eventually will be retrieved, resulting in potentially major changes that have to be made late in the design process to adjust for these weaker profiles. Given that the tool is an approximation of reality rather than an exact representation, applying a correction factor for the model overestimating is the most straightforward way to deal with this issue. Table 68 is presented here again to show the deviations of the results:

	A	B	C (lc1)	D	E	F	G	Average
Id1;id2	+1	0	-1	0	+1	+1	+2	+0,57
Id3;id4	0	+1	0	+2	0	0	0	+0,43

Table 68: Profile deviation quickscan output V2, source: own work

The results show an average deviation of about half a profile class. It is not possible to subtract half a profile class from each element, as half profile classes do not exist. The first and simplest correction factor that could then be applied to the results would be (class – 1). Table 68a shows these results:

	A	B	C (lc1)	D	E	F	G	Average
Id1;id2	0	-1	-2	-1	0	0	+1	-0,43
Id3;id4	-1	0	-1	+1	-1	-1	-1	-0,57

Table 68a: Profile deviation quickscan output V2, source: own work

The average deviation stays the same, however, is now negative meaning it underestimates rather than over estimates. In that light, a -1 correction factor looks like an improvement, with only 2 overestimations of just one profile class. Another consequence is the number of correct matches drops from 7 to 4, making the results less accurate than before the correction is applied. Therefore, a different approach has been tried that does not focus on the profile classes, but on the calculated section moduli. This should lead to a more precise correction, allowing for 'half profile classes' to be somewhat included. This correction factor is based on the fact that the tool calculates a required section modulus and then rounds up to the nearest ceiling

within the section moduli list, ensuring the selected profile is strong enough. This can become problematic when a section modulus threshold is exceeded by just a few mm³. For example, if the tool calculates a required section modulus of 326, an IPE 240 with a section modulus of 324 is considered to be insufficient, therefore the larger IPE270 (sec. modulus: 429) is selected, whereas the 2 mm³ excess could very well be caused by the model's margin. On the other hand, if the required section modulus would for example be 427, 429 is definitely required and just rounding down a profile class would be the wrong move to make. The range step in section moduli between each profile is different, varying from a 14 mm³ between IPE80/IPE100 up to 628mm³ between IPE550/IPE600. This further illustrates why simply subtracting a profile class is problematic. In order to subtract half a profile class, the floor and ceiling profile class of any given required section modulus needs to be defined. To come back to the earlier example; IPE240 and IPE270. Any required section modulus that falls within the 324-429 range (spanning 105mm³) gets assigned an IPE270. Subtracting half a profile would be equal by subtracting half the range between the floor and ceiling profile, in this case 52mm³. This means required section moduli in the lower section of the range are rounded towards the floor profile (e.g. 364, 364-52 = 312, rounded tot 324, IPE240), whereas higher values are round up to the ceiling profile (e.g. 404, 404-52 = 362, rounded tot 429, IPE270). By applying this 'half a profile class' correction factor to the tool, the output results are as follows (Table 68b):

	A	B	C (lc1)	D	E	F	G	Average
ld1;id2	0	0	-1	0	0	+1	+1	+0,14
ld3;id4	0	+1	0	+1	-1	0	0	+0,14

Table 68b: Profile deviation quickscan output V2, source: own work

The tool now only suggests profile deviations with a maximum of one class, and on average an overestimation of +0,14. This shows that the new approach of a correction factor leads to more fruitful results. The number of correct predictions also increased, implying that the accuracy of the tool is also improved. However, it still remains a case of overestimation. This could also be due to the relatively small batch size, therefor it is recommended that for further development and research, more cases are tested in order to further finetune the applied correction factor. An element of script has been included in the tool to provide the correction factor calculations

5.3.5 Version Management

The various iterations and reworks of the script have led to different versions of the model being part of the final product. An overview of the different script versions is shown in Figure 31. The figure shows the gradual development of the tool over time. Eventually the 3DBAG input should get the extra supporting elements included as well. The additional analyses are described in more detail in the next chapter.

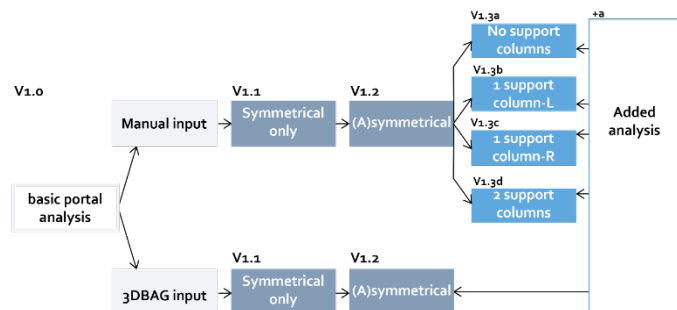


Figure 31: version management, source: own work

6. DECONSTRUCTION AND REUSE

This chapter will go into depth about the practice of reclaiming the elements from the industrial halls. In order to be able to properly reuse the structural elements for new purposes, the practice of deconstruction has to be applied, instead of the usual demolition process. A distinction can be made between proper deconstruction – taking the structure apart bolt by bolt – or simplified deconstruction – cutting out the beam elements, leaving out the specific connecting knots. Both have consequences for the remaining element length, economical and circular performance and for the logistics and efficiency of the process. After deconstruction has taken place, the elements need to be assessed on quality, which influences the remaining structural performance of the retrieved elements. Furthermore, the effects of reuse on cost and its potential impact on the environment are indicated. At the end of this chapter, three new elements are included to the quickscan tool to include the effects of the steps that take place after mapping out the available structural steel components.

6.1 Deconstruction processes

According to Bertino et. al (2020) the method of deconstruction is an approach focused on the selective dismantling of building components, with the aim of future reuse or recycling purposes. The Spanish building code (2018) describes it as follows: deconstruction of steel structures is considered an ordered process of demolition with the goal to separate the components, materials and possible waste for reuse, remanufacture, recycling or repurposing. In practice, deconstruction can take place on multiple levels:

1. functions – removing façade elements from a loadbearing structure
2. within function – disassembling loadbearing structure into elements
3. materials – disassembling a façade, separating insulation, cladding, windows

As this research is focused on reclaiming structural components, the first and second level are relevant. In order to take out the loadbearing structure the elements resting on that structure (façade and roof) first need to be removed as well. Separating materials is relevant for the recycling process, but as reuse is considered more circular than recycling and therefore preferred, not that relevant to the topic of this research. Most of the available literature on structural steel reuse involves the topic of design for deconstruction – not a wrong thing per se, but it requires new products to be designed and introduced. The halls that are central to this specific thesis are already built and generally not designed with deconstruction, but demolition as an end-of-life phase in mind due to the cost of deconstruction. However, the extent to which the principles of design for deconstruction (DfD) apply to these industrial hall structures can give insight to the ability to deconstruct such structures in a proper way. According to the EPA (2015) design for deconstruction requires designers to:

1. Maximize clarity and simplicity
2. Minimize building complexity
3. Minimize different types of materials

4. Minimize number of components
5. Use mechanical fasteners instead of sealants and adhesives
6. Simplify connections
7. Make connections visible/accessible
8. Separate building layers or systems

Almost all of these features of buildings that are meant to be deconstructed apply to industrial hall structures. The structure itself is generally clear and simple; a repetition of a specific portal in one direction, with only the end portals differing in setup. For the loadbearing structure, only steel beams are used. Because industrial halls are almost solely built for functional use, the loadbearing structure and therefore also the connections are uncovered, visible and easily accessible from the inside of the structure. The façade and roof are applied as an outside layer on the structure and do not envelop the structural elements. This ensures the outer layer can be separately removed, leaving the structure standing. Based on the principles of DfD, it suggests that industrial halls lend themselves very well for the process of deconstruction. An example from practice that affirms the ability to deconstruct portal halls is a British company called Portal Power. As a supplier of new and pre-used hall structures, disassembly and relocation of industrial halls is one of the services that Portal Power offers. Their portfolio consists of all sorts of projects, from industrial buildings to horse stables, that are either being converted on site or disassembled and transported to a new location. It must be noted that in this case, the relocated building has a function similar to its prior life, with a similar structural setup (portal hall). For a broader application in the circular economy, it would be preferable if the components could be applied for other purposes.

6.1.1 Considerations and Consequences of Deconstruction

The choice for deconstruction instead of demolition is based on different aspects, but most important of all are cost and time efficiency. Compared to regular demolition, deconstruction is an intensive process that requires planning, labour and the right machinery. If the costs for deconstruction are outnumbering the cost savings that reusing reclaimed steel has over using new steel, the incentive of steel reuse is lost (Gorgolewski & Morretin, 2009; Geyer et. al, 2002).

	Demolition	Deconstruction
Duration	Several days	Several weeks
Economics	Net Income = (Price paid by owner) - (Pre-Demolition + Demolition + Transport + Disposal)	Net income = (Price paid by owner + Salvage Value) - (Pre-Deconstruction + Deconstruction + Processing + Transport + Disposal)

Table 76: demolition vs deconstruction cost, based on: CIB 2001

According to Geyer (2002), the cost of demolition is around double the cost of deconstruction, but demolition also comes with the cost of disposal. According to a study conducted by the US Environmental Protection Agency (2015), the cost of deconstruction can be reduced by up to 30% when materials are salvaged and reused. As industrial halls are relatively homogenous in material composition, the

materials might not be disposed but at least recycled. The example of possible disposal costs introduces the concept of avoided costs and incurred costs (CIB, 2001). These refer to the savings made by reselling and by not disposing the materials (Table 76). However, hard numbers for these savings are hard to define because they depend on many factors – such as market demand, local and regional policies and demolition companies being private companies – making it hard to directly compare demolition and deconstruction. A survey held by the EIB (2019) suggests that demolition companies mainly see the added cost (90%) and a mismatch between supply and demand (70%) as the main reasons why in the end, demolition is chosen over deconstruction and material reclamation.

6.1.2 Disassembly Of Connections

Connections between structural elements are crucial to the process of deconstruction (Huuhka & Hakanen, 2015; Gorgolewski 2008). In the developed quickscan tool, two types of connections are implemented that are relevant to steel portal halls: rigid connections and pinned connections (IdeaStatica, n.d.). The connection types do not only influence the mechanical behaviour of the hall structure, but also the deconstruction process. Hollander & Eldik (2017) define the two connection types respectively as flexible and hinge connections and add that hinge connections follow certain standards, where as flexible (read moment) connections have to be put together by the structural designer. Examples of both connection types are shown in Figure 32.

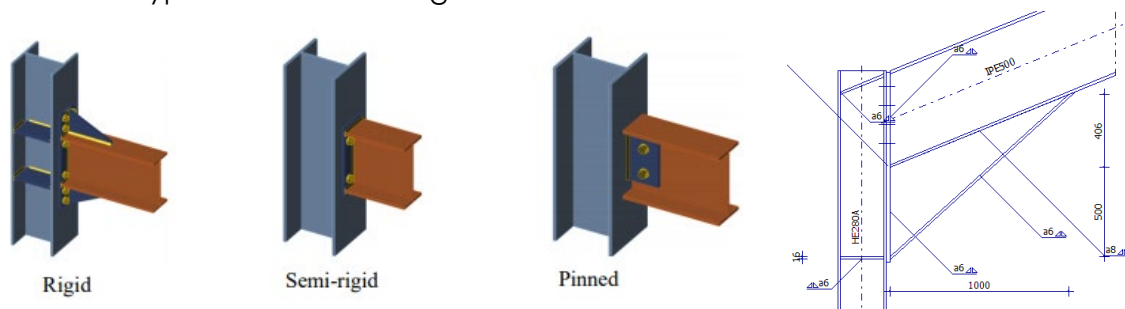


Figure 32: connection types, source: Ideastatica.com

A bolted connection has the benefit of being fully demountable as it involves only dry connection types. Disassembling a bolt connection is relatively simple, especially with the use of pneumatic tools (Infosteel, n.d.). A welded connection is not demountable and will require cutting the connections loose from the structural members. In this case the material that is cut out will be lost and can only be recycled at best. In some cases an extra triangular plate is mounted between the column and the spanning beam. This provides an extra rigid connection and can help with handling larger moments especially in 3-pinned portal, where the maximum moments generally occur at the location where a beam and a column connect. Such a plate is welded to at least one of the structural components. After deconstruction, this plate needs to be cut off to ensure the beam can be reused in a new project.

Because megabarns typically have pitched roofs, the connection between column and beam is practically never a 90 degree angle. This means the beams are cut diagonally at both ends, before they are connected to the columns and to each other in the middle (see Figure 32). The consequence of this design choice is that in the case of a bolted connection, once the beam is disassembled, it is left with angled ends on both sides, that severely limit the reusability of the element, as it can only be connected to another beam in the exact same angle as the roof pitch. This does not pose a problem when the structure is relocated, like in the example of Portal Power, but does create an issue for reuse in another context like an orthogonal structure. This means after deconstruction, the beams need to be cut straight if reuse in another context is preferred. Some steel will get lost in that process, but can be recycled as scrap steel. It will also influence the length of the elements that can be reused. The length that needs to cut off is defined by the angle of the roof – the steeper the angle, the more material is lost. When the roof angle = x° , the length lost for the spanning beams can be defined as:

$$\text{Length lost [m]} = 2 * \tan(x) * \text{profile height [m]}$$

Example: for an IPE220 element of 10m of a portal with a roof with a 20 degree pitch, this leads to a loss of:

$$2 * \tan(20) * 0,22 = 0,16\text{m lost}$$

An element has been added to the quickscan tool that performs this calculation based on the suggested profile height, roof pitch and suggested element length. The outcome of the calculation is subtracted from each element length. This script part has not been included in the evaluations described in the previous paragraph, as those evaluations check whether the quickscan tool can predict the elements present in the hall. It will however be included in the final product as it brings the output closer to predict the actual reusable portion of steel.

6.2 Element quality assessment

Regarding the quality of steel, two factors come in to play. On the one hand the steel grade matters, on the other hand the remaining steel quality due to degradation. To start with steel grade; this is the composition of the steel being used. Small variations in the material composition can strongly influence the performance of the steel (Vanilla Steel, n.d.). As mentioned in paragraph 2.3, carbon steel is the steel type used for most construction projects. Based on the available data used for the quickscan tool, there is no direct way to assess the steel grade within the tool. The only guarantee it can give is that no matter the steel grade, a certain structural performance is achieved. It is however possible and relatively easy to assess the steel grade and composition in a non-destructive way, using optical emission spectrometry (NDO Nederland, 2023). In case of the analysed halls in paragraph 5.2, the available static reports all indicated steel grade S235JR has been used

The other factor, steel quality due to degradation, is possible to include in the tool to some extent. The main reason steel degrades is because of corrosion. Depending on the conditions of both the exterior environment and the interior of a structure, steel can corrode and lose thickness. This loss of thickness impacts the cross-sectional properties of a beam, reducing its area and decreasing the section modulus of the profile. According to Li and Yang (2022), the effect of degradation is taken into account during the design process, accepting that degradation is bound to happen. This means a steel structure is designed for a certain lifespan in which corrosion does take place but within acceptable boundaries. In order to include the effects of degradation in the tool, certain factors must be defined; the effect of degradation on a cross section over a given period of time, the interior and exterior conditions in which the steel corrodes, the amount of time that passed since construction and the cross sectional properties (area and section modulus) of the beam. The goal is not to calculate corrosion as accurately as possible, but to give the user information on what to expect from the remaining quality of the steel components. Based on the *BS EN ISO 12944-2* norm, the conditions of an industrial hall fall somewhere between corrosion category C2 (low) and C3 (medium). This results in a cross sectional material loss of $20\mu\text{m}$ (0.020mm) per year. It must be noted that the effects of corrosion reduce overtime because of saturation (Steel Construction Info, n.d.).

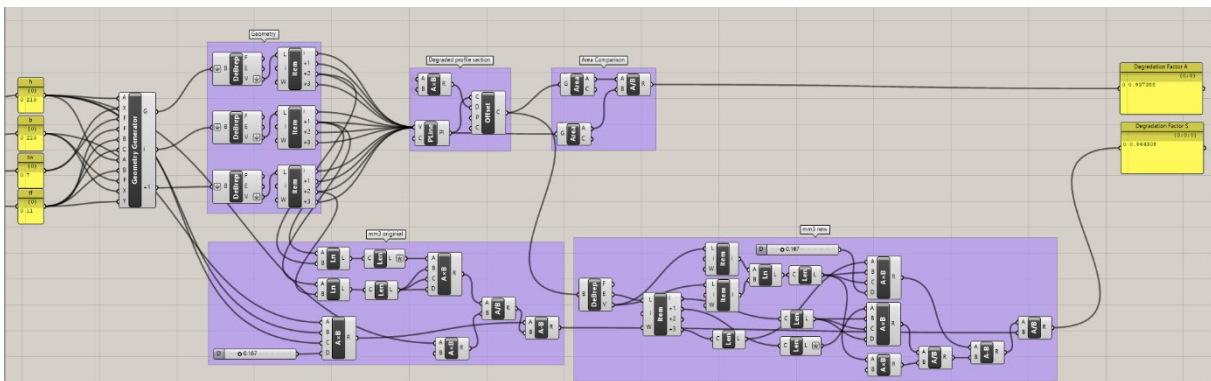


Figure 18: performance factor grasshopper script

A new part of script was developed to include performance reduction by corrosion in the output data of the quickscan tool. The year of construction of an industrial hall can be retrieved from the 3DBAG-data set. Subtracting this from the current year gives the period a hall has been standing in years. Multiplying this by a corrosion factor of 0.020mm/year , this results in a total loss of thickness. If the cross section is seen as an outline, by including an inward offset equal to the total loss of thickness, a new, reduced cross section is created, of which the new area and the section modulus can be calculated. The suggested profile remains part of the output, as designers need these dimensions for their design. However the new area and section modulus need to be included to indicate the remaining structural performance. The script executes a simple area and section modulus calculation based on the width, height, flange and web thickness given from a cross sectional table. This results in area and section modulus values that deviate a little from the original profile,

because it does not take into account the slightly chamfered edge between the web and the flanges. Therefore, instead of having a new area and section modulus as output, the script calculates a remaining performance factor ($\text{Area}_{\text{corrosion}}/\text{Area}_{\text{original}}$; $\text{Section modulus}_{\text{corrosion}}/\text{Section modulus}_{\text{original}}$). This factor indicates the remaining expected performance of a beam, e.g. 0,965 suggests a beam still has 96,5% of its original (cross-sectional) performance. After 15 years, which is the expected lifespan of an industrial hall (Hollander & Eldik, 2007), the remaining performance factor of a profile would be around 0.9, which matches values that Yang and Li (2022) provide in 'Steel Corrosion and Degradation of its Mechanical Properties'. By including this analysis to the script, the effects of material degradation are considered as well. Figure 33 shows the applied script for this part.

6.3 Effectiveness of reuse

In order for designers and other stakeholders to engage in the process of steel component reuse, the costs, benefits and environmental savings need to be indicated early in the process (Gorgolewski & Morretin, 2009; Huuhka & Hakanen, 2015). The effectiveness of the quickscan tool can be improved by having the tool estimate the impact of reusing the expected steel output of a hall. The only way of doing so is by generalizing situations, using values and indicators from literature and comparing the reuse scenario with a non-reuse scenario. Three domains of impact can be identified:

1. Economical (€)
2. Environmental(CO_2)
3. Energetic (MJ)

6.3.1 Economical

The economic impact for a design with a reuse scenario is defined by the added costs of deconstruction and storage – the cost benefit of using reused elements. The economic benefit (R) of reusing steel element can then be defined according to the following formula, based on CIB (2001), Table 77 explains the values:

$$R = (p_{\text{new}} - p_{\text{reused}}) * m_{\text{steel}} - (C_{\text{transport}} + C_{\text{storage}} + (C_{\text{dec}} - C_{\text{dem}} - C_{\text{recycle}}))$$

The market value of steel will strongly influence ($p_{\text{new}} - p_{\text{reused}}$). This is the difference in price per price difference between a new beam and a reused beam. If a reused beam is more expensive than a new beam, the financial incentive to use reclaimed materials is gone. Similarly, if selling a reused beam brings in less money than selling it to a scrapyard, there is no financial incentive to sell it for reuse either. This creates a goldilocks zone in which the market price of a reused beam should be. This goldilocks zone will shift over time because of fluctuating market prices, but at the time the research for this paper was conducted – early 2023 – the following market prices were found (Brink Staalbouw, 2023):

Symbol	Value	Unit
p_{new}	Price new steel	€/kg
p_{reused}	Price reuse steel	€/kg
m_{steel}	Mass reclaimed steel	kg
$C_{\text{transport}}$	Cost transport	€/kg
C_{storage}	Cost storage	€/kg
C_{dec}	Deconstruction cost	€/kg
C_{dem}	Demolition cost	€/kg
C_{recycle}	Recycling cost	€/kg

Table 77: Values cost calculations, source: own work

Scrap steel: 1.14 euro/kg
New steel beam: 1.5 euro/kg
Reused steel beam: 1.14 > 1.5 euro/kg

The mass of reclaimable steel (m_{steel}) can be retrieved from the calculations made by the quickscan tool, following: (weight/meter) * (element length) * (element quantity) – all values the tool provides. This means the cost saving part of the calculation can be executed. However, cost factors are considerable harder to quantify as they are mostly location- and project dependent. Transport costs are estimated around 1.85 euro/km for , according to research institute Panteia (2018). This is considered for truck up to 20 tonnes, averaging out to 9 cents per kg per 100km.

As mentioned before in paragraph 6.1, accurate information on the cost of deconstruction and demolition is difficult to obtain and quantify. Attempts have been made to contact deconstruction and demolition companies, but no useful results have been acquired that way. As the data is still missing for ($C_{\text{dec}} - C_{\text{dem}} - C_{\text{recycle}}$), it is not possible to include a complete cost analysis to the tool. Due to the time scope of this research, the decision was made to include the benefit analysis ($(p_{\text{new}} - p_{\text{reused}}) * m_{\text{steel}}$) in the tool and pause the development of the cost analysis for future development.

6.3.2 Environmental & Energetic impact

To compare the environmental impact of reusing steel versus using new steel, we analyze the CO₂ emissions of both scenarios. The production of new steel generates an average of 1.37 kg of CO₂ per kilogram of material produced, accounting for the average recycling content (Neenu, 2022). However, we need to account for the additional emissions resulting from transporting reclaimed materials to and from a storage location. On average, a truck emits 1.10 kg of CO₂ per kilometer (Milieubarometer, 2015). Since the structural components from a hall can be transported on a single truck, we need to consider the maximum transport distance. In a worst-case scenario with only one storage depot located in the centre of the Netherlands, the maximum transport distance would be 2 * 200 km, resulting in a total of 400 km. This distance corresponds to 440 kg of CO₂ emissions caused by the transport of reused elements. In comparison, the retrieved structural steel components from a hall amount to an order of magnitude greater than 10,000 kg (10^4). This implies that reusing these components can save a significant amount of CO₂ emissions, totalling manifolds of 13,700 kg. Consequently, the emissions from transportation become insignificant, representing less than 1% of the emissions caused by new production.

A similar calculation can be applied to the energetic performance of reuse. On average it costs about 20.1 MJ to produced 1 kg of steel, with the average recycling share included (Neenu, 2022). The energy to transport steel equals 1,98MJ/ton per

km, or about 0,198MJ/kg per 100km (RVO, 2023). Given the maximum distance of 400km of transport, a minimum of 19,3 MJ/kg of energy can be saved by reusing. An element of script is added to the tool, converting the weight of reclaimed elements to CO₂ emissions and energy that have been saved. This ensures the eco-impact of reuse is included in the quickscan tool as well.

6.3.3 Extra elements for the quickscan tool

As a result of this chapter, four extra analytical elements are included in the quickscan tool:

1. Material loss due preparation for circular economy
2. Material performance loss due to degradation
3. Eco-impact of reuse
4. Cost savings due to material price

These analyses provide additional information on the effects of deconstruction and reuse on the retrieved structural components' properties. They were not included in the case analysis of chapter 5, which focused on evaluating the tool's accuracy in predicting component lengths, types, and quantities found in industrial halls. The analyses in this chapter include the necessary steps to provide designers with a more realistic material output, considering factors like material degradation and loss. These steps are applied to the tool's resulting output, as described in chapter 5. See Figure 34. for analyses 1, 3 and 4. Figure 35 shows the relation between these added elements and the quickscan tool. The results of the full analysis are listed and exported as an excel file.

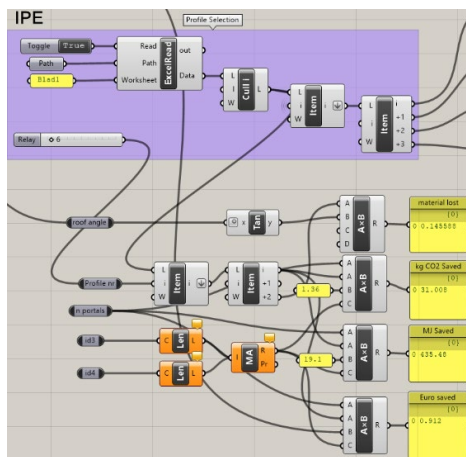


Figure 34: analysis 1, 3 & 4, source: own work

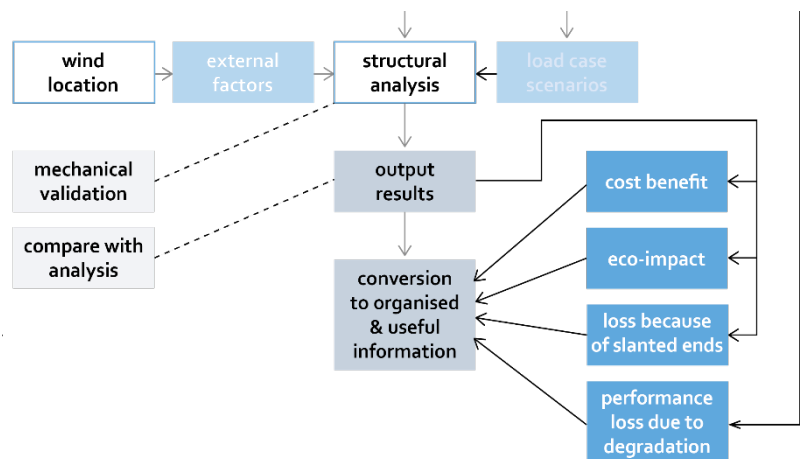


Figure 35: relation between added analysis and quickscan tool, source: own work

7. FINAL PRODUCT

In this chapter the latest version of the tool is displayed, this being the final product coming from this research. It discusses how the tool can be applied and how application of the tool benefits the process of reusing steel. Furthermore, the limitations of the tool are discussed, indicating where further development and research is needed, as well as showing the opportunities that can be seized if the tool is continued to be developed.

7.1 Overview final tool

To give an overview of the script that is the quickscan tool, a schematic visualization is shown in figure 36. Screenshots of the grasshopper script are added to the appendix (G), marking in similar colors where each 'function' is located within the script. Figure 36 also shows what part of the script is controlled by the user, and which part of the script needs to remain untouched. It also shows the cyclical nature of applying the tool; the user should interpret the results and be able to tweak the script input if necessary.

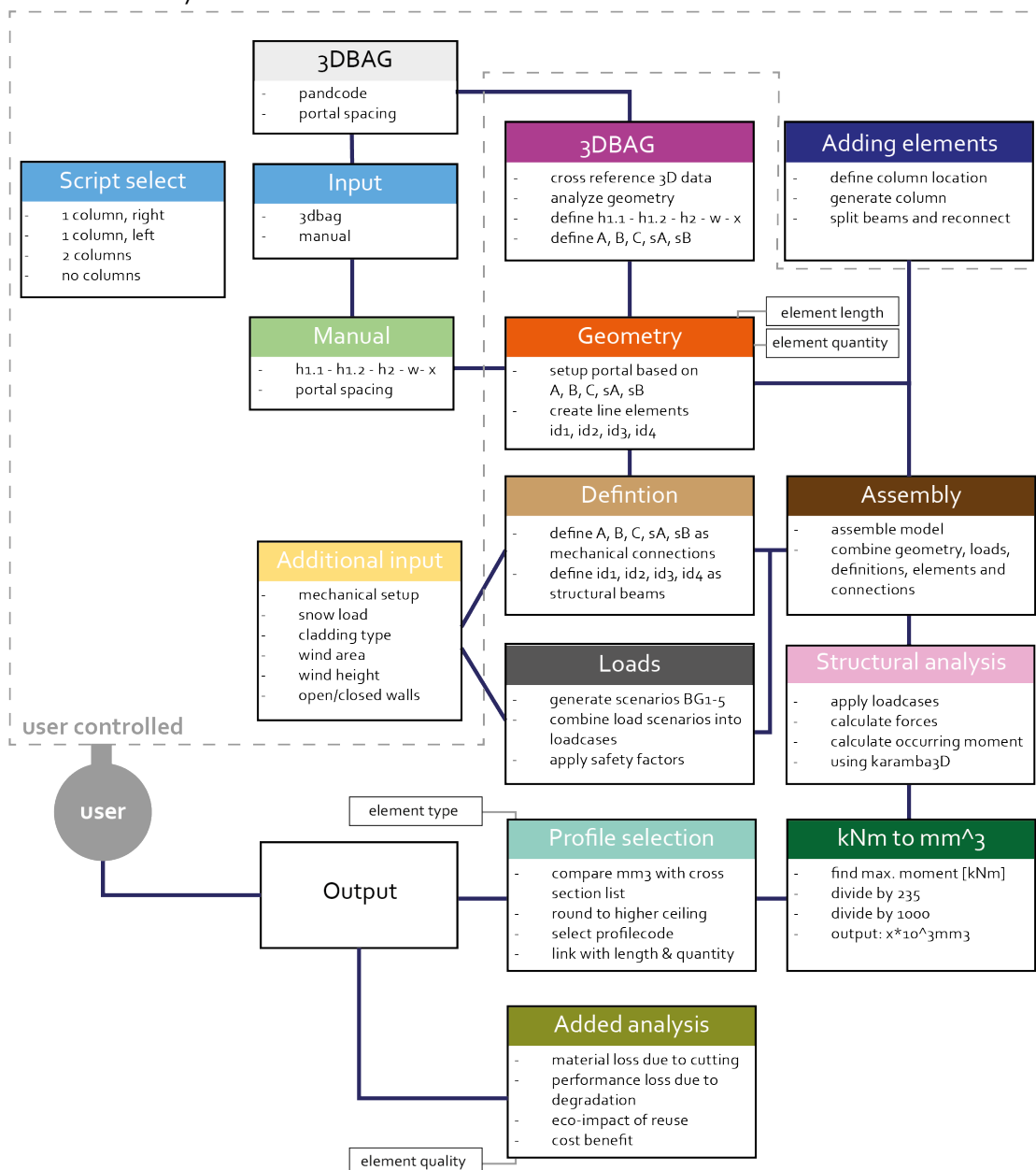


Figure 19: final tool overview, source: own work

The output of the tool consists of the following elements and is formatted as shown in Table 78.

Element	Length [m]	Type	Quantity	Material loss [m]	Performance S
id_1	3,3	HEA240	16	0,143	0,949
id_2	6,6	HEA240	16	0,143	0,949
id_3	17,38	IPE300	16	0,179	0,939
id_4	14,51	IPE300	16	0,179	0,939

Element	Performance A	CO ₂ savings [kg]	Energy savings [MJ]	cost benefit [euro]
id_1	0,942	8.832	62.022	1688,54
id_2	0,942	4.416	124.043	3377,09
id_3	0,932	16.267	228.451	6219,61
id_4	0,932	13.577	190.677	5191,21

Total savings hall

CO ₂ savings [T]	Emb. energy Saved [GJ]	Euro saved salvaging
43,1	605,2	€ 16.476,45

Table 78: excel output quickscan tool, source: own work

7.2 Tool application

The idea behind the tool is to take away the need to send someone to every single hall in the Netherlands to get an indication of the available structural steel components present in a hall. Instead, users of the tool will be able to quickly scan one, two or even a whole set of buildings from their computer, without having to travel to the location. This will save time (about 4-5 hours per structure), money, CO₂ emissions because of reduced travelling and allows for a batch applications, analysing lists of buildings based on pand codes, due to the inclusion of the 3DBAG input. This means large chunks of data on availability of steel can be retrieved, mapping out the used steel stock and potentially plan urban mining operations ahead of time. Designers can use this information early in the process, when their design is not set yet. Based on the output of the tool, they can take into account the structural performance of elements that will come available in the near future and adjust their design to these performance values. The tool can also be used in a deductive manner; if the performance of steel that potentially comes available in the near future does not at all match the required performance for the design brief, it can be ruled out to use reclaimed steel, meaning other sources of circular material need to be sought.

As the data used in the tool is publicly available, launching the tool as an open source web-app would be an ideal approach. Owners of hall structures can use to tool to indicate the potential resell value of if they decide to deconstruct their halls, designers can seek for available structures that might provide the elements they need, the government could use the tool to get data on availability of materials and

use it to promote circular reuse of structural steel components. If the data alone does not suffice, for example when it is assumed that extra supporting elements are included or that the static setup is significantly different, hall owners could be contacted to send additional images of interior and/or connections. As the tool is indicative rather than exact, the accuracy of the position of supporting elements, simply knowing whether they are present and where they approximately are can help to improve the results, again without requiring someone to physically visit those halls. The grasshopper script alone is not workable as a tool yet, due to it showing the whole script that goes behind the calculations. In order to take user experience into account, a suggestive interface (Figure 37) has been designed that shows how the input can be organized and what is required from users to fill in the tool correctly. This will also define the order in which the input values should be defined – see Table 79. Extended user-interface illustrations are added in Appendix H. Hypothetically, the tool could be converted to be a web app, as examples of companies offering 'online grasshopper tools' are prevalent. However doing this properly would result in a research project of its own, falling outside of the scope of this thesis.

Figure 20: user-interface, source: own work

Step	Input
1.	Extra supporting elements? <ul style="list-style-type: none"> - Yes, 2 - Yes 1, right - Yes, 1 left - No
2.	3DBAG input available? <ul style="list-style-type: none"> - Yes - No
	<i>Script version selection</i>
3.	3DBAG / Geometrical input (h1.1, h1.2, h2, w, x)
4.	Cladding type
5.	Wind area
6.	Open/closed sides
7.	Static setup (if needed: optimization)
8.	Price/kg new steel beam
9.	Price/kg reused beam
10.	In case of no 3DBAG: year of construction
11.	Button to export to excel sheet

Table 79: input order, source: own work

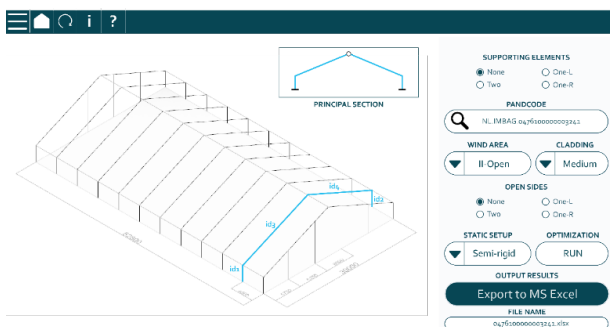


Figure 21a: user-interface, source: own work

7.3 Discussion: Limitations

In this paragraph the limitations of the tool are reflected on. This helps to better understand how to interpret the output results of the tool, as well as indicating where future improvements can or should be made. The limitations of the tool are listed in this paragraph.

- **Wind direction coming from one side**

The wind load analysis is based on a wind load case only coming from the left side. For symmetrical halls, this does not create a problem as the exact same wind load from the right side would cause similar maximum moments. However for asymmetrical halls, wind from one directions acts differently on a portal than wind from the other direction, due to suction and pressure coefficients being reverse and applied on different surface areas. It would be possible to include a second wind load case from the right side, creating a loadcase 2.1 and 2.2. However, this would make the tool more complex adding a whole extra windload component, whereas the steps that need to be taken are exactly the same as already has been described in paragraph 4.4. That is why the decision was made not to include flipped wind-direction in the final tool for now.

- **Front and end portal**

The current version of the tool only retrieves information on the structural steel components that are part of the middle portals. This means front and end portals are not included, although they contain structural steel as well. These portals are not included because their variety in organizations does not allow the standardization in analysis that the other portals allow. The only statement that can be made about these front and end portals is that they generally contain smaller profile sizes than the mid-hall portals; they resemble portals with more than 2 extra supporting columns.

- **Combined beams, and complex structural solutions**

The analysis results of Case D (par. 5.2) show that some halls include profiles that are upgraded, adjusted, combined or structurally strengthened in one way or another. These profiles have a different structural behavior then regular beams, but without prior knowledge, the tool is not able to identify they are used instead of regular beams. The output results in this indicate an element with a similar structural performance. However, as with the combined HEA280-IPE270 profile found in case D, this would neither be correct, as not the whole 13,5 meters of profile has this structural performance equivalent, only the first two meters. Combined profiles like these are not common, but can also not be ruled out. Interior images of a hall could be of help out here, but making those a requirement for the tool to function would severely limit the rate of analyzing and mapping out the available steel.

- **IPE Columns**

As aforementioned, columns are generally HEA-profiles, whereas beams are generally IPE-profiles, because of their respective cross sectional properties being beneficial for the applied situations. However, some hall designers choose to also use

IPE profiles as columns, for example case D and case G1. This could be due to aesthetic reasons, material availability or (most likely) cost savings. This IPE profile would need to have an equivalent structural performance to the suggested HEA profile and would therefore be a relatively tall cross section. Like the combined beams described above, applying IPE profiles as columns is not common, but the fact that it can happen weakens the reliability of the output results. It would be possible to have the tool suggest both HEA and structurally equivalent IPE profiles as columns, informing the user of the tool that HEA columns are most likely to be found in a hall, with IPE columns being a possibility.

- **No guarantee**

The limitations that have been presented up till now show a sign of a bigger limitation of the tool; it cannot guarantee which profiles can be found in a hall, it can only suggest what can best be assumed to be in there. Although still useful and more detailed than just guessing, it is difficult to state with certainty the profiles that can be retrieved. The tool can be useful in early design stages when no specific requirements are set, when element lengths and elements quantities are needed with a rough idea of available profiles. But to really know whether the components are equivalent to the tool's prediction, some site inspection might still be necessary.

7.4 Discussion: Opportunities

In this paragraph the opportunities of future development of the tool are considered. This helps to better understand how the tool could be applied in a broader context and how further development can improve the tool's effectiveness. The limitations of the tool are listed down below:

- **Applying tools to other structures than agrarian halls**

For the purposes of this research, agrarian halls were the focus of the case study and therefor central to the development of the tool. However, even without adjustments, the tool can also be applied to other hall structures, such as storage halls, sports halls and other portal structures. Flat roofs and pent roofs can be included as well, as long as the main structural setup involves a portal frame. It must be noted that in these structures, the variety of structural solutions is wider. Spans of large, flat roofs for example can consist of trusses, which are constructed of a variety of profiles. In this case, the model's profile suggestion is not relevant anymore; however it can still indicate the structural performance of these trusses, providing an equivalent section modulus and an approximate truss height. Designers could decide to include the whole truss in their new design, rather than all the separate components the truss is made of.

- **Linking tool with other computational tools**

The output of the model is a list of elements with a specific length, structural performance and a quantity of these elements. These elements can be introduced to the circular economy and then be distributed over various projects, but it would also be possible to research what structures can be developed using just the steel coming from one hall. An example of such a project is a research paper by Brütting

et al. (2019), in which they analyze a power grid tower structure and then use computational tools to generate a new structure using the steel from the tower as efficiently as possible. Combining the quick scan tool from this research with equivalent computational tools can create a powerful method to translate and transform industrial structures into new structures promoting reuse.

- **Batch process & linking it to an online database**

The inclusion of the 3DBAG dataset to generate the geometry of a hall allows for a batch analysis to be executed. Multiple cityJSON files could be uploaded, as well as multiple pand codes that can be used as input. This would allow users to scan a given area to get insight of the amount of reclaimable steel that is present in that area. In this case, exact profiles might not be relevant but rather an indication of the total weight of the portion of reusable steel. This would require a lot of computational power as the current setup of the model would require to run them simultaneously. The results of such a batch process can be uploaded into an online database, mapping when and where what sort of steel becomes available. This would reduce unnecessarily applying the same analysis multiple times to one building. As the data, especially from the 3DBAG, is linked to a location, transport emissions and costs can more accurately be identified, as the distance between the available material and the project location is now known.

- **Including other materials & second order elements**

Within the scope of this research, steel has been the material at the center of the analysis as it is the most used material for industrial halls (90% according to Hollander & Eldik, 2007). However, the tool could be adjusted to include other materials such as wood and concrete. This does require material specific knowledge and needs to include extra factors that are relevant to the structural properties of these materials, such as the effect of creep and material quality standards. Additionally, the tool now focuses on first-order structural components only, but a further developed tool could include an indication of second-order elements, such as purlins and profiles connecting the portals in the length direction. These are harder to identify, as they come in more sizes and shapes, similar to the extra supporting columns described in paragraph 5.3.2.

8. CONCLUSION

The Dutch government and the European Union have a desire to shift towards a circular economy before 2050, with a circular economy indicating closed material loops and no creation of waste products. The ongoing nitrogen-oxide crisis in the Netherlands provided an opportunity for a case to apply research into reusing structural components, as it is likely that this crisis will cause farmers in the Netherlands to close down their businesses. The suggested government solution of buying out so-called mega farmers will result in empty structures ready for demolition, this thesis attempted to take a more detailed dive into the concept of reusing structural components of these halls rather than recycling them, in order to stimulate a shift towards a more circular construction economy.

8.1 Research questions

The research central to this graduation project attempted to answer the following research question regarding the topic of reusing industrial building components:

'How can structural steel elements of industrial buildings be analysed and mapped out in order to be introduced in a circular urban context?'

In order to answer this main question, various sub-questions were set up. As results from researching these sub-questions will help to answer the main question, they will be discussed first before the main question is answered.

8.1.1 What are current barriers for steel reuse to become common practice?

There are a number of factors that come into play that prevent steel reuse from becoming common practice. Those factors can be categorized as happening on a system level, or happening on a component level. Additionally, these factors involve the effects of market demand and technical feasibility. The factors are depicted in Figure 38. The main reasons revolve around a lack of information on the supply side, making it hard for designers to implement the reclaimed elements in their projects. More information on availability (what/when/where) early in the process can help both designers and project managers to plan for reuse, rather than having to react on sudden availability of material requiring them to change the design. Furthermore, the potential benefits of reusing components compared to using new ones should be quantified and communicated clearly, creating incentive to adopt a reuse strategy.

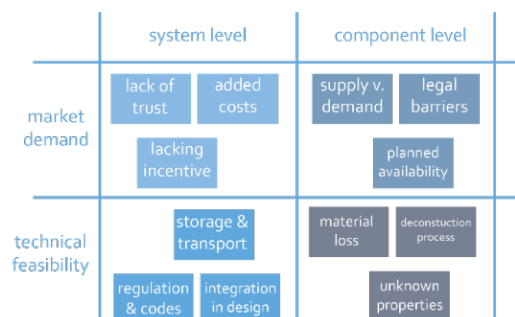


Figure 22: barriers in steel reuse, source: own work

8.1.2 What is the economic and environmental impact of steel reuse?

The economic impact of steel reuse is hard to predict, because of the many variables influencing the balance between economical cost and benefits. Money can be saved by buying reused elements, as long as they are priced cheaper per kilogram than new elements, but earn the current owner more money than selling it

as scrap steel. The two biggest unknowns, deconstruction and storage, have the largest impact on the actual cost of steel reuse. However it must be noted that these costs are not simply added, but replace the costs of what otherwise would be demolition and landfill costs, albeit that those options are generally cheaper. The environmental benefits are much more easily quantified. About 1.36 metric tonnes of CO₂ can be saved for every metric tonne of steel that is being reused instead of being recycled. Compared to other building materials, this is a relatively large CO₂-saving per unit weight. Because recycling steel is an energy intensive process, embodied energy savings turn out to be significant. About 19.1 MJ of energy can be saved for every kilogram of steel being reused instead of recycled – being energy that can then be used for other purposes.

8.1.3 How can industrial buildings be analysed to provide the necessary data for potential reuse?

To approach industrial buildings on a larger scale, it is needed to generalize their structural setup in order to predict what kind of structural components can be reclaimed. Once a generalized structural model is selected, reverse-engineering using codes, design requirements and external factors can be applied in order to make an estimate of the element dimensions, type and quantity. An additional analysis on material degradation and material loss due to deconstruction can help to provide a realistic image of the actual reusable portion of the components. Some factors relevant for the reverse-engineering process are unknown. Methods such as reverse optimization, deductive reasoning and generalizing examples from literature can help to make a well-informed approximation of these unknown factors.

8.1.4 What data is required to predict the available steel in a hall?

In order to predict the type, dimensions, quantity and quality of elements in a steel hall, the following data listed in table 80. is required. Using this data in a reverse-engineering strategy, one is able to indicate the maximum occurring moments. This in turn will provide the required section modulus the structural

Required Data	
Geometric properties	Design requirements
Load scenarios	Building codes
Loadcases	Structural formulas
Static setup	Year/construction

Table 80: required data, source: own work

components, via which the element type can be indicated. Lengths and quantities are drawn from the geometry information, whereas year of construction and further design requirements help to indicate the predicted quality of the elements.

8.1.5 What sources of data are available?

During the research process, various sources have been used to retrieve the required data in order to perform the analysis. The main sources are listed in Table 81. The BAG3D dataset turned out to be especially useful, streamlining the process of setting up the geometry of the portals. If directly available data sources do not suffice, or extra information is required, simple

Data sources
3DBAG
AHN Viewer
Wind load tables
Satellite & Street view

Table 81: required data, source: own work

interior pictures can help to indicate the missing information. With the results coming from the subquestions, a quickscan tool has been developed that helps to answer the main research question can now be answered:

8.1.6 How can structural steel elements of industrial buildings be analysed and mapped out in order to be introduced in a circular urban context?'

Structural steel components in industrial buildings can be analysed and mapped out by developing a tool that predicts what kind of structural components can be retrieved from those industrial buildings based on reverse-engineering. By only using data that is publicly available, an accurate estimate of element length and quantity be made. Profile types can be indicated fairly accurately, within a margin of error of 1 profile. An indication of elements quantity and remaining performance can be provided, but this remains a generic prediction – elements can degrade locally and faster if conditions are worse. Applying the developed tool will give insight in expected availability of components. By providing this information to designers in an early phase of the design process, ensuring they can make decisions based on the upcoming availability of materials, being able to implement it in their projects properly.

8.2 Future Research

The tool presented in chapter 7 is the result of this research. Due to its limit in scope, there is room to further develop this tool to make it more accurate, more widely applicable and providing more information on the impacts of reuse. The following research directions are suggested:

- Evaluating the application on other hall types than agrarian ones, to find out the broader potential of the quickscan tool to be used to map out available materials.
- More in depth research on the economic aspects and implications of reuse, adding these to the tool to provide a more detailed insight in the consequences of component reuse.
- Developing a streamlined process of reclaiming, tagging, assessing and storing the potentially reusable components to facilitate reuse.
- Creating a database for the information from the analyses to be stored in and making this publicly available as a data set.
- The inclusion of second-order loadbearing components in the tool, providing a more comprehensive list of material that is actually reclaimable and reusable.
- Approaching other structural typologies in a similar way, exploring the possibility to develop a comparable quickscan method for other building types. This could be focused on steel, however other construction materials such as timber and concrete could be considered as well.

9. REFLECTION

This reflection is written to evaluate the graduation process and to discuss the potential societal impact of this thesis.

Graduation process:

My graduation process involves circular building methods and approaches, which I believe is one of the central themes of the Building Technology Gradation Studio. In order to achieve a durable, circular and environment-friendly built environment, innovation on reusing construction material is required in order to move away from a construction sector that is organized in a linear way, causing large amounts of waste and emissions. The aim was to combine the knowledge about circularity and durability from the FPD-department with the structural knowledge of the SD-department and use that combination to explore and add knowledge to the reuse of structural steel components.

The research method that was used, combining literature review, case studies and applying research by design turned out to be a suitable approach for this research paper. The cases used in the case study did not only help to gain knowledge on what kind of components can be expected from the types of halls analyzed, they could then also function as testcase for the tool to be applied to and evaluated on. Using Grasshopper as a computational tool turned out to be an effective choice. The variety of plug-ins available allow for different sources of data to be seamlessly introduced and the Karamba3D software providing real-time structural calculations ensured a short feedback loop, helping to spot oddities and errors relatively soon and enforcing the iterative process of design. What I think missed in this research approach is the link with practice. Although I aimed to involve stakeholders in the process, as I did reach out to stakeholders in the beginning, in the end I started focusing more on the tool-aspect rather than the broader context. This might also have been due to lack of response from stakeholders I reached out to. The perspective from practice could have helped to develop a tool that does not mainly provide in the needs of designers wanting to implement reuse, but also in the needs of other actors in the steel construction sector. This could have resulted in an end product that is more relevant to the industry sector.

Although at first glance, developing a quickscan tool does not sound like designing. However, as the report shows and experience has learned, developing such a tool follows the cyclical nature and iterative process that is key to any design process. Likewise, research has been used to lay a foundation of background knowledge that helped to identify what output the tool should provide, as well as providing the technical knowledge needed to build the tool. During the process of constructing and evaluating the tool, research was conducted to find solutions to problems that occurred, both theoretical and practical – like watching a youtube video to learn how to achieve certain actions in grasshopper. As mentioned this process is cyclical; the design sometimes requires more research to be improved, whereas sometimes, research done leads to the tool being changed because of new findings.

Right from the start I knew the nitrogen-oxide crisis context of this research would be a controversial topic, given the fierce protests and recent changes in the political landscape. The closure of farms and shrinking the agrarian sector is a sensitive topic. One hall owner I reached out to mentioned the Dutch saying that translates as 'One

man's dead is another man's bread', pointing out the somewhat opportunistic nature of doing reuse research within this context. Personally, I see the topic of reusing steel from such halls as 'one man's trash is another man's treasure' but I could see his point of view. In the end I have chosen to shift the societal context of the nitrogen-oxide crisis more to the background, underlining the general need to reclaim materials from existing buildings because of the circularity targets set for 2050.

Societal impact

The quickscan tool that has been developed for this graduation projects is one of many small steps that are currently taken in preparation of a circular construction sector. However, instead of focusing on the circularity of newly introduced building materials, structures and components, for this graduation project the decision was made to underline the need to analyze the existing building stock and start treating it as a source of construction material. While the steel sector (and other branches) proudly claim to recycle a lot, direct reuse should be the approach that is aimed for, given its true circular nature. The goal of this graduation project was to innovate by using reverse-engineering as a method to analyze the existing building stock. This projected innovation has been achieved, as in the end a tool has been developed that can actually achieve this goal. By applying the tool on a broad scale, a lot of potential material sources can be mapped out and be anticipated for, streamlining and promoting the reuse of steel structures early on. If this tool were to be expanded on, or different versions of a similar tool are developed, not only steel, but all sorts of sourced construction material can be indicated, ensuring more insight is gained on the actual availability of materials in the current building stock.

If the tool helps to increase reuse rates, it will help to shift the current linear economy to a circular one, helping to reach the targets set by the European Union and the Dutch government. By steering choices on reuse over recycling, a larger shift might occur helping reuse to become more practice, rather than the niche it is. When reuse is chosen over recycling, CO₂-emissions and embodied energy waste will be reduced in the steel sector, which is beneficial to the local and global environment. The developed tool's goal is not only functional, it represents a shift in perspective, providing an idealistic view on the current industrial building stock as an urban mine. The tool will aid designers in their ability to implement reused and reclaimed elements in their projects early on, as it provides them the knowledge of what material to expect to be retrieved both when and where, before deconstruction of these structures has taken place. This allows for reclaimed elements to be seriously considered in design projects, rather than added as a potential afterthought. However, this also requires a different attitude from designers, as they should be willing to change their design to fit and optimally use reclaimed components.

10. REFERENCE LIST

- 3D Geoinformation TU Delft. (2021). 3D BAG [Dataset]. From <https://3dbag.nl/en/viewer>
- AHN. (n.d.). *Actueel Hoogtebestand Nederland*. Geraadpleegd van <https://www.ahn.nl/>
- Allwood, J. M. (2014). Squaring the Circular Economy. *Handbook of Recycling*, 445–477. <https://doi.org/10.1016/b978-0-12-396459-5.00030-1>
- Arends, J. (2020). *Handleiding Ontwerpen Draagconstructie*. TU Delft
- Barendsz, M. A. & Eldik, C. (2019). *Hallen: Kenmerken en constructiesystemen van stalen hallen en het ontwerp van een éénbeukige geschoorde hal volgens Eurocode 3*. Bouwen Met Staal.
- Bekaert. (2020). *ULS and SLS*. <https://www.bekaert.com/en/product-catalog/construction/news/uls-and-sls>
- Bertino, G., Kisser, J., Zeilinger, J., Langergraber, G., Fischer, T. & Österreicher, D. (2021). Fundamentals of Building Deconstruction as a Circular Economy Strategy for the Reuse of Construction Materials. *Applied Sciences*, 11(3), 939. <https://doi.org/10.3390/app11030939>
- Bhaskar, A., Abhishek, R., Assadi, M., & Somehesaraei, H. N. (2022). Decarbonizing primary steel production : Techno-economic assessment of a hydrogen based green steel production plant in Norway. *Journal of Cleaner Production*, 350, 131339. <https://doi.org/10.1016/j.jclepro.2022.131339>
- de Blois, M., Korevaar, G., & Blok, K. (2018). *Op weg naar een klimaatneutrale infrasector in Nederland*. TU Delft.
- Brink Staalbouw. (2022). *Ontwikkeling staalprijzen*. Geraadpleegd van <https://brinkstaalbouw.nl/staalprijsindex>
- Brütting, J., De Wolf, C. & Fivet, C. (2019). The reuse of load-bearing components. *IOP Conference Series: Earth and Environmental Science*, 225, 012025. <https://doi.org/10.1088/1755-1315/225/1/012025>
- Brütting, J., Desruelle, J., Senatore, G. & Fivet, C. (2019). Design of Truss Structures Through Reuse. *Structures*, 18, 128–137. <https://doi.org/10.1016/j.istruc.2018.11.006>
- Casadata. (2017). *Staalconstructies voor veestallen*. www.Casadata.Nl.
- Cossu, R., & Williams, I. D. (2015). Urban mining: Concepts, terminology, challenges. *Waste Management*, 45, 1–3. <https://doi.org/10.1016/j.wasman.2015.09.040>
- Crowther, P. (2018). "Re-Valuing Construction Materials and Components Through Design for Disassembly", [Crocker, R.](#), [Saint, C.](#), [Chen, G.](#) and [Tong, Y.](#) (Ed.) *Unmaking Waste in Production and Consumption: Towards the Circular*

Economy, Emerald Publishing Limited, Bingley, pp. 309-321. <https://doi.org/10.1108/978-1-78714-619-820181024>

CBS. (2020). Smaller material footprint, more recycling than the EU average. CBS. From: <https://www.cbs.nl>

Dirkse, H. S. G. (2023). *Het effect van stijgende bouwkosten op nieuwbouwprojecten en grondprijzen* - Rabobank. From: <https://www.rabobank.nl/kennis/d011296949-het-effect-van-stijgende-bouwkosten-op-nieuwbouwprojecten-en-grondprijzen>

EPA. (2015). *Design for Deconstruction*. epa.gov. From: <https://www.epa.gov/sites/default/files/2015-11/documents/designfordeconstrmanual.pdf>

Economisch Instituut voor de Bouw [EIB], Kok, J., & Koning, M. (2019). *Toekomst perspectieven sloopsector 2019*. From: https://www.eib.nl/pdf/Toekomstperspectieven%20sloopsector%202019_web.pdf

European Council. (2023). *Energy price rise since 2021*. From: <https://www.consilium.europa.eu/en/infographics/energy-prices-2021/>

Geyer, R., Jackson, T. & Clift, R. (2002). *Economic and Environmental Comparison Between Recycling and Reuse of Structural Steel Section*.

Girao Coelho, A., Pimentel, R., Ungureanu, V., Hradi, P. & Kesti, J. (2017). *European recommendations for reuse of steel products in single-storey buildings*.

Gorgolewski, M. & Morretin, L. (2009). The Process of Designing with Reused Building Components. In *Lifecycle Design of Buildings, Systems and Materials: Vol. p.105-109*. <http://www.irbnet.de/daten/iconda/CIB14291.pdf>

Gorgolewski, M. (2008). Designing with reused building components: some challenges. *Building Research & Information*, 36(2), 175–188. <https://doi.org/10.1080/09613210701559499>

Hatcher, G., Ijomah, W., & Windmill, J. (2011). Design for remanufacture: a literature review and future research needs. *Journal of Cleaner Production*, 19(17–18), 2004–2014.

Helbig, C., Huether, J., Joachimsthaler, C., Lehmann, C., Raatz, S., Thorenz, A., Faulstich, M. & Tuma, A. (2022). A terminology for downcycling. *Journal of Industrial Ecology*, 26(4), 1164–1174. <https://doi.org/10.1111/jiec.13289>

Hollander, J. & Eldik, C. (2007). *Stalen hallen: Ontwerpgrafieken voor portalen met scharnierende en flexibele verbindingen*. Bouwen met Staal.

Hopkinson, P., Chen, H. M., Zhou, K., Wang, Y., & Lam, D. (2019). Recovery and reuse of structural products from end-of-life buildings. *Proceedings of the Institution of Civil Engineers - Engineering Sustainability*, 172(3), 119–128. <https://doi.org/10.1680/jensu.18.00007>

- HQTS. (2022). Steel Quality Control: What are the Types of Quality Inspections? HQTS. Geraadpleegd van <https://www.hqts.com/how-and-why-steel-quality-control-should-be-conducted/>
- Huuhka, S. & Hakanen, J.H. (2015). Potential and barriers for reusing load-bearing building components in Finland. 39. 215-224.
- Huysman, S., Debaveye, S., Schaubroeck, T., Meester, S. D., Ardente, F., Mathieux, F. & Dewulf, J. (2015). The recyclability benefit rate of closed-loop and open-loop systems: A case study on plastic recycling in Flanders. *Resources, Conservation and Recycling*, 101, 53–60. <https://doi.org/10.1016/j.resconrec.2015.05.014>
- Iacovidou, E. & Purnell, P. (2016). Mining the physical infrastructure: Opportunities, barriers and interventions in promoting structural components reuse. *Science of The Total Environment*, 557–558, 791–807. <https://doi.org/10.1016/j.scitotenv.2016.03.098>
- Ijomah, W. L. (2010). The application of remanufacturing in sustainable manufacture. *Proceedings of the Institution of Civil Engineers - Waste and Resource Management*, 163(4), 157–163. <https://doi.org/10.1680/warm.2010.163.4.157>
- Kim, S. & Kim, S. A. (2020). Framework for Designing Sustainable Structures through Steel Beam Reuse. *Sustainability*, 12(22), 9494. <https://doi.org/10.3390/su12229494>
- King, A. M., Burgess, S. C., Ijomah, W., & McMahon, C. A. (2006). Reducing waste: repair, recondition, remanufacture or recycle? *Sustainable Development*, 14(4), 257–267. <https://doi.org/10.1002/sd.271>
- Li, C. Y., & Yang, W. (2021). *Steel Corrosion and Degradation of Its Mechanical Properties*. CRC Press.
- Liu, W., Zuo, H., Wang, J., Xue, Q., Ren, B., & Yang, F. (2021). The production and application of hydrogen in steel industry. *International Journal of Hydrogen Energy*, 46(17), 10548–10569. <https://doi.org/10.1016/j.ijhydene.2020.12.123>
- Madaster Nederland. (2022). *Madaster: het kadaster voor materialen en producten*. Geraadpleegd van <https://madaster.nl/>
- Mahpour, A. (2018). Prioritizing barriers to adopt circular economy in construction and demolition waste management. *Resources, Conservation and Recycling*, 134, 216–227. <https://doi.org/10.1016/j.resconrec.2018.01.026>
- NDO Nederland. (2023). *OES-meting: inzicht in de chemische samenstelling van metaal* | NDO Nederland. From: <https://ndo-nederland.nl/niet-destructief-onderzoek/oes-meting/>
- Nieuwenhuis, M. (2019). *Aantal megastallen neemt steeds verder toe*. From: <https://www.parool.nl/nieuws/aantal-megastallen-neemt-steeds-verder-toe~b994e03b/>

- NSC. (2017). *Structural steel reuse*. newsteelconstruction.com.
<https://www.newsteelconstruction.com/wp/structural-steel-reuse/>
- Oosterhoff, J. (2013). *Kracht plus vorm: inleiding in de constructieleer van bouwwerken*. Bouwen Met Staal.
- Ploeger, H., Prins, M., Straub, A., & Van den Brink, R. (2019). Circular economy and real estate: the legal (im)possibilities of operational lease. *Facilities*, 37(9/10), 653–668. <https://doi.org/10.1108/f-01-2018-0006>
- Spanish Government. (2018). *Codiga Estructural*. From:
https://cdn.mitma.gob.es/portal-webdrupal/CPH/codigo_estructural/english/chapter_26_deconstruction_of_steel_structures.pdf
- Seitz, M. A., & Peattie, K. (2004). Meeting the closed-loop challenge: the case of remanufacturing. *California management review*, 46(2), 74-89.
- Steel Construction Info. (n.d.). *Corrosion of structural steel*. Geraadpleegd van https://www.steelconstruction.info/Corrosion_of_structural_steel
- Thormark, C. (2001). Conservation of energy and natural resources by recycling building waste. *Resources, Conservation and Recycling*, 33(2), 113–130.
[https://doi.org/10.1016/s0921-3449\(01\)00078-7](https://doi.org/10.1016/s0921-3449(01)00078-7)
- Tingley, D. D., & Davison, B. (2011). Design for deconstruction and material reuse. *Proceedings of the Institution of Civil Engineers - Energy*, 164(4), 195–204.
<https://doi.org/10.1680/ener.2011.164.4.195>
- Vanilla Steel. (2022). *Different Steel Grades and Their Designation*. From:
<https://www.vanillasteel.com/content/steel-grades>
- Wienerberger. (2020). *Brick as a Service*. From:
<https://www.wienerberger.nl/product/gevel/systemen/clickbrick/brick-as-a-service.html>
- WRAP. (2008). *Reclaimed building products guide*. The Old Academy.
- Xing, K., Kim, K. P., & Ness, D. (2020). Cloud-BIM Enabled Cyber-Physical Data and Service Platforms for Building Component Reuse. *Sustainability*, 12(24), 10329.
<https://doi.org/10.3390/su122410329>
- Yang, S., Ong, S. & Nee, A. (2015). Towards Implementation of DfRem into the Product Development Process. *Procedia CIRP*, 26, 565–570.
<https://doi.org/10.1016/j.procir.2014.07.026>

Case	Company	URL
A	Swierstra	https://www.planviewer.nl/imro/files/NL.IMRO.0140.OMGBtngbOJeth2-VA01/i_NL.IMRO.0140.OMGBtngbOJeth2-VA01_illustratie2.pdf
B	FG Bedrijfs-ontwikkeling	https://repository.officiële-overheidspublicaties.nl/externebijlagen/exb-2019-20934/1/bijlage/exb-2019-20934.pdf
C	BTB Jan de Groot	https://repository.officiële-overheidspublicaties.nl/externebijlagen/exb-2014-881/1/PDF/exb-2014-881.PDF
D	DLV Advies	https://docplayer.nl/135977189-Statistische-berekening-nieuwbouw-vleeskuikensstal-stal-6-voor-de-oosters-vof-projectnummer-b.html
E	Constr. Bureau F. Wiggers	https://repository.officiële-overheidspublicaties.nl/externebijlagen/exb-2015-32122/1/bijlage/exb-2015-32122.pdf
F	IBZ	https://www.noordenveld.nl/ruimtelijkeplannen/NL.IMRO.1699.2015PB014-vg01/b_NL.IMRO.1699.2015PB014-vg01_bd32.pdf
G	LTO Vastgoed	https://repository.officiële-overheidspublicaties.nl/externebijlagen/exb-2015-8918/1/Bijlage/exb-2015-8918.pdf

Table 81: Sources for drawings & static reports of case halls

Appendix A – Structural formulas

	Property	Unit
A	Area	mm ²
L	Length	mm
F	Force	N
Q	Distributed load	N/m
M	Moment	Nmm
E	E-modulus	N/mm ²
Wy	Section modulus	mm ³
Iy	2nd moment of area	mm ⁴
Iz	2nd moment of area	mm ⁴
w	Displacement	mm

	Max. stress [N/mm ²]	ULS
Due to Force	$F_{normal}/A_{profile}$	Max. stress < Yield strength
Due to Moment	M_d/W_y	Max. stress < Yield strength

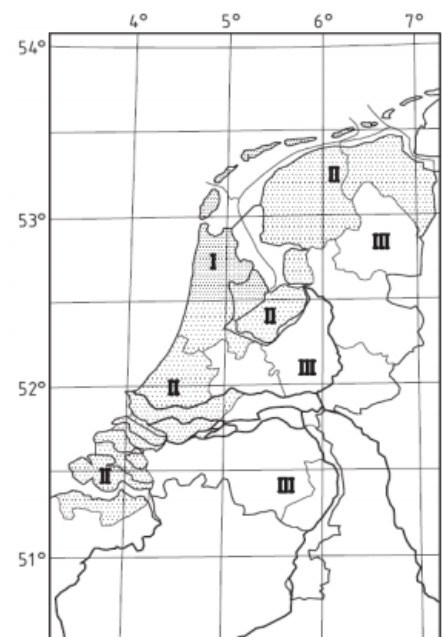
	Buckling forces [kN]	ULS
$F_{critical}$	$E \cdot I_z \cdot \pi^2 / (L^2)$	$F_{max} < F_{critical} / 5$

	Bending [mm]	SLS
w	$5/384 \cdot (Q \cdot L^4 / E \cdot I_y)$	$w < 0,004 \cdot l$

Load Case	ULS
lc1	$1,1 \cdot BG_1 + 1,3 \cdot BG_2$
lc2	$1,1 \cdot BG_1 + 1,3 \cdot BG_3 + 1,3 \cdot BG_4$
lc3	$1,35 \cdot BG_1$
lc4	$0,9 \cdot BG_1 + 1,3 \cdot BG_5$
Load Case	SLS
lc1	$1,0 \cdot BG_2$
lc2	$1,0 \cdot BG_3 + 1,0 \cdot BG_4$

Appendix B – Wind table

Hoogte m	Gebied I			Gebied II			Gebied III	
	kust	onbe- bouwd	be- bouwd	kust	onbe- bouwd	be- bouwd	onbe- bouwd	be- bouwd
1	0,93	0,71	0,69	0,78	0,60	0,58	0,49	0,48
2	1,11	0,71	0,69	0,93	0,60	0,58	0,49	0,48
3	1,22	0,71	0,69	1,02	0,60	0,58	0,49	0,48
4	1,30	0,71	0,69	1,09	0,60	0,58	0,49	0,48
5	1,37	0,78	0,69	1,14	0,66	0,58	0,54	0,48
6	1,42	0,84	0,69	1,19	0,71	0,58	0,58	0,48
7	1,47	0,89	0,69	1,23	0,75	0,58	0,62	0,48
8	1,51	0,94	0,73	1,26	0,79	0,62	0,65	0,51
9	1,55	0,98	0,77	1,29	0,82	0,65	0,68	0,53
10	1,58	1,02	0,81	1,32	0,85	0,68	0,70	0,56
15	1,71	1,16	0,96	1,43	0,98	0,80	0,80	0,66
20	1,80	1,27	1,07	1,51	1,07	0,90	0,88	0,74
25	1,88	1,36	1,16	1,57	1,14	0,97	0,94	0,80
30	1,94	1,43	1,23	1,63	1,20	1,03	0,99	0,85
35	2,00	1,50	1,30	1,67	1,25	1,09	1,03	0,89
40	2,04	1,55	1,35	1,71	1,30	1,13	1,07	0,93
45	2,09	1,60	1,40	1,75	1,34	1,17	1,11	0,97
50	2,12	1,65	1,45	1,78	1,38	1,21	1,14	1,00
55	2,16	1,69	1,49	1,81	1,42	1,25	1,17	1,03
60	2,19	1,73	1,53	1,83	1,45	1,28	1,19	1,05
65	2,22	1,76	1,57	1,86	1,48	1,31	1,22	1,08
70	2,25	1,80	1,60	1,88	1,50	1,34	1,24	1,10
75	2,27	1,83	1,63	1,90	1,53	1,37	1,26	1,13
80	2,30	1,86	1,66	1,92	1,55	1,39	1,28	1,15
85	2,32	1,88	1,69	1,94	1,58	1,42	1,30	1,17
90	2,34	1,91	1,72	1,96	1,60	1,44	1,32	1,18
95	2,36	1,93	1,74	1,98	1,62	1,46	1,33	1,20
100	2,38	1,96	1,77	1,99	1,64	1,48	1,35	1,22
110	2,42	2,00	1,81	2,03	1,68	1,52	1,38	1,25
120	2,45	2,04	1,85	2,05	1,71	1,55	1,41	1,28
130	2,48	2,08	1,89	2,08	1,74	1,59	1,44	1,31
140	2,51	2,12	1,93	2,10	1,77	1,62	1,46	1,33
150	2,54	2,15	1,96	2,13	1,80	1,65	1,48	1,35
160	2,56	2,18	2,00	2,15	1,83	1,67	1,50	1,38
170	2,59	2,21	2,03	2,17	1,85	1,70	1,52	1,40
180	2,61	2,24	2,06	2,19	1,88	1,72	1,54	1,42
190	2,63	2,27	2,08	2,20	1,90	1,75	1,56	1,44
200	2,65	2,29	2,11	2,22	1,92	1,77	1,58	1,46



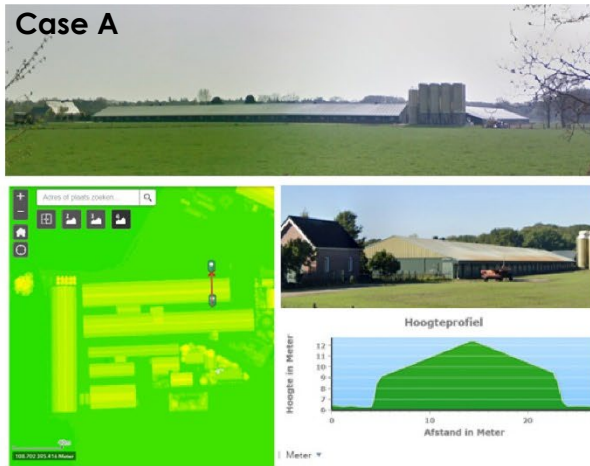
Appendix C – Extended Case Table

	Adress	Location	Province	Area [m ²]	Length [m]	Width [m]	Height [m]	Spacing [m]	Wind Area	3DBAG	Drawings/stat analysis
A	Jeth 2	Britswert	FR	1620	30	54	9	4,8	II-open	no	Drawings
B	Mastdreef 19	Breda	NB	2074	17	122	6,5	4,8	III-open	no	Both
C	Helmweg 29	Callantsoog	NH	1300	26	50	8,8	5	I-open	yes	Drawings
D	Oosterseweg 1	Elshout	NB	2340	26	90	7,8	5	III-open	yes	Static analysi
E	Bontekoeweg 2	Baak	GL	3209	34,5	93	9,8	5	III-open	yes	Static analysi
F	Hoofdstraat 52	Een	DR	2566	32,9	78	10	5,4	III-Open	no	Drawings
G	Baaksevoetpad 2	Hengelo	GL	8803	-	-	-	-	III-Open	yes*	Drawings

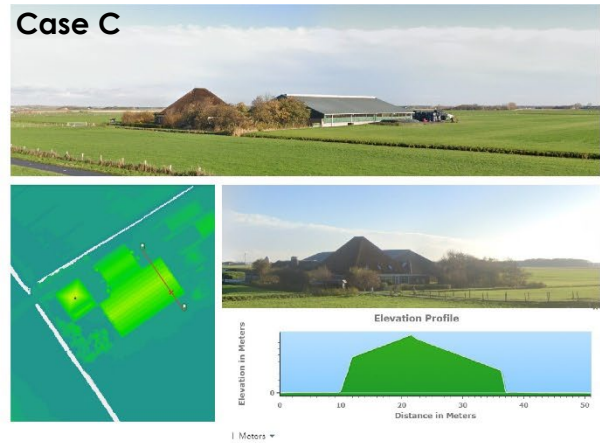
	Area [m ²]	Length [m]	Width [m]	Height [m]	Spacing [m]
G1	1369	14,8	92,5	5	5
G2	688	14,8	46,5	5	5
G3	1898	17,1	111	5,7	5
G4	4848	30,3	160	7,3	5,5

Appendix D – Analyses

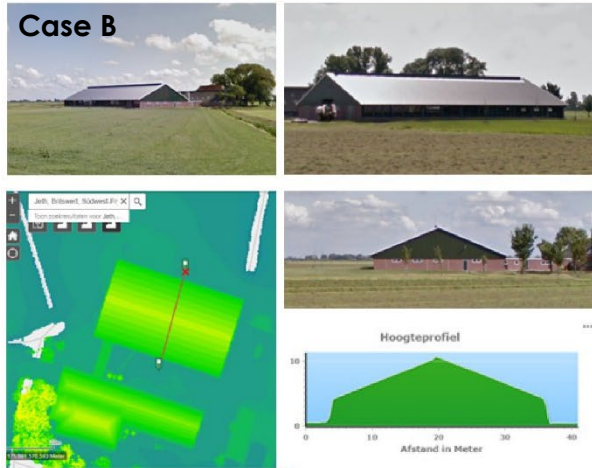
Case A



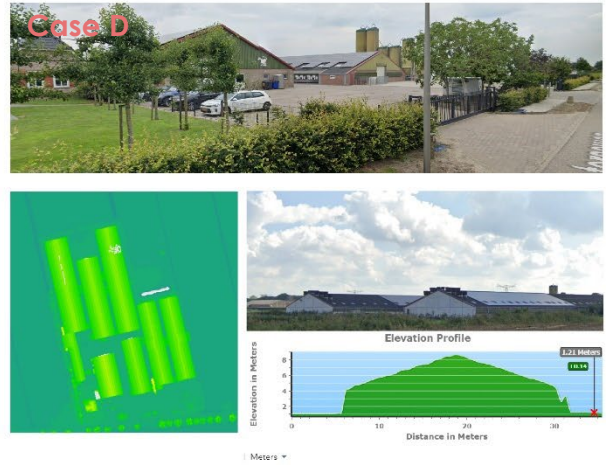
Case C



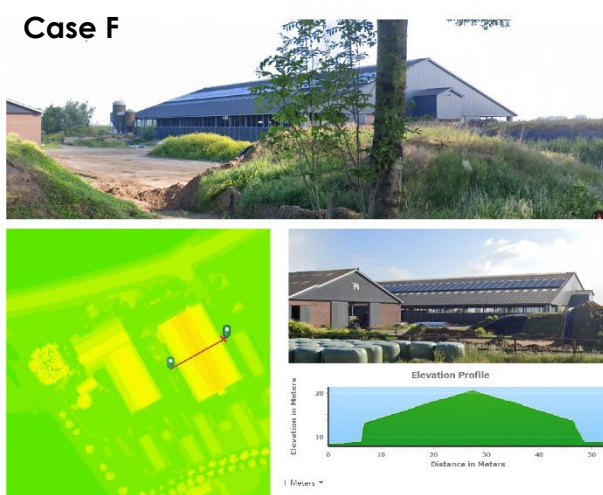
Case B



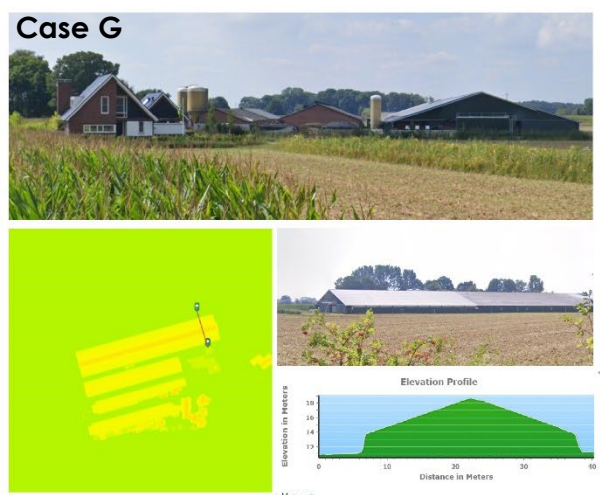
Case D



Case F



Case G



Appendix E – Structural verification

Calculations for Lc1 – Deadload + snow load

Elements	Properties	Load	Safety factor	Ftot [kN]
ld1	3m	0,26kN/m	1,1	0,86
ld2	3m	0,26kN/m	1,1	0,86
ld3	10,44m	0,26kN/m	1,1	2,98
ld4	10,44m	0,26kN/m	1,1	2,98
Cladding	0,10kN/m ²	0,5kN/m	1,1	2 * 7,39
Snow	0,56kN/m ²	2,80kN/m	1,3	2 * 38,00
Total				98,46

Table 82: Occuring loads lc1, source: own work

LC1 - Vertical reaction forces

$$r_A + r_B = 98,46 \text{ kN}$$

$$r_A = r_B = 98,46/2 = 49,23 \text{ kN}$$

Value Karamba3D model: 50,0 kN

$$\text{Deviation Karamba3D Model: } 0,77/49,23 \cdot 100 = +1,6\%$$

LC1 - Horizontal reaction forces

Moment around C = 0

$$r_A \cdot 10 = F_{\text{snow}} \cdot 5 + F_{\text{id1}} \cdot 10 + F_{\text{id3}} \cdot 5 + F_{\text{cladding-id1}} \cdot 10 + F_{\text{cladding-id3}} \cdot 5 + h_A \cdot 6$$

$$49,23 \cdot 10 = 38 \cdot 5 + 0,86 \cdot 10 + 2,98 \cdot 5 + 1,65 \cdot 10 + 5,75 \cdot 5 + h_A \cdot 6$$

$$492,3 = 190 + 8,6 + 14,9 + 16,5 + 28,75 + h_A \cdot 6$$

$$233,55 = h_A \cdot 6$$

$$h_A = 38,9 \text{ kN}$$

Value Karamba3D model: 39,5kN

$$\text{Deviation Karamba3D Model: } 0,6/38,9 \cdot 100 = +1,5\%$$

LC1 - Max. occurring moment in element id1:

$$M_d = F \cdot l$$

$$F = h_A = 38,9 \text{ kN}$$

$$l = 3,00 \text{ m}$$

$$M_d = 116,7 \text{ kNm}$$

Value Karamba3D model: 118,39kNm

$$\text{Deviation Karamba3D Model: } 1,7/116,7 \cdot 100 = +1,5\%$$

LC1 - Required section modulus due to stress due to moment:

Required W_y = Maximum occurring moment

$$116,7 \cdot 10^6 / 235 = 497 \cdot 10^3 \text{ mm}^3$$

Smallest HEA profile that suffices: HEA220 (515 > 497)

Profile selection by quickscan tool: HEA220 (515 > 504)

$$\text{Deviation Karamba3D Model: } 7/497 \cdot 100 = +1,5\%$$

Calculations for lc2 – Deadload + windload + overpressure

Elements	Properties	Load	Safety factor	Ftot [kN]
ld1	3m	0,26kN/m	1,1	0,86
ld2	3m	0,26kN/m	1,1	0,86
ld3	10,44m	0,26kN/m	1,1	2,98
ld4	10,44m	0,26kN/m	1,1	2,98
Cladding	0,10kN/m ²	0,5kN/m	1,1	2 * 7,39
Wind	6m/area II/built 0,58 kN/m ²	2,9kN/m	1,3	
ld1 wind	3m; f = 0,8	2,32kN/m	1,3	9,05
ld2 wind	3m; f = 0,4	1,16kN/m	1,3	4,53
ld3 wind	10,44m; f = 0,9	2,61kN/m	1,3	35,42
ld4 wind	10,44m; f = 1,3	3,77kN/m	1,3	51,17
ld1 overpr.	3m; f = 0,3	0,87kN/m	1,3	3,93
ld2 overpr.	3m; f = 0,3	0,87kN/m	1,3	3,93
ld3 overpr.	10,44m f = 0,3	0,87kN/m	1,3	11,8
ld4 overpr.	10,44m f = 0,3	0,87kN/m	1,3	11,8

Table 83: Occuring loads lc2, source: own work

LC2 - Vertical reaction forces

As the loads are not applied symmetrically, reaction force rB is defined by using the fact that the moment around A = 0. This leads to the following equation:

$$\begin{aligned} dA1 &= 1,5m & dA3 &= 5m & dA5 &= 4,5m \\ dA2 &= 20m & dA4 &= 15m & \alpha &= 16,7^\circ \end{aligned}$$

$$\begin{aligned} &F_{\text{deadload}} + F_{\text{cladding}} (id2) * dA2 + F_{\text{deadload}} + F_{\text{cladding}} (id3) * dA3 + F_{\text{deadload}} + F_{\text{cladding}} (id4) * dA4 + \\ &F_{\text{wind}} + F_{\text{overpressure}} (id1) * dA1 + F_{\text{wind}} - F_{\text{overpressure}} (id2) * dA1 + \cos(\alpha) * F_{\text{wind}} + F_{\text{overpressure}} (id3) * dA3 + \\ &\sin(\alpha) * F_{\text{wind}} + F_{\text{overpressure}} (id3) * dA5 - \cos(\alpha) * F_{\text{wind}} - F_{\text{overpressure}} (id4) * dA4 + \sin(\alpha) * F_{\text{wind}} - F_{\text{overpressure}} \\ &(id4) * dA5 - rB * dA2 \\ &2,5 * 20 + 8,73 * 5 + 8,73 * 15 + 12,98 * 1,5 + 0,60 * 1,5 + \cos(16,7) * 47,22 * 5 + \sin(16,7) * 47,22 * \\ &4,5 - \cos(16,7) * 39,36 * 15 + \sin(16,7) * 39,36 * 4,5 - rB * 20 \\ &rB = 19,2/20 = 0,96 \end{aligned}$$

Value Karamba3D model: 1,01

Deviation karamba model: + 4%

Appendix F – 3DBAG Input G2-G4

3DBAG input of case G2, G3 and G4

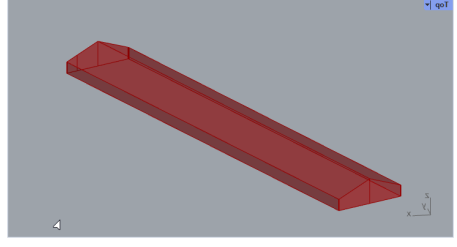
	3DBAG output [m]	Real value	Deviation	Geometry in Rhino by Grasshopper
h1.1	2,53	2,2	+1,2%	
h1.2	2,53	2,2	+1,2%	
h2	6,0	5,8	+3,3%	
w	16,7	16,2	+3%	
l	112	110,9	+0,9%	
x	0,5	0,5	0	
ld1 length	2,53	2,2	+1,2%	
ld2 length	2,53	2,2	+1,2%	
ld3 length	9,07	8,9	+2,2%	
ld4 length	9,07	8,9	+2,2%	

Table 84: geometry output case G2 based on 3DBAG, source: own work

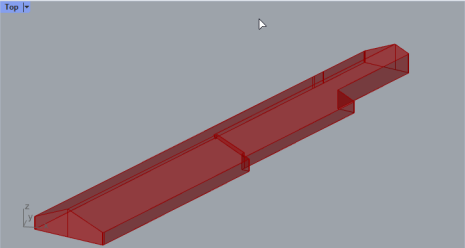
	3DBAG output [m]	Real value	Deviation	Geometry in Rhino by Grasshopper
h1.1	2,1	2,0	+5,0%	
h1.2	2,1	2,0	+5,0%	
h2	5,1	5,0	+2,0%	
w	14,2	13,9	+2,1%	
l	105	103,8	+1,1%	
x	0,5	0,5	0%	
ld1 length	2,1	2,0	+5,0%	
ld2 length	2,1	2,0	+5,0%	
ld3 length	7,6	7,5	+1,3%	
ld4 length	7,6	7,5	+1,3%	

Table 85: geometry output case G3 based on 3DBAG, source: own work

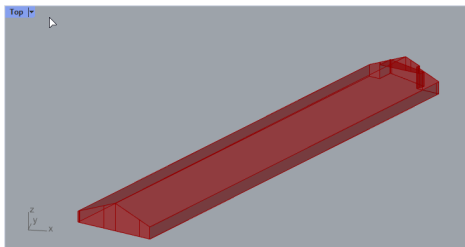
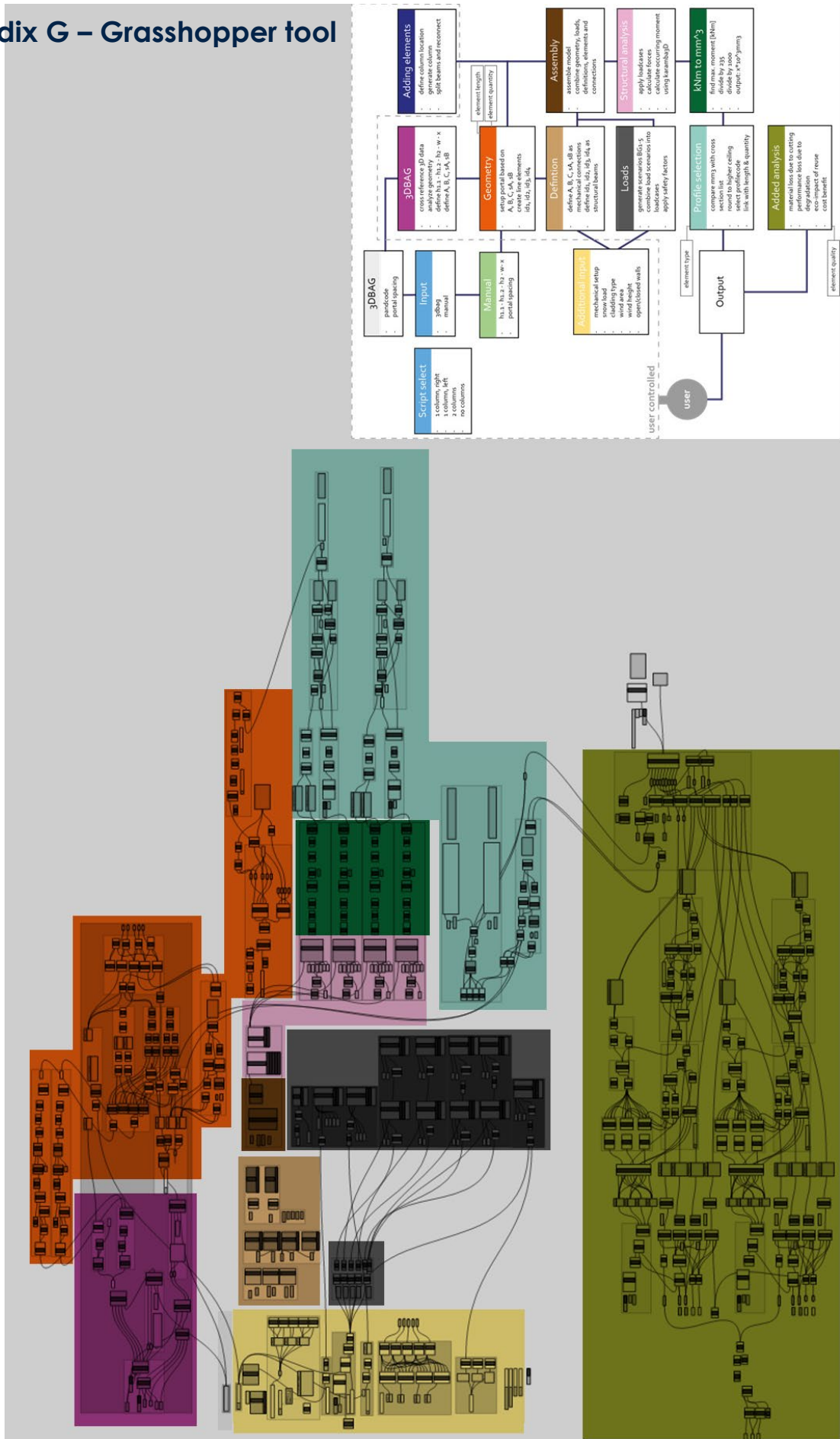
	3DBAG output [m]	Real value	Deviation	Geometry in Rhino by Grasshopper
h1.1	2,0	2,0	0%	
h1.2	2,0	2,0	0%	
h2	5,1	5,0	+2%	
w	15,0	14,5	+3,3%	
l	93,2	92,5	+0,7%	
x	0,5	0,5	0%	
ld1 length	2,0	2,0	0%	
ld2 length	2,0	2,0	0%	
ld3 length	8,1	7,8	+3,7%	
ld4 length	8,1	7,8	+3,7%	

Table 86: geometry output case G3 based on 3DBAG, source: own work

	C	D	E	G1	G2	G3	G4	Average
ld1	+2,8%	-0,3%	+3%	+4%	+1,2%	+5%	0%	+2,24%
ld2	+3,1%	-0,3%	+2,8%	+4%	+1,2%	+5%	0%	+2,26%
ld3	0%	-0,7%	+1,1%	-3,9%	+2,2%	+1,3%	+3,3%	+0,62%
ld4	-1,6%	-0,7%	+1,3%	-3,9%	+2,2%	+1,3%	+3,3%	+0,42%

Table 87: deviations based on 3DBAG, source: own work

Appendix G – Grasshopper tool



Appendix H – User Interface Illustrations

Screenshots of what the tool could potentially look like to users.

